LBL--28512

DE90 009067

Matrix Photochemistry of Small Molecules: Influencing Reaction Dynamics on Electronically Excited Hypersurfaces

Sandra Lee Laursen
Ph.D. Thesis

Materials and Chemical Sciences Division
Lawrence Berkeley Laboratory
University of California
Berkeley, CA 94720

January 1990

DISCLAIMER

This report was prepared as an account of work sponsored by an agency of the United States Government. Neither the United States Government nor any agency thereof, nor any of their employees, makes any warranty, express or implied, or assumes any legal liability or responsibility for the accuracy, completeness, or usefulness of any information, apparatus, product, or process disclosed, or represents that its use would not infringe privately owned rights. Reference herein to any specific commercial product, process, or service by trade name, trademark, manufacturer, or otherwise does not necessarily constitute or imply its endorsement, recommendation, or favoring by the United States Government or any agency thereof. The views and opinions of authors expressed herein do not necessarily state or reflect those of the United States Government or any agency thereof.

The U.S. Department of Energy has the right to use this thesis for any purpose whatsoever including the right to reproduce all or any part thereof.

This work was supported by the U.S. Department of Energy under Contract No. DE-AC03-76SF00098.

MASTER

DISTRIBUTION OF THIS DOCUMENT IS UNLIMITED

Matrix Photochemistry of Small Molecules: Influencing Reaction Dynamics on Electronically Excited Hypersurfaces

Sandra L. Laursen

Abstract

Investigations of chemical reactions on electronically excited reaction surfaces are presented. The role of excited-surface multiplicity is of particular interest, as are chemical reactivity and energy transfer in systems in which photochemistry is initiated through a metal atom "sensitizer." Two approaches are employed: A heavy-atom matrix affords access to forbidden triplet reaction surfaces, eliminating the need for a potentially reactive sensitizer. Later, the role of the metal atom in the photosensitization process is examined directly.

Photolysis of 1,2-dichloroethene in xenon matrix gives a product not seen in Kr, $Cl_2 \cdot C_2H_2$, as well as products common to both matrices, the π-hydrogen-bonded complex $HCl \cdot C_2HCl$ and the *cis-trans* isomerization product. Comparison with prior Hg (^3P)-sensitized results shows that the new product is formed only on a triplet reaction surface, accessed via matrix-induced intersystem crossing enhanced by the external heavy atom. Product formation in Xe at photon energies below the S_1 threshold indicates that direct excitation to the reactive triplet surface also occurs.

At photolysis energies low in the S_1 manifold, chlorine is eliminated from 1,1-dichloroethene in solid Xe, but not in Kr, further evidence of triplet surface chemistry and a matrix heavy-atom effect. At higher energies, a novel product appears, identified as a second $HCl \cdot C_2HCl$ isomer, σ-hydrogen-

bonded through the acetylenic proton. The product dependence on wavelength, parent, and matrix indicates that it is formed through a triplet-surface process under geometric constraints specific to the 1,1 isomer. Loss of Cl from a dissociative triplet state to form an excited chlorovinyl radical, with further cage reaction of the energetic fragments, is postulated.

Studies of Cd photosensitization were initiated after design and construction of a Knudsen cell source. Absorption studies of Cd in rare gas matrices agree with prior work but reveal new details of matrix effects on electronic spectra. In particular, matrix trends in frequency shift depend on the multiplicity of the upper state, as may oscillator strength changes between the matrix and gas phases. Representatives of two hydrocarbon classes, cycloalkanes and alkynes, were unreactive in the presence of excited Cd atoms, and possible reasons are discussed.

George C. Pimentel / Yuan T. Lee

"Only God can make a tree, but George can make a chemist—me."

—from a fortune cookie

dedicated to my grandmothers,

Metta Laursen and Karen Christensen-Trankar,

who tended my roots

and to GCP,

who watered often

Acknowledgments

First and foremost I am grateful to my late research advisor, George Pimentel. I never failed to leave his office without a scribbled list of ideas to ponder and tactics to try, a renewed sense of determination, and a realization that the experiment I had considered a bust was in fact a nugget of valuable information—never stepped out his door without feeling like a better scientist than the one that stepped in. Teaching with George was an immense pleasure too; it is no overestimation to predict that his voice as a teacher will echo throughout my life. I treasure those four years, and I regret that there were but four of them. Last summer George's daughter Jan mentioned that her family lost some things by having to share George with the rest of us, but in return they gained many other benefits. So, too, out of George's death came pleasures I otherwise would have missed—a chance to become closer to Jeanne, Jan, Tess and Chris, and many other special people in George's "enormous family."

George also deserves at least partial credit for the collection of interesting souls that were found in the lab. Ed Orton and Carolyn Hoener were both laboratory mainstays and buddies, Vicki Grassian was always good for a stimulating conversation about photochemistry or feminism, and Jim Harrison saved my sanity more times than he knows. Other Pimentel group members proved to be loyal friends and Bad Clams. Trish, Yvonne and Tucker were delightful neighbors and Vickie an exemplary Roma companion, while the Sauer group graciously incorporated me into their communal social life. Pam, Jane and Ishita deserve special thanks as charter members of the North Berkeley Mutual Aid Society, founded that panicky second-year autumn.

Heinz Frei was generous with his scientific expertise and enthusiasm, and Yuan Lee and Dan Neumark contributed helpful advice at critical stages late in the game. The LCB staff, especially Phil Eggers, Gary Smith, Lois Soule and Vangie Peterson, provided ever-friendly and efficient support. The machine shops on B-level and on the hill did yeoman service at crucial times, and Ed Orton's synthesis of dideuterated 1,1-dichloroethene proved invaluable.

And, yes, life did go on outside the lab. My family was always interested, supportive, and proud, and without them I would never even have tried this. Janet, Ruth and Mari, especially Mari, who had to put up with the worst of me, supplied their love and their friendship, "and that's everything." I thank many other supporters, including family and friends, teachers and unofficial mentors too numerous to list, although the Bruisers occupy a niche all their own.

Finally, but not least importantly, financial support for this work came from a National Science Foundation Graduate Fellowship and the Office of Energy Research, Office of Basic Energy Sciences, Chemical Sciences Division of the U. S. Department of Energy under Contract No. DE-AC03-76SF00098.

Table of Contents

List of Tables

List of Figures

Chapter I

Chapter II

Chapter III

Chapter I

Xenon Matrix Photochemistry of the 1,2-dichloroethenes

INTRODUCTION

Haloethene photochemistry has been studied in the gas phase using both direct photolysis and mercury (^3P) photosensitization.[1,2,3,4] Elimination of HX (X = F, Cl, Br) is the most common reaction pathway for photoexcited mono- and dihaloethenes in the gas phase, although isomerization, Cl atom detachment and molecular Cl_2 elimination have also been reported.[5] VUV photolysis of the dichloroethenes isolated in cryogenic matrices likewise yields HCl and its matrix cage partner C_2HCl as the principle products.[6,7]

However, recent matrix isolation studies of the metal atom (^3P) sensitized photochemistry of some haloethenes contrast with gas-phase results in the finding of other primary products than the HX elimination product.[8,9,10,11] For both chlorodifluoroethene and dichloroethene, insertion of Hg into the CCl bond occurs upon selective excitation of Hg codeposited with the olefin in krypton matrix. The formation of the organomercuric halide indicates that chemical reactivity plays a role in photosensitization along with energy transfer, and exemplifies the type of transient reaction intermediates which participate in the sensitization process.

The second important realization from these studies is that matrix photochemistry of these molecules is constrained to the reaction surface of the initial singlet or triplet excited state. For *cis*- and 1,1-dichloroethene in solid krypton, chlorine elimination occurs upon Hg (^3P)-sensitized photolysis, but not upon direct singlet excitation, indicating that the Cl_2 elimination channel is made accessible via triplet excitation. This aspect, namely the extent to which the photochemistry is determined by the initial excitation surface, has been the focus of these investigations of the photochemistry of

the 1,2-dichloroethenes in xenon matrix. The heavy-atom environment facilitates intersystem crossing and thus may be expected to alter the accessibility of normally spin-forbidden reaction channels. The use of an external heavy atom instead of a triplet sensitizer simplifies the reaction dynamics by excluding the chemical reactivity of the sensitizer from involvement in the energy transfer process.

The technique of matrix isolation in conjunction with infrared spectroscopy provides a number of advantages for the study of excited-state chemistry. The infrared "fingerprints" of various chromophores enable identification of nearly all possible product molecules, and the narrow band widths and lack of rotational structure permit even complex reaction mixtures to be distinguished. Moreover, the cryogenic temperatures and inert gas solvents inhibit secondary reaction and help stabilize normally reactive transient species so that primary reaction processes can be discerned. One twist here, however, is that the matrix material plays a dynamical role and thus cannot be considered completely "inert." Since very little thermal energy resides in the cryogenic system, the use of laser photolysis sources allows preparation of a narrow distribution of initial states and thus facilitates determination of reaction onset energies, branching ratios and quantum yields, information which helps to map hypersurface contours.

Presented here is the photochemistry of *cis*- and *trans*-1,2-dichloroethene in xenon matrix, using laser and Hg-Xe lamp irradiation at wavelengths longer than 200 nm. Comparison with the results in Kr matrix allows elucidation of reaction dynamics on surfaces of different multiplicity, while variations of the photolysis wavelength gives specific information about the reaction surface contours involved.

EXPERIMENTAL SECTION

The cryogenic apparatus, infrared spectroscopy, and Hg-Xe lamp photolysis were essentially the same as those described by Cartland and Pimentel.[8] In a typical experiment, 0.5 mmol of a xenon/dichloroethene mixture at M/R (matrix/reactant) = 100 was deposited with a flow rate of 0.3 mmol/hour onto a CsI substrate (Harshaw) held at 25 K with an Air Products Displex model CS-202 closed-cycle helium refrigerator. The matrix was cooled to 12 K for subsequent spectroscopy and photolysis. Gaskets of 0.015-in indium foil (Indium Corp. of America) held the substrate in good thermal contact with the copper sample holder. Temperature was monitored with an Au (0.07% Fe) vs. chromel thermocouple mounted on the cold tip and could be adjusted with a resistance heater. One apparatus (used with the IR44) was equipped with a digital temperature indicator/controller (R. G. Hansen and Associates), while the other was supplied separately with a variable power source for the heater and a digital multimeter for thermocouple voltage readout. Kr was deposited at 20 K and Xe at 25 K. The cryostat could be rotated 180° to permit exposure to the deposition ports, IR interrogation beam, or photolysis sources.

Infrared spectra were taken with an IBM-Bruker IR97 FTIR spectrometer, or in some experiments with an IBM IR44 FTIR. All laser photolysis experiments were performed on the IR97. Both spectrometers were equipped with a globar source, Ge-coated KBr beam splitter, and liquid nitrogen-cooled Hg/Cd/Te detector. Spectra were collected between 4000 and 400 cm^{-1} with a resolution of 0.5 cm^{-1} and were referenced to a spectrum of the external CsI windows and cold (12 K) substrate. The sample compartment was sealed and

purged with nitrogen to minimize gas-phase H_2O and CO_2 absorptions, although some spectra show such features due to limitations of the spectral subtraction software and operator patience. Selected IR features were integrated using a compensating polar planimeter.

The cryostat could also be mounted in the optical path of a Perkin-Elmer model 450 dual-beam spectrophotometer for recording UV absorption spectra. This instrument is described fully in Chapter III, as it was used extensively in the studies reported there. Spectra were recorded in transmittance mode against the nitrogen-purged reference compartment. In UV studies, cryostat windows and substrate were of BaF_2 or CaF_2 (Harshaw) and the baseline was electronically adjusted at room temperature, then re-recorded at 12 K.

Photolyses were performed with both monochromatic and broadband light sources. The second harmonic (532 nm) of a Quanta-Ray DCR Nd:YAG laser was used to pump a PDL-1 pulsed dye laser equipped with a WEX-1 wavelength extension system with KDP mixing crystals. Generation of the dye second harmonic in the WEX and mixing of this with the 1.064 μm fundamental of the Nd:YAG laser enabled tunability of the photolysis wavelength over the range 217-265 nm. In these experiments rhodamine 640 dye (Exciton) was used to attain a photolysis wavelength of 237 nm. Typically the laser power at a pulse frequency of 10 Hz was 700 μJ/pulse at the target as measured with a Scientech 380105 power meter. Some experiments were also performed using the fourth harmonic of the Nd:YAG laser at 266 nm. Photolysis intensities are reported here as milliwatt-hours (mWh), the product of photolysis time and average power.

Photolyses were also conducted with a focused 1000-W high pressure Hg-Xe arc lamp (Hanovia model 977-B1) mounted in an Oriel model 6140 air-cooled housing and equipped with a 2-in f/1.0 UV-grade fused silica, two-element, focusing lens and a 3-in water-cooled water filter. Broadband photolyses were limited to wavelengths longer than about 200 nm by the air cutoff, or to narrower regions by appropriate filters. Normally a 1-in aperture was used to restrict the lamp beam to a size near that of the substrate, in order to minimize radiative heating of the copper sample holder.

The dichloroethenes were obtained from Aldrich with reported purities of 97%, *cis*-dichloroethene (*cis*-DCE), and 98%, *trans*-dichloroethene (*trans*-DCE). The liquids were transferred to bulbs under nitrogen in a glovebox and degassed using liquid nitrogen. After cryogenic distillation at -77° C (CO_2(s)/2-propanol) the reserved middle fraction was stored in the dark at -20° C. Acetylene (Pacific Oxygen Co., 99.5%) was bubbled through concentrated H_2SO_4 to remove acetone, bulb-to-bulb distilled from a -77° C slush bath to a liquid nitrogen bath, and treated with a freeze-pump-thaw cycle before mixture preparation. Chlorine (Matheson) was of uncertain vintage and purity and was not further purified. Xenon (Airco 99.9995%) and krypton (Airco 99.995%) were used without further purification. Matrix/reactant mixtures, 100:1 unless specified otherwise, were prepared at pressures of 10^{-5} torr or less, using standard manometric techniques, on a mercury diffusion-pumped manifold with greased stopcocks (Apiezon N) and mineral oil-covered Hg manometer.

RESULTS

Xenon Matrix Infrared Spectra of the Dichloroethenes

Table 1 lists the IR absorption features observed for the 1,2-dichloroethenes in xenon matrix at 12 K. Spectra can be seen as negative features in the difference spectra of Figures 3 and 6. Vibrational mode assignments are made by analogy with the krypton matrix spectra of reference 9, hereafter referred to as I. Even under carefully controlled deposition conditions the xenon samples generally exhibited greater spectral complexity than the Kr equivalents, including more extensive splitting and broader and more variable lineshapes, as well as the usual matrix frequency shifts (1-7 cm^{-1}). Lines assigned to specific perturbations are noted as such in the table; other additional lines are assumed to be due to site splitting or aggregation.

Matrix UV Spectra of the Dichloroethenes

Transmittance spectra were recorded for 1:100 matrices of all three dichloroethenes in Kr and Xe and all showed a smooth, featureless rise starting near 230 nm, although scattering from the matrix made it difficult to determine the true onset. As our interest lay primarily in the possible spectral differences between matrices, rather than in the absorbing species itself, crude spectra were calculated for comparative purposes. A few data points in the region of interest (200-235 nm) were converted to absorbance units, the cold substrate background normalized out, and the matrix scattering linearly extrapolated from the absorption-free long-wavelength region and subtracted. These corrected curves are shown in Figure 1 for all three DCEs, and in all cases the xenon matrix spectrum is red-shifted from the krypton spectrum by 2-4 nm.

Table 1: Xenon Matrix Spectra of the 1,2-Dichloroethenes

cis-dichloroethene/Xe 1:100		*trans*-dichloroethene/Xe 1:100	
ν, cm^{-1}	Assignment	ν, cm^{-1}	Assignment
3084.0 (m)[a]	ν_8, asym. CH str.	3090.8 (m)[a]	ν_9, CH str.
3081.6 (w)		3084.5 (w)	
1589.9 (s)		1665.2 (w)	?
1588.9 (vs)	ν_2, CC str.	1658.7 (w)	
1586.9 (m)			
1565.5 (w)[b]			
1564.3 (w)	$\nu_4 + \nu_{10}$		
1562.4 (w)			
1298.7 (m)	ν_9, in-plane	1196.8 (s)	ν_{10}, CH bend
1297.8 (m)	CH bend		
1278.3 (w)	$\nu_4 + \nu_{11}$		
857.5 (vs)[b]	ν_{10}, asym. CCl str.	904.8 (s)	ν_6, CH bend
855.7 (vs)		901.4 (m)	
854.0 (m)			
850.4 (m)			
715.6 (m)[b]	ν_4, sym. CCl str.	819.0 (vs)[b]	ν_{11}, CCl str.
712.6 (m)		817.0 (m)	
709.3 (w)		815.8 (s)	
		813.1 (m)	
697.9 (vs)	ν_{12}, out-of-plane		
696.9 (s)	CH bend		
695.7 (m)			
568.7 (m)[b]	ν_{11}, CCl deform.		
566.4 (m)			

[a]Relative peak heights: w=weak, m=medium, s=strong, vs=very strong

[b]Splitting due to $^{35/37}Cl$ isotopes.

Figure 1: Matrix UV Spectra of the Dichloroethenes
(see text for correction procedure)

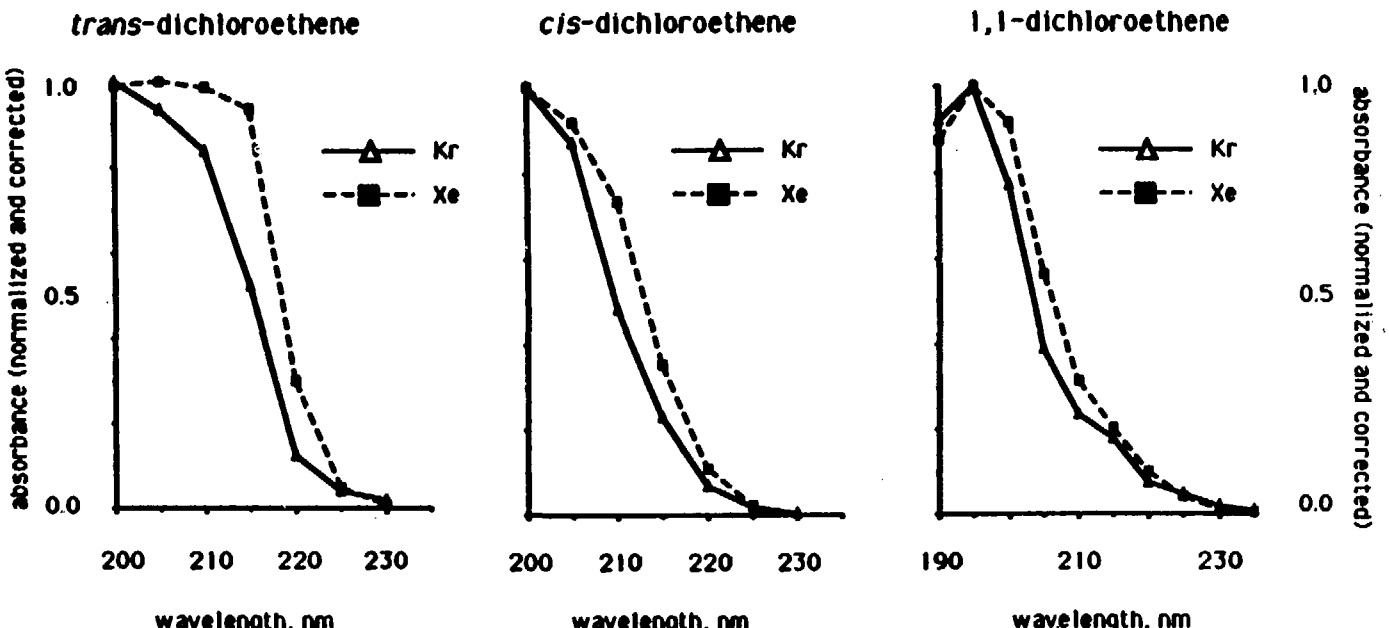

Photolysis of *cis*-dichloroethene

One hour of 237 nm photolysis (7.2 mWh) of an 0.51 mmol *cis*-DCE/Kr matrix (M/R = 100) resulted in the difference spectrum shown in Figure 2. The product frequencies, listed in Table 2, are in good agreement with those observed upon broadband ($\lambda > 200$ nm) Hg-Xe lamp photolysis of a similar sample in I. Thus the photoproducts at 237 nm are seen to be the same as the products of broadband UV irradiation: the isomer *trans*-DCE and the T-shaped, hydrogen-bonded complex $HCl{\cdot}C_2HCl$. Additional bands seen in Figure 2 can be assigned to annealing of strong parent *cis*-DCE features and to CO_2 and H_2O. Four hours of Hg-Xe lamp irradiation through a Pyrex cutoff filter ($\lambda > 300$ nm) caused no spectral changes in a *cis*-DCE/Kr 1:100 sample at 12 K except for apparent annealing of the *cis*-DCE parent.

For an 0.51 mmol *cis*-DCE/Xe matrix (M/R = 100), photolysis at 237 nm (3.2 mWh) gave the difference spectrum in Figure 3. The product band positions are listed in Table 2. By comparing the product frequencies with the *trans*-DCE/Xe data in Table 1 and the Kr photoproduct absorptions in Table 2, two of the products can be identified as those also observed in krypton. Strong bands at 818.9/815.9, 904.9/901.5, 1196.7 and 3090.5 cm^{-1} (descending intensity) match up with features of *trans*-DCE, and bands at 3312.0/3328.6, 2107.7, and 602.7 cm^{-1} correlate with the three strongest absorptions of the chloroacetylene-HCl complex. The remaining prominent features at 3264.4 cm^{-1} and the doublet at 727.9/736.4 cm^{-1} indicate the presence of a new photoproduct not formed in krypton under the same conditions. This can be recognized as the acetylene-chlorine cage pair produced in I by mercury-sensitized photolysis of *cis*-DCE in Kr matrix. Growth curves, displayed in Figure 4, indicate that all three products are primary photoproducts. In

Table 2: Products of 237 nm Photolysis of *cis*-DCE

cis-DCE/Kr 1:100 (7.2 mWh) ν, cm^{-1}	*cis*-DCE/Xe 1:100 (3.2 mWh) ν, cm^{-1}	Assignment		
	3334.1 (.003) [a]			
	3328.6 (.008)			
	3318.0 (.007)			
3308.7 (.004) [a]	3312.0 (.012)	C	ν_1	HCl•C_2HCl
	3277.1 (.002)[b]			
	3264.4 (.009)	D	ν_3	Cl_2•C_2H_2
	3090.5 (.003)	A	ν_9	*trans*-DCE
2778 (.005)	2829 (.002)			
2767 (.004)	2771 (.002)	C	ν_8[c]	HCl•C_2HCl
	2113.1 (.001)			
	2109.2 (.006)			
2099.8 (.004)	2107.7 (.009)	C	ν_2	HCl•C_2HCl
	2102.8 (.004)			
	2099.8 (.003)			
1199.1 (.010)	1196.7 (.009)	A	ν_{10}	*trans*-DCE
908.4 (.011)	904.9 (.017)	A	ν_6	*trans*-DCE
903.5 (.015)	901.5 (.006)			
902.1 (.009)	898.6 (.003)			
899.0 (.005)				
823.2 (.051)[d]	818.9 (.027)[d]	A	ν_{11}	*trans*-DCE
820.2 (.034)	815.9 (.021)			
817.3 (.008)	813.0 (.004)			
	736.4 (.015)[e]	D	ν_5	Cl_2•C_2H_2
	727.9 (.015)			
602.4 (.004)	602.7 (.007)	C	ν_4	HCl•C_2HCl

[a]Absorbances in parentheses refer to peak heights.

[b]Splitting due to Fermi resonance with combination band $\nu_2 + \nu_4 + \nu_5$.

[c]Stretching frequency for HCl submolecule.

[d]Splittings due to $^{35/37}Cl$ isotopes.

[e]Splitting of degenerate π_u bend due to presence of Cl_2 cage partner.

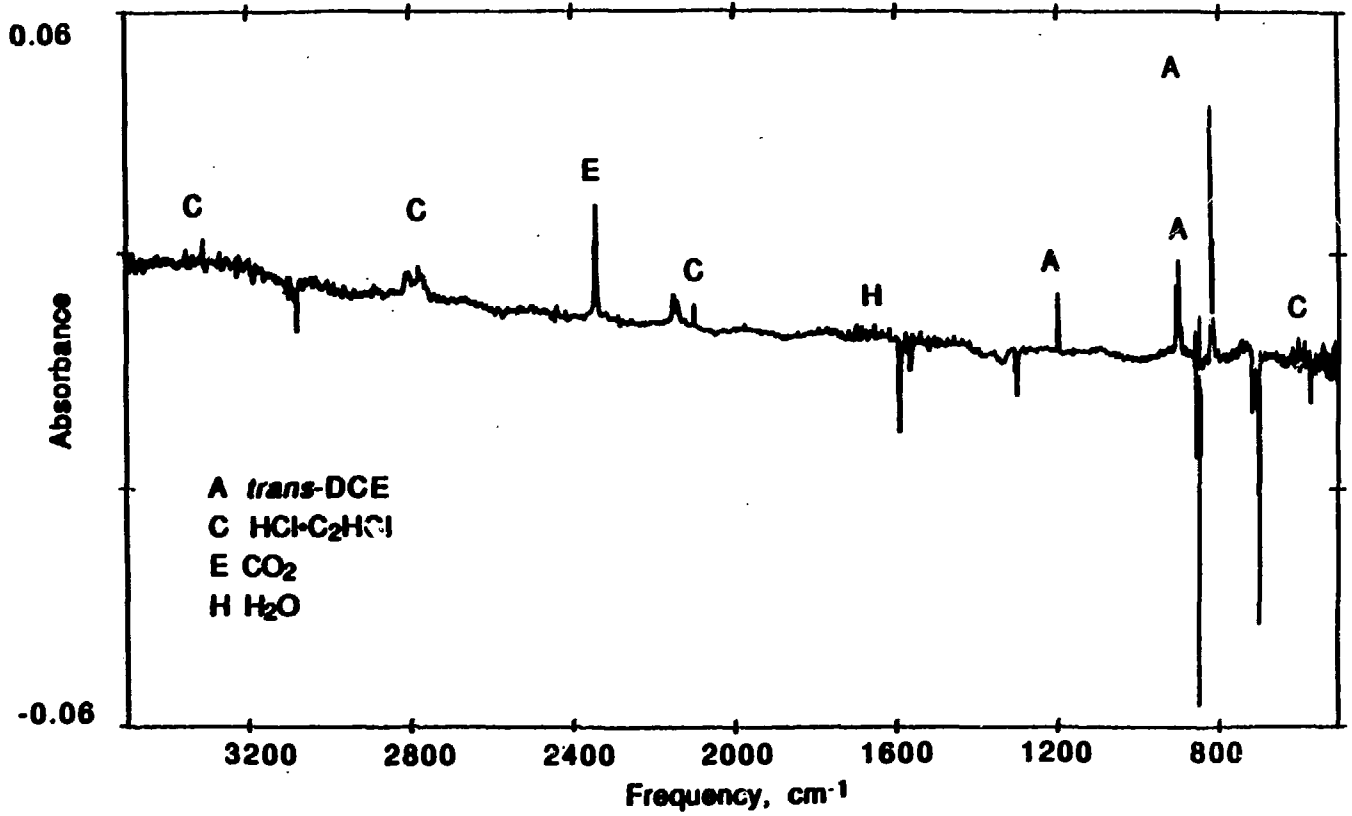

Figure 2: Difference Spectrum of *cis*-DCE/Kr 1:100 at 12 K, after 7.2 mWh laser photolysis at λ = 237 nm

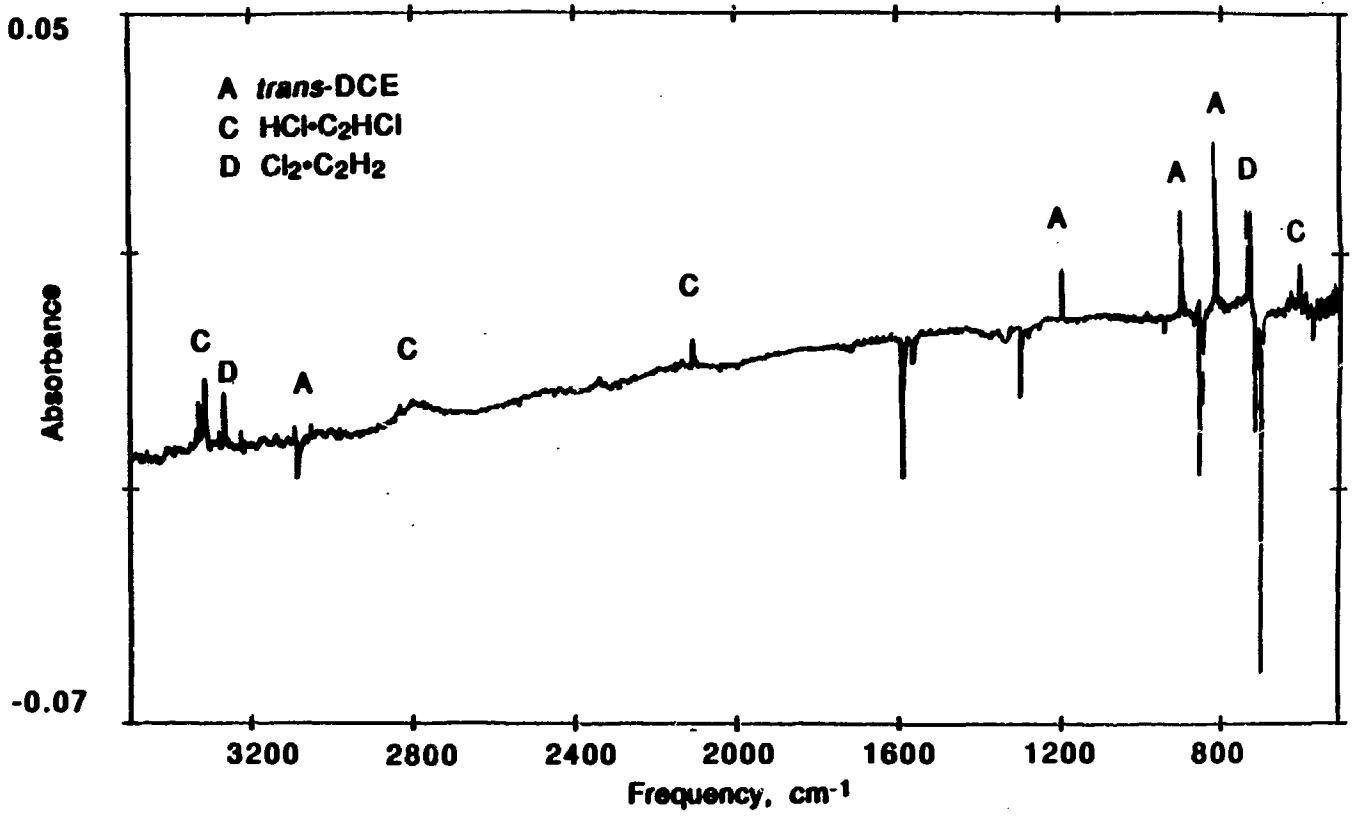

Figure 3: Difference Spectrum of *cis*-DCE/Xe 1:100 at 12 K, after 3.2 mWh laser photolysis at λ = 237 nm

Figure 4: *cis*-DCE/Xe Photoproduct Growth at λ = 237 nm

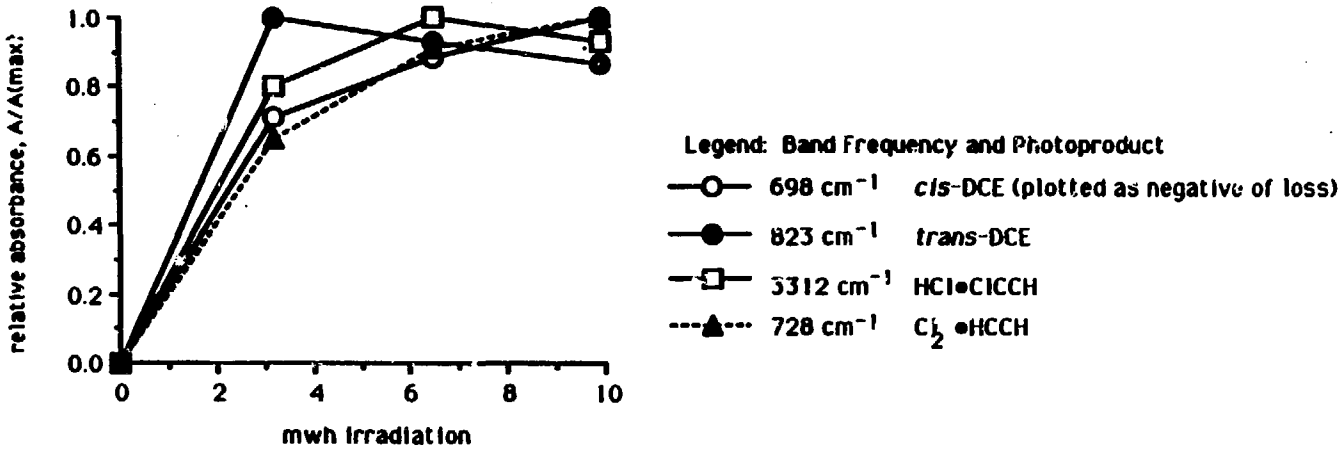

summary, 237 nm photolysis of *cis*-DCE in xenon matrix causes isomerization to form *trans*-DCE, elimination of HCl to form $HCl{\cdot}C_2HCl$, and elimination of Cl_2 to form $Cl_2{\cdot}C_2H_2$.

Three hours of irradiation of *cis*-DCE/Xe 1:100 with λ = 266 nm (average power 15 mW) produced absorptions at 818.9/815.7, 905.0/901.9, and 1196.7 cm^{-1}, and a doublet at 736.3/728.5 cm^{-1}. A portion of the difference spectrum is presented in Figure 5. The photoproducts can be identified respectively as *trans*-DCE and $Cl_2{\cdot}C_2H_2$, and it is concluded that excitation at 266 nm induces slow isomerization and chlorine elimination from *cis*-DCE in xenon matrix.

Broadband (λ > 200 nm) irradiation of a *cis*-DCE/Xe 1:100 matrix produced a product spectrum very similar to Figure 3. The only significant difference observed was an overall lower intensity for the absorption features of $Cl_2{\cdot}C_2H_2$, relative to those of the isomerization and HCl elimination products. A more dilute sample (1:400) gave the same products, with an overall sharpening of both parent and product features. Diminishing of some features within the lineshape of a given parent band is indicative that multimers contribute to the absorption at that particular frequency. Again, the same photoprocesses are seen to occur under both laser and lamp photolysis in the ultraviolet, but here with differing relative importance.

After 3.5 hours of Hg-Xe lamp photolysis of *cis*-DCE/Xe 1:100 through the Pyrex filter (λ > 300 nm), small but distinct product absorptions appeared at 819.1/815.9 and 905.2 cm^{-1}, in addition to negative parent features at 698.1/697.2, 857.8/856.0, and 715.9 cm^{-1}. Thus, a slow isomerization of *cis*-DCE to *trans*-DCE occurs upon prolonged long-wavelength irradiation in solid Xe, although none took place in Kr.

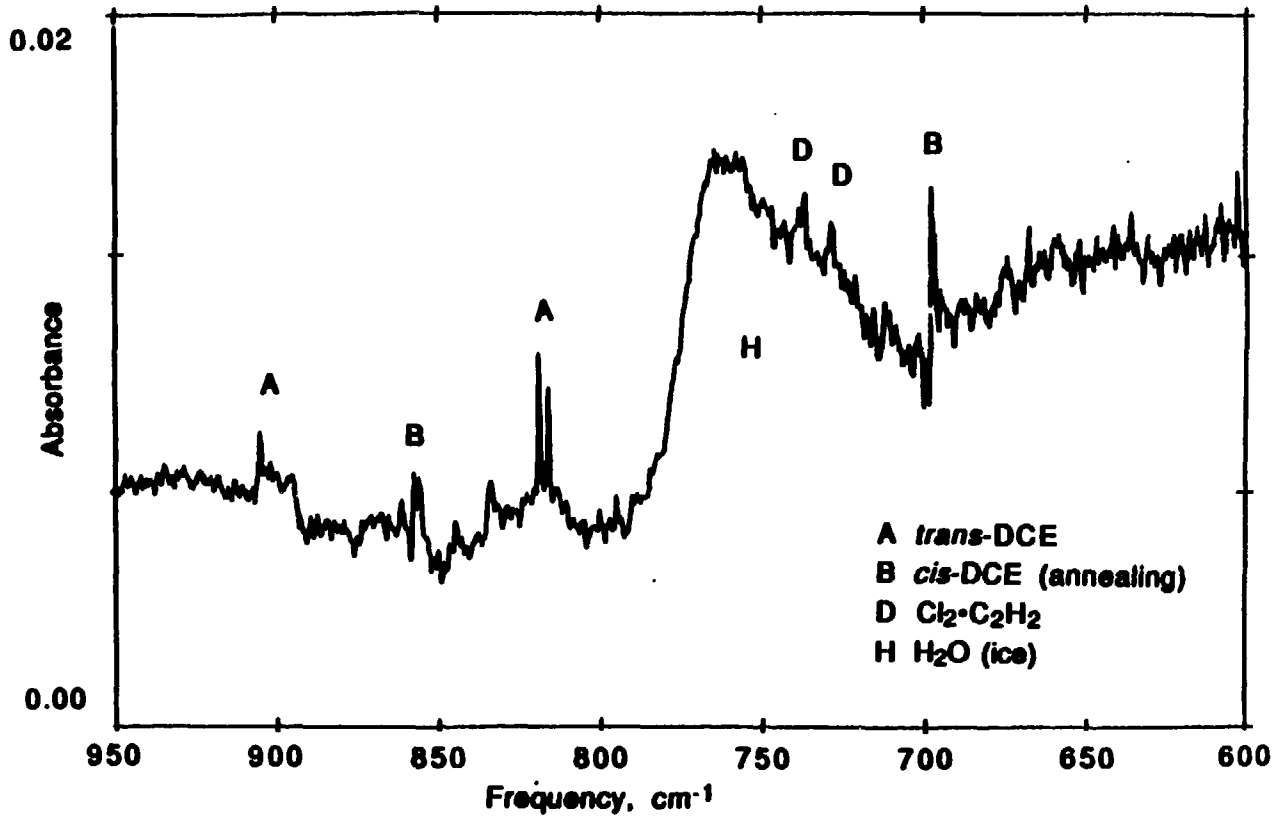

Figure 5: Difference Spectrum of *cis*-DCE/Xe 1:100 at 12 K, after 44 mWh laser photolysis at λ = 266 nm

Photolysis of *trans*-dichloroethene

Laser photolysis at 237 nm (8.8 mWh) of an 0.58 mmol *trans*-DCE/Kr matrix (M/R = 100) produced weak absorptions at 861.0, 699.4, 1302.0, and 718.3 cm^{-1}, identified by comparison to I as *cis*-DCE. Weak bands were also produced at 2099.8 and 602.3 cm^{-1}, indicating the presence of $HCl{\cdot}C_2HCl$, which may be a product of secondary photolysis of *cis*-DCE. In krypton matrix, *trans*-DCE photoreacts slowly at 237 nm to form the *cis* isomer and the HCl elimination product.

In contrast, an 0.54 mmol sample of *trans*-DCE 1:100 in xenon was found to be very reactive when irradiated at 237 nm. Absorptions appeared after only 10 minutes of photolysis (0.6 mWh) and became strong with continued irradiation, as can be noted in the difference spectrum in Figure 6 and in the list of product absorptions in Table 3. One product, with principal features at 698.0/697.0, 857.6/855.8, 1588.9/1589.8, 715.7/712.6 and 1298.6/1297.7 cm^{-1}, is easily recognized as the *cis* isomer. Absorptions at 3312.4/3328.7, 2107.9 and 602.7 cm^{-1} belong to the elimination product, $HCl{\cdot}C_2HCl$, previously identified, and the remaining prominent features at 727.9/736.4 and 3264.2 cm^{-1} are associated with the $Cl_2{\cdot}C_2H_2$ product. Again, growth curves show that all three species are primary photoproducts. The bands labeled "K" in Figure 6 were identified as $CsNO_3$,[12] produced in an earlier experiment by reaction of NO_2 with the CsI substrate. Thus isomerization and the two eliminations are the primary processes induced by 237 nm irradiation of *trans*-DCE isolated in xenon.

Unfiltered Hg-Xe lamp photolysis of a *trans*-DCE/Xe 1:100 matrix gave a difference spectrum similar to Figure 6, the most notable distinction being a

Table 3: Products of 237 nm Photolysis of *trans*-DCE

trans-DCE/Kr 1:100 (8.8 mWh) ν, cm^{-1}	*trans*-DCE/Xe 1:100 (3.2 mWh) ν, cm^{-1}	Assignment		
	3334.3 (.002) [a]			
	3328.7 (.006)			
	3318.5 (.004)			
	3312.4 (.010)	C	ν_1	$HCl \cdot C_2HCl$
	3276.8 (.001)[b]			
	3264.2 (.005)	D	ν_3	$Cl_2 \cdot C_2H_2$
	2830 (.002)			
	2799 (.002)			
2781 (w) [a]	2772 (.002)	C	ν_8[c]	$HCl \cdot C_2HCl$
	2109.3 (.003)			
2099.8 (.004)	2107.9 (.006)	C	ν_2	$HCl \cdot C_2HCl$
	2102.0 (.002)			
	1591.5 (.003)			
	1589.8 (.006)			
1591.9 (.002)	1588.9 (.008)	B	ν_2	*cis*-DCE
	1587.0 (.003)			
1302.0 (.002)	1298.6 (.004)	B	ν_9	*cis*-DCE
	1297.7 (.004)			
861.0 (.006)[d]	857.6 (.011)[d]	B	ν_{10}	*cis*-DCE
859.3 (.005)	855.8 (.010)			
	736.4 (.015)[e]	D	ν_5	$Cl_2 \cdot C_2H_2$
	728.7 (.007)			
	727.9 (.014)			
718.3 (.002)	715.7 (.006)[d]	B	ν_4	*cis*-DCE
	712.6 (.004)			
	709.7 (.002)			
699.4 (.005)	698.0 (.023)	B	ν_{12}	*cis*-DCE
	697.0 (.013)			
602.3 (.002)	602.7 (.006)	C	ν_4	$HCl \cdot C_2HCl$

[a] Absorbances in parentheses refer to peak heights; w = weak.

[b]Splitting due to Fermi resonance with combination band $\nu_2 + \nu_4 + \nu_5$.

[c]Stretching frequency for HCl submolecule.

[d]Splitting due to $^{35/37}Cl$ isotopes.

[e]Splitting of degenerate π_u bend due to presence of Cl_2 cage partner; see text.

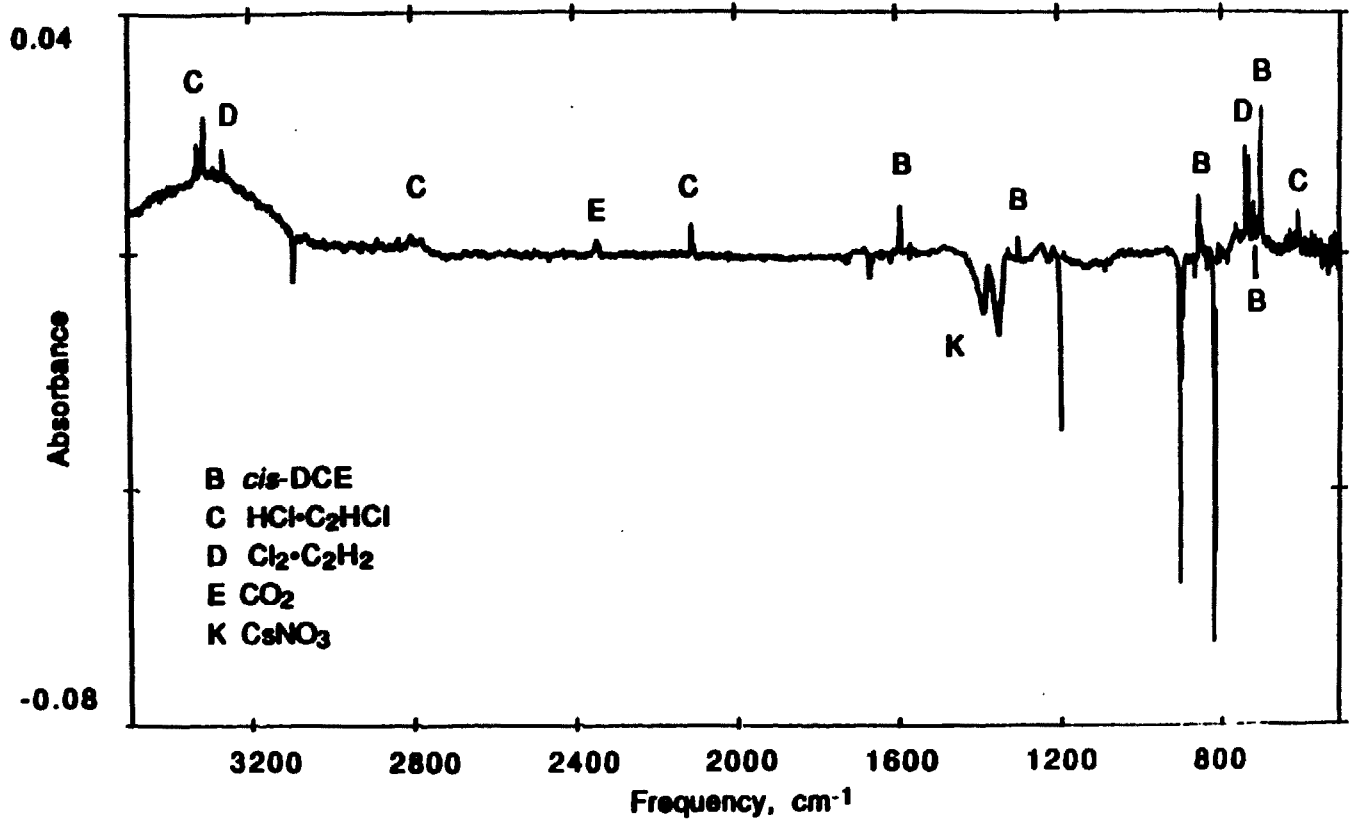

Figure 6: Difference Spectrum of *trans*-DCE/Xe 1:100 at 12 K, after 3.3 mWh laser photolysis at λ = 237 nm

lower relative intensity for the $Cl_2 \cdot C_2H_2$ product. As observed for the *cis* isomer, UV photolysis initiates the same photochemical reactions, but with a relative importance dependent on the source.

Longer-wavelength ($\lambda > 300$ nm) irradiation of a *trans*-DCE/Xe 1:100 matrix caused small depletions of the strong parent features at 904.7 and 819.0/816.0 cm^{-1} and growth of bands at 698.0 and 857.9/855.9 cm^{-1} after 3 hours. As in the *cis*-DCE/Xe experiment, photoisomerization proceeds on a slow time scale. In contrast, no new features were observed when *trans*-DCE/Kr 1:100 was subjected to 3 hours of Hg-Xe lamp photolysis at $\lambda > 300$ nm.

Codeposition and Photolysis of $C_2H_2/Cl_2/Xe$

Mixtures of C_2H_2/Xe 1:100 and Cl_2/Xe 1:25 were codeposited to give a sample of approximate composition C_2H_2/Cl_2/Xe 1:4:200. In such a sample, assuming a perfect statistical distribution, 19-26% of the acetylene molecules would have a single chlorine neighbor, and 2-4% would have two Cl_2 nearest neighbors, depending on the number of substitutional sites (one or two) occupied by the acetylene. For comparison, the acetylene mixture was also deposited alone (major features 727.6, 3280.5/3267.0, 1317.1 cm^{-1}), but the mixed-sample spectrum in the regions of the IR-active acetylene modes was sufficiently complex to inhibit the spectral distinguishing of a small number of $Cl_2 \cdot C_2H_2$ pairs from the very strongly absorbing isolated C_2H_2, multimers and other acetylene-impurity complexes. The results of Hg-Xe lamp photolysis show that such pairs were, however, present. After just 10 min unfiltered ($\lambda > 200$ nm) irradiation, some parent bands were depleted up to 50%, and many product features had grown in. Absorptions at 635.0/612.1, 3328.7/3314.7/3311.9/3301.7, 2839, and 2109.3/2108.3 cm^{-1} indicate the formation of $C_2HCl \cdot HCl$. The presence of *trans*-DCE is seen in features at 819.0/815.8/813.4,

905.3/901.4, and 1196.5 cm^{-1}, and *cis*-DCE features appeared at 698.2/697.2, 857.8, and 715.8 cm^{-1}. A number of additional features grew in with photolysis but were not identified: 843.1, 573.6, 1240.4/1237.5, 921.2, 973.8, 673, 1221 cm^{-1}. Most are probably due to photoreactions of chlorine with impurities introduced into the matrix by small air leaks or with the unpurified chlorine sample.[13]

Branching Ratios

Relative absorption coefficients were determined as in I in order to estimate branching ratios for the laser photolysis experiments. For *cis*-DCE/Kr, the integrated absorbance of the ν_2 *cis*-DCE band at 1590.9 cm^{-1}, divided by the number of millimoles of *cis*-DCE deposited, gave an effective extinction coefficient of 94 cm^{-1}/mmol. This is in good agreement with the value obtained by Cartland and Pimentel in Kr, 87 cm^{-1}/mmol.[9] In xenon the effective extinction coefficient obtained was 82 cm^{-1}/mmol. From the experiment with *trans*-DCE in Kr an effective extinction coefficient of 52 cm^{-1}/mmol was derived for ν_{10} (1199.4 cm^{-1}) of *trans*-DCE, which compares well to that determined in I, 57.5 cm^{-1}/mmol. In Xe this coefficient was calculated to be 65 cm^{-1}/mmol. Comparison of the Kr matrix values suggests that random errors are on the order of 10%, while the Xe coefficients perhaps differ slightly more.

Upon 237 nm photolysis of an 0.51 mmol *cis*-DCE/Kr matrix, the two products formed were *trans*-DCE and HCl·C_2HCl. The intensity of the ν_2 *cis*-DCE feature sustained an 11% loss after one hour, and integrated absorbances of 0.023 cm^{-1} for ν_{10} (1199.1 cm^{-1}) of *trans*-DCE and 0.0045 cm^{-1} for ν_2 (2099.8 cm^{-1}) of C_2HCl were produced. Using the extinction coefficient of 52 cm^{-1}/mmol for ν_{10} of *trans*-DCE (I), the *cis*-to-*trans* isomerization yield is 78%. The

remaining 22% is thus attributed to the only other product, $HCl \cdot C_2HCl$; however, comparison with the data to be presented and with that in I indicates that the extinction coefficient thereby derived for $HCl \cdot C_2HCl$ is not reliable.

Photolysis of an 0.20 mmol matrix at 237 nm in xenon caused a 46% depletion of the *cis*-DCE ν_2 band intensity after one-half hour. The following integrated absorbances were obtained for the three products: ν_{10} (1196.7 cm^{-1}) of *trans*-DCE, 0.010 cm^{-1}; ν_2 (2107.7 cm^{-1}) of $HCl \cdot C_2HCl$, 0.026 cm^{-1}; ν_3 (3264.4 cm^{-1}) of $Cl_2 \cdot C_2H_2$, 0.020 cm^{-1}. For *trans*-DCE, this converts to a 16% yield. The two elimination products must then account for the remaining 84% of the parent depletion.

For the *trans*-DCE experiment in krypton, the 237 nm photoproduct absorptions of *cis*-DCE and $HCl \cdot C_2HCl$ were not sufficiently intense to permit calculation of yields. Comparison of relative intensities with other experiments suggests, however, that *cis*-DCE is the major photoproduct and that $HCl \cdot C_2HCl$ is a minor, and possibly secondary, photolysis product.

After 1 hour of 237 nm excitation of an 0.54 mmol matrix, the ν_{10} *trans*-DCE feature at 1196.8 cm^{-1} was depleted by 13%. Integrated absorbances were measured for the three photoproducts: ν_2 (1588.9 cm^{-1}) of *cis*-DCE, 0.024 cm^{-1}; ν_2 (2107.9 cm^{-1}) of $HCl \cdot C_2HCl$, 0.022 cm^{-1}; and ν_3 (3264.2 cm^{-1}) of $Cl_2 \cdot C_2H_2$, 0.0073 cm^{-1}. This indicates an isomerization yield of 43%, and a combined yield of 57% for the two elimination processes.

At this point the yields of the two photoelimination products for the xenon experiments can be found by applying the method of simultaneous equations to the conservation of mass for each reaction:

$$\text{mmol parent depleted} = \Sigma(\text{mmol product}) = \Sigma(A/\varepsilon)$$

where A is the experimental integrated absorbance and ε the unknown extinction coefficient for each photoproduct. Using product absorbances from the *cis*- and *trans*-DCE/Xe experiments discussed above and the effective extinction coefficients derived for the two dichloroethenes, we obtain as solutions extinction coefficients of 128 cm^{-1}/mmol for ν_2 of $HCl{\cdot}C_2HCl$ and 35 cm^{-1}/mmol for ν_3 of $Cl_2{\cdot}C_2H_2$. Relative yields from *cis*-DCE in xenon are thus 16% *trans*-DCE, 22% $HCl{\cdot}C_2HCl$, and 62% $Cl_2{\cdot}C_2H_2$. From *trans*-dichloroethene in xenon, the photoproducts are 43% *cis*-DCE, 26% $HCl{\cdot}C_2HCl$, and 31% $Cl_2{\cdot}C_2H_2$. In each case, the new, chlorine elimination product is formed in significant yield.

DISCUSSION

Structure of $Cl_2 \cdot C_2H_2$ Photoproduct

The vibrational bands of the $Cl_2 \cdot C_2H_2$ product in Xe show some interesting spectroscopic differences from the same features in Kr. The ν_3 CH stretch in Xe shifts 2.6 cm^{-1} to the red from the isolated acetylene frequency of 3267.0 cm^{-1}, and the higher component of the Fermi doublet ($\nu_2 + \nu_4 + \nu_5$) is observed at 3.4 cm^{-1} lower than the 3280.5 cm^{-1} band of isolated C_2H_2/Xe, although with less intensity than the low-frequency component. This contrasts with the $Cl_2 \cdot C_2H_2$ spectrum in Kr, in which the lower component shifted far to the red (12.9 cm^{-1}) of isolated acetylene, apparently far enough to remove the Fermi resonance, since no second component was observed at all.

Turning to the ν_5 band, a doublet was observed in both Xe and Kr, indicating breaking of the $D_{\infty h}$ acetylene symmetry by the chlorine cage partner. The magnitude of the splitting is similar, 8.5 cm^{-1} in Xe and 6.2 cm^{-1} in Kr, but the average shift of the band position from the C_2H_2 ν_5 singlet (727.7 cm^{-1} in Xe, 732.5 cm^{-1} in Kr) is much smaller in Xe (+4.4 cm^{-1}) than in Kr (+12.4 cm^{-1}).

The large blue shift of both ν_5 components and the large downward shift of ν_3, suggesting an acidic interaction of the CH bond, led Cartland and Pimentel

to consider an "end-on" structure as in T_1 more likely than the T_2 structure deduced for the $HCl \cdot C_2HCl$ complex by McDonald et al.[7] However, the smaller average shifts of both ν_3 and ν_5 for the $Cl_2 \cdot C_2H_2$ pair in Xe more closely resemble the behavior of the well-characterized, π-hydrogen-bonded $HX \cdot C_2H_2$ complexes with structure T_2,[7,14,15] and thus the T_2 geometry is favored for the photoproduct in xenon matrix. In recent codeposition studies Ault has suggested the same structure for the acetylene complexes of Cl_2 and ClF in Ar matrix, with the halogen molecule acting as a Lewis acid toward the CC bond.[16] The appearance of different photoproduct geometries in krypton and xenon is no doubt influenced by the difference in cage sizes in the two matrices and the possibly differing number of substitutional sites occupied by the reactant molecule. Since, in the similar metal atom-sensitized photoreaction of vinyl chloride, the $HCl \cdot C_2H_2$ photoproduct frequencies were identical for all three sensitizers, Hg, Cd and Zn,[15] the presence of the metal atom in the krypton case is presumably not responsible for the spectroscopic differences discussed here, even though it may play a role in the product geometry change.

Structure of $HCl \cdot C_2HCl$ Photoproduct

The large degree of splitting seen in the spectral features of the π-hydrogen-bonded $HCl \cdot C_2HCl$ photoproduct of both *cis*- and *trans*-DCE deserves brief comment. Splittings are probably due to trapping in several slightly different substitutional sites and nearest-neighbor interactions due to imperfect isolation, as evidenced by the spectral simplifications which resulted from dilution of the matrix. Significant differences of complex geometry are expected to induce more substantial spectral changes, as will be seen in Chapter II. Of particular note is the HCl absorption near 2800 cm^{-1},

which is split into several bands of this sort. Over time additional bands developed at 2838 and 2839 cm^{-1}, corresponding to Q(0) and R(0) rotation-vibration transitions of free HCl in solid Xe.[17,18] Apparently even when hydrogen-bonded to chloroacetylene, hydrogen chloride undergoes hindered rotation in the xenon cage.

237 nm Photolysis

The UV absorption spectra of the gaseous 1,2-dichloroethenes exhibit maxima near 190 nm but with a red tail reaching nearly to 240 nm.[1] Matrix spectra are consistent with the gas-phase data, although, as noted already, it is difficult to determine the exact onset of absorption due to scattering from the matrix. Thus it is not surprising that some photochemistry does occur when these compounds are irradiated at 237 nm, although this wavelength is surely near the threshold of absorption. Consistent with the latter point are the small extent of reaction (11% depletion of *cis*-DCE/Kr after 7.2 mWh) and the observation that neither dichloroethene reacts when directly irradiated through a 246-257 nm interference filter (I).

As does broadband ($\lambda > 200$ nm) photolysis, laser irradiation of *cis*-DCE in Kr matrix induces formation of two products, *trans*-DCE and $HCl{\cdot}C_2HCl$. In contrast, the same molecule in xenon reacts to form a new product, $Cl_2{\cdot}C_2H_2$, in addition to those previously observed. Clearly, changing the matrix material from krypton to xenon has altered the product distribution for the photoreaction. The observation that assisted in the identification of the new xenon photoproduct, that it is also formed via mercury photosensitization in Kr, provides as well a clue to the reaction pathway. Cartland and Pimentel (I) concluded that the Hg (^3P)-initiated Cl_2 elimination chemistry "takes place (at least in the Kr matrix) on a triplet surface that is not accessed with

the higher energy, singlet excitation." In the Xe case, access to a triplet reaction surface could be facilitated by the heavy-atom matrix environment through spin-orbit coupling.

237 nm Photolysis in Kr. The diagram in Figure 7, adapted from I, shows the relevant energy levels for the reactants and possible products in this system. Sources of the energies which appear on this and other diagrams are compiled in Appendix A. For $\lambda > 200$ nm excitation, the singlet (π,π^*) state has been considered the major contributor to photochemical activity.[1] Singlet (n,π^*) and (n,σ^*) states are also accessible in this energy regime, particularly to the long-wavelength side of the broad DCE absorption, although these transitions have low oscillator strength and initiate little of the gas-phase photochemistry.[1] Since *cis-trans* isomerization is readily accomplished probably only through the nonplanar (π,π^*) state, it is assumed that the observation of a significant amount of *trans*-DCE photoproduct in Kr means that the $^1(\pi^*\leftarrow\pi)$ transition is being excited by the 237 nm photons. The possibility that this isomerization is accomplished through the triplet (π,π^*) state, rather than the singlet, is eliminated by noting that *cis*-DCE was unreactive during prolonged photolysis at $\lambda > 300$ nm in Kr. If the $^3(\pi^*\leftarrow\pi)$ transition, with a vertical energy of 91 kcal/mol,[19] were active, the 95 kcal/mol energy input should have caused formation of *trans*-DCE photoproduct. However, the possible influence on the photochemistry of the (n,σ^*) and (n,π^*) states must not be ignored.

Following the argument of Cartland and Pimentel (I), the absence of Cl_2 elimination shows that, although a triplet state, $Cl_2(\tilde{A}\,^3B_0^+{}_u)\cdot C_2H_2$, is energetically accessible, triplet reaction surfaces are not involved in the photoreaction in Kr. Internal conversion from $^1[CHClCHCl]^*$ into high

Figure 7: Energy Level Diagram for 1,2-DCE/Kr

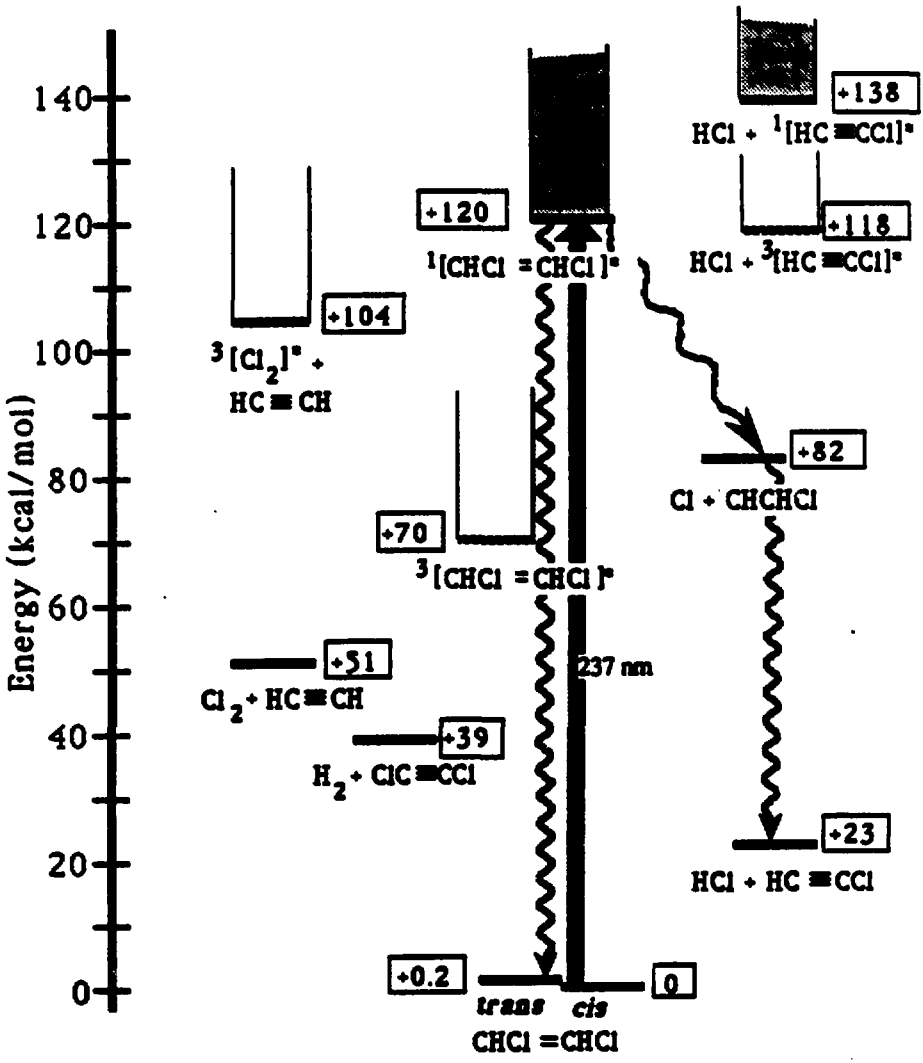

vibrational states of the ground singlet state would provide access to a singlet ground-state surface with sufficient energy to form any of the three possible elimination products. Since neither Cl_2 nor H_2 elimination is observed, this mechanism is not very satisfactory as an explanation for the appearance of the $HCl \cdot C_2HCl$ product. However, the ground state of Cl + CHCHCl is also energetically accessible, so chlorine atom detachment could follow excitation into the $^1(n,\sigma^*)$ state. The vibrationally hot β-chlorovinyl radical could then either recombine with the Cl atom, forming dichloroethene, or lose a hydrogen atom to form $HCl \cdot C_2HCl$. The observation of *cis*- and *trans*-dichloroethene as photoproducts of 1,1-DCE in Kr matrix bears evidence that CCl bond rupture and recombination does occur in these systems (I).

237 nm Photolysis in Xe. Having noted the availability of a triplet excited state and the heavy atom effect of the xenon environment, it is logical to conclude that chlorine is eliminated from 1,2-DCE through this $^3[Cl_2]^* \cdot C_2H_2$ state via xenon-induced intersystem crossing from the initial singlet excitation surface. Interconversion of isomers may be effected through either $^1[CHClCHCl]^*$ or $^3[CHClCHCl]^*$ states. Some HCl elimination may proceed through a $HCl \cdot ^3[C_2HCl]^*$ state, estimated to lie about 20 kcal/mol below the singlet chloroacetylene state[20] by analogy to acetylene.[21] Figure 8 shows the energy levels and reaction pathways for the xenon matrix system.

The enhanced reaction rates in Xe over Kr, as measured by parent depletion with photolysis time, can be ascribed to the opening of a new reaction channel in Xe. In addition, matrix UV absorption spectra (figure 1) show a red shift of the absorption onset in Xe as compared to Kr, suggesting that the extinction coefficient at the 237 nm photolysis wavelength—very near the

Figure 8: Energy Level Diagram for 1,2-DCE/Xe

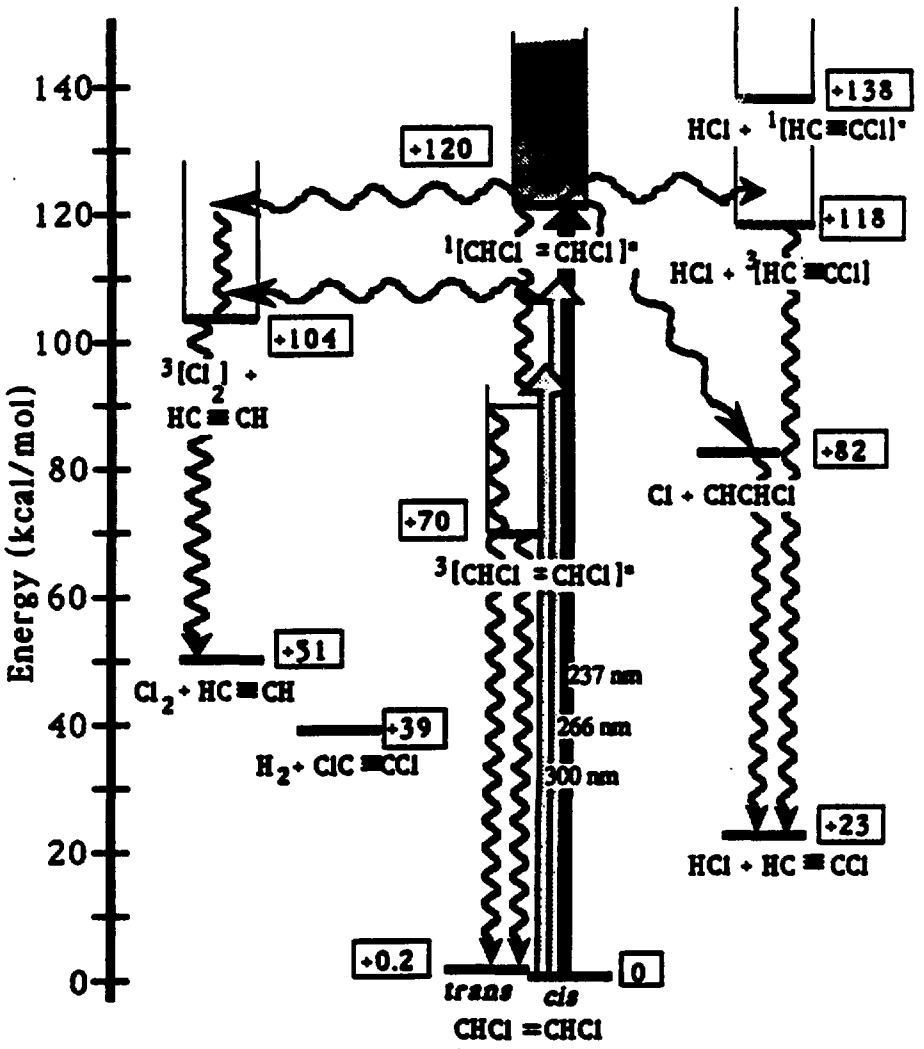

absorption onset—is higher in Xe than in Kr, although the data show no obvious absorption in either matrix at 237 nm. Such shifts in electronic band origins with matrix material are well known for atomic species,[15,22] and have recently been catalogued for diatomics.[23]

Attribution of the photochemical differences to a matrix heavy-atom effect raises the additional question as to why Kr, itself a rather heavy nucleus, does not induce intersystem crossing and triplet-surface chemistry. Indeed, Morgan and Pimentel have observed heavy-atom effects on emission lifetimes and quantum yields for (dimethylamino)benzonitrile (DMABN) in both Kr and Xe, relative to Ar.[24] Although the rate constant for phosphorescence changes by a factor of 300 from Ar to Xe, that for intersystem crossing changes by a factor less than five. Furthermore, the change in k_{isc} is just as large from Kr to Xe (1.8:3.3) as from Ar to Kr (1:1.8). While these quantitative results surely do not apply here, they are exemplary of both the magnitudes of matrix-induced rate changes and the variation of these magnitudes among different processes, and they also provide an opportunity to note the distinction between photophysical and photochemical manifestations of the heavy atom effect. Clearly it is the rate of intersystem crossing *relative* to the rates of other competing reaction and relaxation processes, which latter depend on the guest molecule as well as on the matrix host, that is crucial in chemically manifesting the heavy atom effect. For some molecules, the relative rate enhancement necessary to observe a change in product distribution might be achieved by using Kr instead of Ar, for example, but for the DCEs the heavier Xe matrix is required.

Broadband Photolysis in Xe

It is evident that the same matrix-induced intersystem crossing mechanism

is at work in the Hg-Xe lamp ($\lambda > 200$ nm) photolyses of *cis*- and *trans*-dichloroethene in solid xenon, since the $Cl_2 \cdot C_2H_2$ product is observed in both experiments. At higher excitation energies, a greater number of competing reaction channels are opened, thus explaining the lower relative importance of Cl_2 elimination at $\lambda > 200$ nm compared with the 237 nm excitation. In addition, as shown in the Cl_2-C_2H_2 codeposition experiments, chlorine is easily excited by the Hg-Xe lamp and reacts readily with acetylene to form $HCl \cdot C_2HCl$, *cis*-DCE and *trans*-DCE. Ault has also observed photoaddition of Cl_2 across the CC triple bond of acetylene in Ar matrix.[16] Thus secondary photolysis of chlorine-acetylene pairs is presumed significant and inhibits buildup of this product.

Direct Triplet Photochemistry

Perhaps the most convincing evidence for an external heavy atom effect on the reaction dynamics is that provided by the longer-wavelength photolyses. Light with wavelengths ($\lambda > 300$ nm) well below the singlet absorption onset is sufficiently energetic to stimulate isomeric interconversion of DCEs in xenon, yet has no effect on krypton-isolated DCE. The excitation energy of 95 kcal/mol exceeds the CHClCHCl $T_1 \leftarrow S_0$ vertical transition energy of 89-91 kcal/mol,[19] and the lengthy photolysis times needed to observe products are consistent with spin-forbidden character in the excited transition. In this case the enhanced spin-orbit coupling of xenon promotes direct absorption into the nonplanar $^3(\pi,\pi^*)$ state of CHClCHCl, from which relaxation to either isomer can occur. When the excitation wavelength is 266 nm, *cis*-DCE undergoes both chlorine elimination and isomerization. The appearance of $Cl_2 \cdot C_2H_2$ signifies the accessibility of the excited state $^3[Cl_2]^* \cdot C_2H_2$ at a photon energy of 107 kcal/mol. The assigned energy level of this state, 104

kcal/mol, is based on the 0-0 transition energy of Cl_2 ($\tilde{A}\,^3B0^+_u \leftarrow \tilde{X}\,^1\Sigma^+_g$) and would therefore be considered a lower limit if the two molecules do not interact. Since this would imply a very low barrier to Cl_2 elimination ($E_a \leq 3$ kcal/mol), perhaps the observations reveal the intermediate to be a triplet excited-state reaction complex with a significant interaction energy and characteristic geometry, rather than merely the sum of $^3[Cl_2]^*$ and ground-state acetylene. Following a similar line of thought, Ault suggests that absorption by a charge-transfer complex is responsible for the reactivity of chlorine-acetylene pairs.[16] In any case, the experimental results provide firm support for photochemistry on a triplet surface accessed via xenon-assisted intersystem crossing.

Branching Ratios and Energy Storage

The ability to control chemistry on electronic hypersurfaces has important implications for photochemical energy storage. Figure 9 demonstrates the changes in photochemical branching ratio at 237 nm achieved by altering the matrix material from Kr to Xe. Less than 20% of the energy is stored by the product $HCl{\cdot}C_2HCl$, formed in 22% yield from *cis*-DCE in Kr, while the major product, *trans*-DCE, at 78% yield, stores no energy. When photolyzed in xenon, however, both dichloroethenes give a large yield of a product $Cl_2{\cdot}C_2H_2$ that stores over 40% of the photon energy, at the expense of the energetically neutral product. Thus selection of the reaction environment for its spin-orbit coupling characteristics can be a means of directing the photoproduct distribution toward more efficient energy storage.

The difference in branching ratios from the two isomers raises the interesting question of its origin. The relative yields of $HCl{\cdot}C_2HCl$ are equal within experimental error, 22% from *cis*-DCE and 26% from *trans*-DCE, while

Figure 9: Branching Ratios and Energy Storage
for the 1,2-dichloroethenes in Kr and Xe Matrices

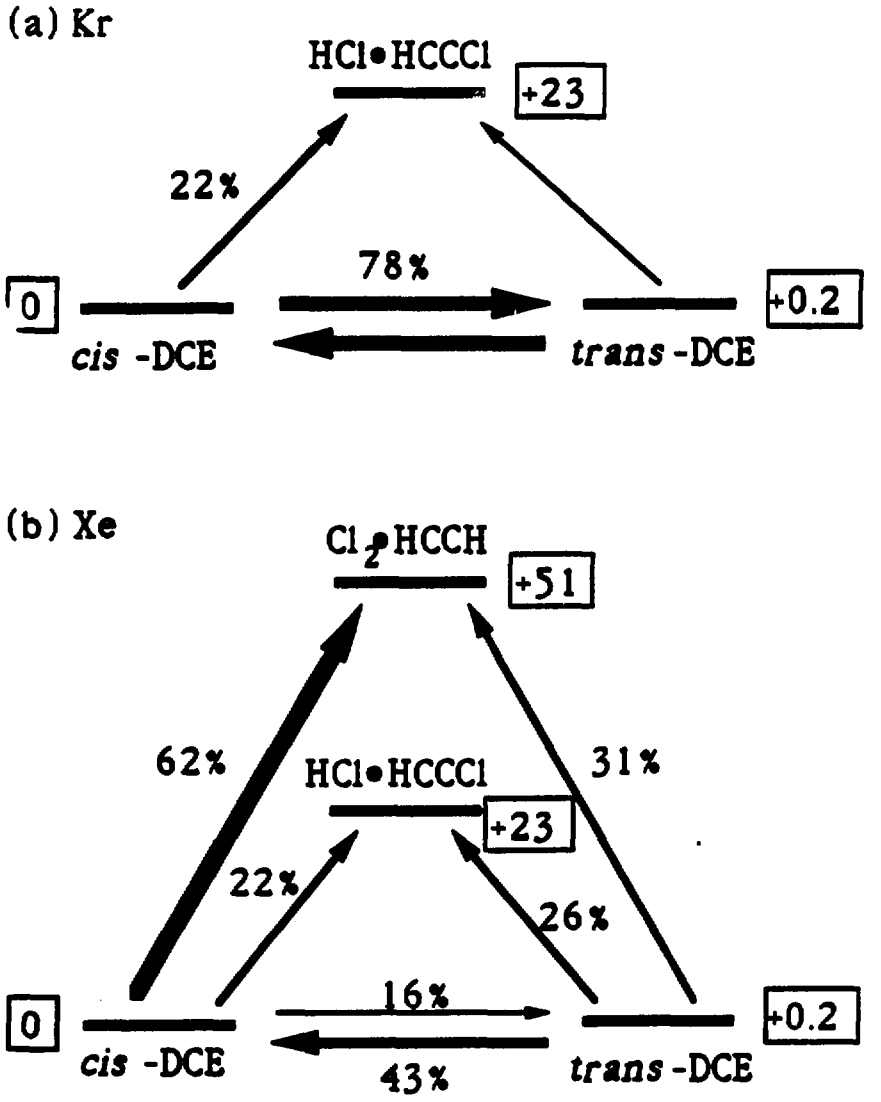

the chlorine elimination yield from the *cis* isomer, 62%, is twice that from the *trans* species. The excited (π,π^*) states are believed to be the same for both isomers, with a dihedral angle 90° from the planar ground state,[25,26] and thus should lead to the same ultimate product distribution, since the excitation wavelength is close to the origin of the excited state. The greater chlorine yield from *cis*-dichoroethene, however, hints that the excited state retains some memory of the geometry of the ground state. In I it was suggested that "proximity of the two halogen atoms may be needed to facilitate reaction with Hg (^{3}P)." Here no mercury is present, but proximity again appears important. In this case the matrix cage may well be implicated, possibly constraining free rotation about the CC axis in the excited state and thus making approach of the chlorine atoms more difficult from an initial *trans* configuration. The similarity of the chloroacetylene yields suggests that HCl•C_2HCl is produced primarily through α,α-elimination, which would be little affected by such a constraint, whereas chlorine must be α,β-eliminated from these two isomers. The results in Chapter II on 1,1-dichloroethene will provide opportunity for additional comment on this issue.

Comparison to Previous Work

We have already discussed in detail the outcome of the present study of DCE photolysis in Xe as compared to the Kr matrix studies of Cartland and Pimentel. Observation of chlorine elimination in Xe supports their conclusion that this process occurs on a triplet surface, whether accessed through selective excitation of Hg (^{3}P) and interaction of the excited mercury atom with the reactant, or through heavy-atom enhancement of intersystem crossing from the initial singlet excited-state surface.

Precedent for such matrix-induced intersystem crossing is seen in the work of Collins and Pimentel, who observed different products of the reaction of imidogen with dimethylacetylene in Ar and Xe matrices and attributed this difference to heavy-atom enhancement of the intersystem crossing rate from a singlet to a triplet surface.[27] Changes in photoproduct distribution in allene-ozone photoreactions in different matrices are similarly explained by Singmaster and Pimentel.[28] Other external heavy-atom effects reported in matrices include a progressive shortening of phosphorescence lifetimes in heavier matrices, observed by Wright, Frosch and Robinson[29,30] and, more recently, by Morgan and Pimentel,[24] and fluorescence lifetime changes from Ar to Xe in studies by Kelly and Rentzepis.[31] Heavy-atom effects on quantum yield have been observed in solution at room temperature. Cowan and Drisko found that addition of an iodine-bearing impurity to a reaction mixture enabled intersystem crossing to the triplet surface and formation of a different product,[32] and Plummer and Chihal used a heavy-atom solvent to achieve a change in photoproduct distribution in their synthetic procedure.[33]

Other workers studying the photolysis of the dichloroethenes in a matrix have reported Cl_2 elimination, as well as HCl and H_2 elimination and isomerization, upon short-wavelength ($\lambda < 200$ nm) irradiation of all three DCE isomers in Ar,[6,7] N_2, CO and Kr.[6] The present work tends to reinforce the conclusion made in I, that elimination chemistry is determined by the singlet or triplet character of the reaction surface accessed, in contrast to contrary speculations in these earlier studies.

Photofragmentation studies of mono- and dichloroethenes in a molecular beam are consistent with the present model. Umemoto *et al.* detect only hydrogen chloride and atomic chlorine as reaction products upon 193 nm excitation and conclude that molecular HCl elimination and Cl atom detachment are the only primary photofragmentation pathways under collision-free conditions.[34] However, their experimental geometry is not conducive to Cl_2 determination, thus it is not certain that this elimination does not also occur. With this caveat in mind, and with the exception of isomerization, which they believe occurs on a slower timescale, the photoprocesses they observe are the same as in solid Kr, with chemistry confined to singlet reaction surfaces only.

Work by Grabowski and Bylina presents an interesting complement to our data on DCE photochemistry in solid Xe.[35] When they measured absorption spectra of liquid 1,2-dichloroethenes under a high pressure of oxygen they found a new, weak absorption in the region 300-400 nm, which they assigned to the $T_1 \leftarrow S_0$ transition. Selective excitation in this wavelength range resulted in *cis-trans* and *trans-cis* isomerization with quantum yields near 0.5. They concluded that isomerization proceeds through a triplet state common to both isomers, consistent with the present findings of photoisomerization in xenon but not in krypton at $\lambda > 300$ nm. Similarly, *cis-trans* isomerization of 1,2-dichloroethene occurred upon SO_2 ($^3B_1$) sensitization with 371 nm excitation,[36] further evidence for triplet-state isomerization.

CONCLUSIONS

The $Cl_2 \cdot C_2H_2$ complex has been identified as a principle product of 237 nm irradiation of *cis-* and *trans*-dichloroethene in Xe matrix, along with the π-hydrogen-bonded complex $HCl \cdot C_2HCl$ and the *cis-trans* isomerization product. The appearance of the chlorine elimination product, not formed in Kr, demonstrates that in xenon chemistry is occurring through a triplet state as well as from the directly excited $^1(\pi, \pi^*)$ state. The heavy-atom environment enhances spin-orbit coupling and thus facilitates intersystem crossing from the initial singlet to a triplet surface, providing access to the otherwise spin-forbidden elimination channel. Observations of Cl_2 elimination and *cis-trans* isomerization in Xe, at photon energies below the singlet absorption threshold, show that the external heavy atom also assists direct $T_1 \leftarrow S_0$ absorption.

It is evident that spin-orbit coupling in the matrix environment has a strong influence on the photochemical reaction dynamics with respect to the ease or difficulty of singlet-triplet transitions. Thus selection of the matrix material may be used to effect changes in products and branching ratios, and to control desirable properties such as capacity for energy storage, exemplified here. The photon energy dependence of various channels provides a glimpse of surface contours and energy relationships on the electronically excited hypersurface and a hint of the importance of excited-state complexes in the photochemistry of these matrix-isolated species.

REFERENCES

[1]Berry, M. J. *J. Chem. Phys.* 1974, *61*, 3114.

[2]Bellas, M. G.; Wan, J. K. S.; Allen, W. F.; Strausz, O. P.; Gunning, H. E. *J. Phys. Chem.* 1964, *68*, 2170.

[3]Strausz, O. P.; Norstrom, R. J.; Salahub, D.; Gosavi, R. K.; Gunning, H. E.; Csizmadia, I. G. *J. Am. Chem. Soc.* 1970, *92*, 6395.

[4]Tsunashima, S.; Gunning, H. E.; Strausz, O. P. *J. Am. Chem. Soc.* 1976, *98*, 1690.

[5]Ausubel, R.; Wijnen, M. H. J. *Int. J. Chem. Kinetics* 1975, *7*, 739; *J. Photochem.* 1975, *4*, 241; *J. Photochem.* 1976, *5*, 233.

[6]Warren, J. A.; Smith, G. R.; Guillory, W. A. *J. Photochem.* 1977, *7*, 263.

[7]McDonald, S. A.; Johnson, G. L.; Keelan, B. W.; Andrews, L. *J. Am. Chem. Soc.* 1980, *102*, 2892.

[8]Cartland, H. E.; Pimentel, G. C. *J. Phys. Chem.* 1986, *90*, 1822.

[9]Cartland, H. E.; Pimentel, G. C. *J. Phys. Chem.* 1986, *90*, 5485. (I)

[10]Cartland, H. E.; Pimentel, G. C. *J. Phys. Chem.* 1989, *93*, 8021.

[11]Cartland, H. E.; Pimentel, G. C. *J. Phys. Chem.*, in press, 1989.

[12]Nyquist, R. A.; Kagel, R. O. *Infrared Spectra of Inorganic Compounds*; Academic Press: New York, 1971; p. 127.

[13]See Cheng, B.; Lee, Y. *J. Chem. Phys.* 1989, *90*, 5930, for example.

[14]Andrews, L.; Johnson, G. L.; Kelsall, B. J. *J. Phys. Chem.* 1982, *86*, 3374.

[15]Cartland, H. E. Ph.D. thesis; University of California, Berkeley, 1985.

[16]Ault, B. S. *J. Phys. Chem.* 1987, *91*, 4723.

[17]Verstegen, J. M. P. J.; Goldring, H.; Kimel, S.; Katz, B. *J. Chem. Phys.* 1966, *44*, 3216.

[18]Keyser, L. F.; Robinson, G. W. *J. Chem. Phys.* 1966, *44*, 3225.

[19]Koerting, C. F.; Walzl, K. N.; Kuppermann, A. *Chem. Phys. Lett.* 1984, *109*, 140.

[20]Evans, K.; Scheps, R. S.; Rice, S. A.; Heller, D. *J. Chem. Soc., Faraday Trans. II* 1973, 69(6), 856.

[21]Lischka, H.; Karpfen, A. *Chem. Phys.* 1986, *102*, 77.

[22]Schnepp, O. *J. Phys. Chem. Solids* 1961, *17*, 188.

[23]Jacox, M. E. *J. Mol. Struct.* 1987, *157*, 43.

[24]Morgan, M. A.; Pimentel, G. C. *J. Phys. Chem.* 1989, *93*, 3056.

[25]Herzberg, G. *Molecular Spectra and Molecular Structure*, vol. III; Van Nostrand: Princeton, 1966; p. 540.

[26]Kato, H.; Hirao, K.; Konishi, H.; Yonezawa, T. *Bull. Chem. Soc. Japan* 1971, *44*, 2062.

[27]Collins, S. T.; Pimentel, G. C. *J. Phys. Chem.* 1984, *88*, 4258.

[28]Singmaster, K. A.; Pimentel, G. C. *J. Mol. Struct.* **1989**, *194*, 215.

[29]Wright, M. R.; Frosch, R. P.; Robinson, G. W. *J. Chem. Phys.* **1960**, *33*, 934.

[30]Robinson, G. W. *J. Mol. Spectrosc.* **1961**, *6*, 58.

[31]Kelly, D. F.; Rentzepis, P. M. *J. Am. Chem. Soc.* **1983**, *105*, 1820.

[32]Cowan, D. O.; Drisko, R. L. *J. Am. Chem. Soc.* **1967**, *89*, 3068.

[33]Plummer, B. F.; Chihal, D. M. *J. Am. Chem. Soc.* **1971**, *93*, 2071; *J. Am. Chem. Soc.* **1972**, *94*, 6248.

[34]Umemoto, M.; Seki, K.; Shinohara, H.; Nagashima, U.; Nishi, N.; Kinoshita, M.; Shimada, R. *J. Chem. Phys.* **1985**, *83*, 1657.

[35]Grabowski, Z. R.; Bylina, A. *Trans. Faraday Soc.* **1964**, *60*, 1131.

[36]Wampler, F. B.; Böttenheim, J. W. *Int. J. Chem. Kinet.* **1976**, *8*, 585.

Chapter II

Xenon Matrix Photochemistry of 1,1-dichloroethene

INTRODUCTION

Reasons for the selection of haloethenes in general, and the dichloroethenes in particular, for investigation of photochemical dynamics in a matrix have already been detailed in Chapter I and elsewhere.[1,2,3,4] In particular, Cartland and Pimentel showed that all three DCE isomers exhibit different photochemistry depending on the multiplicity of the reaction surface excited, the singlet via direct excitation or the triplet surface via Hg (^3P) sensitization.[2] Prior studies in both gas and matrix phases, available information on the excited states of reactants and products, and ease of assignment of IR spectra of these species also contribute to the overall suitability of these molecules for the present studies. To further probe this surface dependence without the complicating factor of metal atom photoreaction, the xenon matrix studies were initiated. The 1,2-dichloroethenes were examined first, as their chemistry was found to be simpler, apparently due to the minimal involvement of free radical processes,[2] and these were found to demonstrate dramatically the effect of a heavy-atom matrix on the photoproduct distribution.[4]

Our interpretation of this effect as matrix-induced intersystem crossing is most easily confirmed through study of the third member of the family, 1,1-dichloroethene. The *cis* and *trans* isomers are expected to, and do, exhibit similar photochemistry because they lie in proximity along a simple reaction coordinate, rotation about the C=C bond. The geometry of 1,1-dichloroethene places it on a quite distinct portion of the ground state surface, yet it shares with the 1,2 isomers many of the same, well-characterized, possible intermediate excited states and products. This provides an opportunity to

generalize and further characterize the matrix heavy-atom effect without a simultaneous drastic change of absorption curves, reaction rates, and other factors—to survey familiar territory from a different benchmark. Certainly, too, the 1,1-DCE isomer provides an additional point of interest, for in this isomer both elimination processes of interest are geometrically limited, HCl to the α,β route and Cl_2 to the α,α route, whereas in the 1,2 isomers only chlorine elimination geometry is defined by the precursor structure.

Thus both a desire for completeness and hopes of further elucidating the photochemical reaction pathways of these molecules motivate examination of the photochemistry of 1,1-dichloroethene in Xe matrix, with comparison to the results in solid Kr. In addition to xenon-induced photoproduct changes similar to those previously observed, a novel photoproduct is observed and is characterized by isotopic substitution and wavelength-dependence studies. Possible photochemical pathways for production of this new product are evaluated and their implications discussed.

EXPERIMENTAL SECTION

The experimental apparatus and procedures were identical to those described in the previous chapter. In one experiment, broadband infrared photolysis ($\nu < 5500$ cm^{-1}) was performed using the spectrometer globar source, filtered through a 5-mm germanium plate to remove any residual visible radiation. All laser photolysis studies were performed on the IR97 instrument, and Hg-Xe lamp and IR photolysis experiments were done on the IR44.

1,1-dichloroethene (1,1-DCE) was obtained from Aldrich (99%) and purified and stored as for the 1,2-dichloroethenes. The 2,2-dideuterated material was prepared according to the method of Liebler and Guengerich.[5] Briefly, dichloroacetyl chloride and lithium aluminum deuteride were reacted to make 2,2-dichloro-1,1-dideuteroethanol.[6] The ethanol was converted to a tosylate with p-toluene-sulfonyl chloride,[7] then this was dehydrated with DBU (diazabicyclo[5.4.0]undec-7-ene) to give the d_2-1,1-DCE. Product purity was verified by infrared and mass spectral analysis, and the product was stored at -20° C.

RESULTS

Matrix Infrared Spectra

The infrared spectrum of 1,1-dichloroethene in krypton matrix has been previously reported[2] and was reproduced in this study. The spectrum of 1,1-DCE isolated in xenon was similar to the gas phase[8] and krypton-matrix spectra, with the added complications of a matrix shift of a few cm^{-1} and the more extensive site splitting common in Xe. The dideuterated species, d_2-1,1-DCE, was studied only in Xe, and its spectrum was assigned by comparison with the gas phase frequencies.[8] Absorption frequencies and intensities for both dihydro- and dideutero-1,1-DCE in xenon matrix are reported for the first time in Table 1, and their spectra can be seen as the negative features in the difference spectra in Figures 2a-b and 7.

Matrix UV Spectra

As reported in Chapter I, transmittance spectra were recorded for samples of 1,1-DCE in Kr and Xe, and corrected absorption curves are shown in Figure 1 in that chapter. Like 1,2-DCE, 1,1-DCE exhibits a structureless, broad absorption beginning around 230 nm, which is red-shifted a few nanometers in Xe relative to Kr.

Photolysis in Kr matrix

Laser photolysis at 239 nm (1.5 mWh) of 1,1-dichloroethene (1,1-DCE) 1:100 in 0.43 mmol Kr produces a number of new absorptions in the infrared spectrum, as seen in Figure 1. These, including some more readily visible upon scale expansion, are listed in Table 2 and can be readily assigned and identified with reference to previous work on this system.[2] Essentially no further growth of these features occurred after 1.5 mWh photolysis. Both

Table 1: Xenon Matrix Spectrum of 1,1-dichloroethene

1,1-DCE/Xe 1:100 ν, cm^{-1}	d_2-1,1-DCE/Xe 1:100 ν, cm^{-1}	Assignment
3121.4 a,b	2353.1 a,b	ν_7, CH_2/CD_2 as. str.
	2247.2 (.009)	
	2239.7 (.016)	
	2237.3 (.022)	ν_1, CD_2 sym. str.
1614.8 sh[b]	1560.1 (.110)	ν_2, CC str.
1612.4 (.139)		
1557.6 (.009)		
1554.4 (.021)		?
1551.7 (.010)		
	1391.7 (.013)	?
	1275.6 (.013)	?
	1265.0 (.006)	
1087.0 (.138)	979.5 (.437)	ν_8, CH_2/CD_2 rock
1085.0 (.120)	978.0 (.331)	
1076.8 (.055)	990.6 (.136)	Fermi resonance?
1075.2 (.093)	986.6 (.171)	
1071.7 (.035)	983.9 (.147)	
866.5 (.285)	693.8 (.191)	ν_{11}, CH_2/CD_2 wag
785.6 (.244)[c]	695.6 (.440)[c]	ν_9, CCl_2 as. str.
784.0 (.152)	692 (.048)	
782.0 (.037)		
745.4 b		$\nu_5 + \nu_{12}$
601.9 (.015)[c]	580.7 (.061)[c]	ν_4, CCl_2 sym. str.
599.5 (.032)	578.7 (.033)	
596.0 (.020)	576.8 (.046)	
	439.3 (.057)	ν_{12}, CCl_2 wag

[a]Absorbances in parentheses refer to peak heights; h_2- and d_2-DCE intensities not normalized to each other. sh=shoulder

[b]weak

[c]Splitting due to $^{35/37}Cl$ isotopes.

Table 2: Products of 239 nm Photolysis of 1,1-DCE/Kr

1,1-DCE/Kr 1:100 (1.5 mWh) ν, cm^{-1}	Assignment		
3314.6 (.005)[a]			
3310.2 (.010)			
3308.7 (.014)	C	ν_1	$HCl \cdot C_2HCl$ (π)
2778.3 (.013)	C	ν_s[b]	$HCl \cdot C_2HCl$ (π)
2776.4 sh			
2772.5 (.006)			
2768.4 (.006)			
2099.6 (.008)	C	ν_2	$HCl \cdot C_2HCl$ (π)
2098.7 (.003)			
1590.9 (.004)	B	ν_2	*cis*-DCE
1298.5 (.002)	B	ν_9	*cis*-DCE
905.7 (.003)	A	ν_6	*trans*-DCE
850.8 (.003)[c]	B	ν_{10}	*cis*-DCE
849.1 (.003)			
823.1 (.006)[c]	A	ν_{11}	*trans*-DCE
819.7 d			
699.6 (.007)			
696.7 (.010)	B	ν_{12}	*cis*-DCE
615.2 (.008)			
601.8 (.012)	C	ν_4	$HCl \cdot C_2HCl$ (π)

[a]Absorbances in parentheses refer to peak heights; sh=shoulder.

[b]Stretching frequency for HCl submolecule.

[c]Splitting due to $^{35/37}Cl$ isotopes.

[d]weak

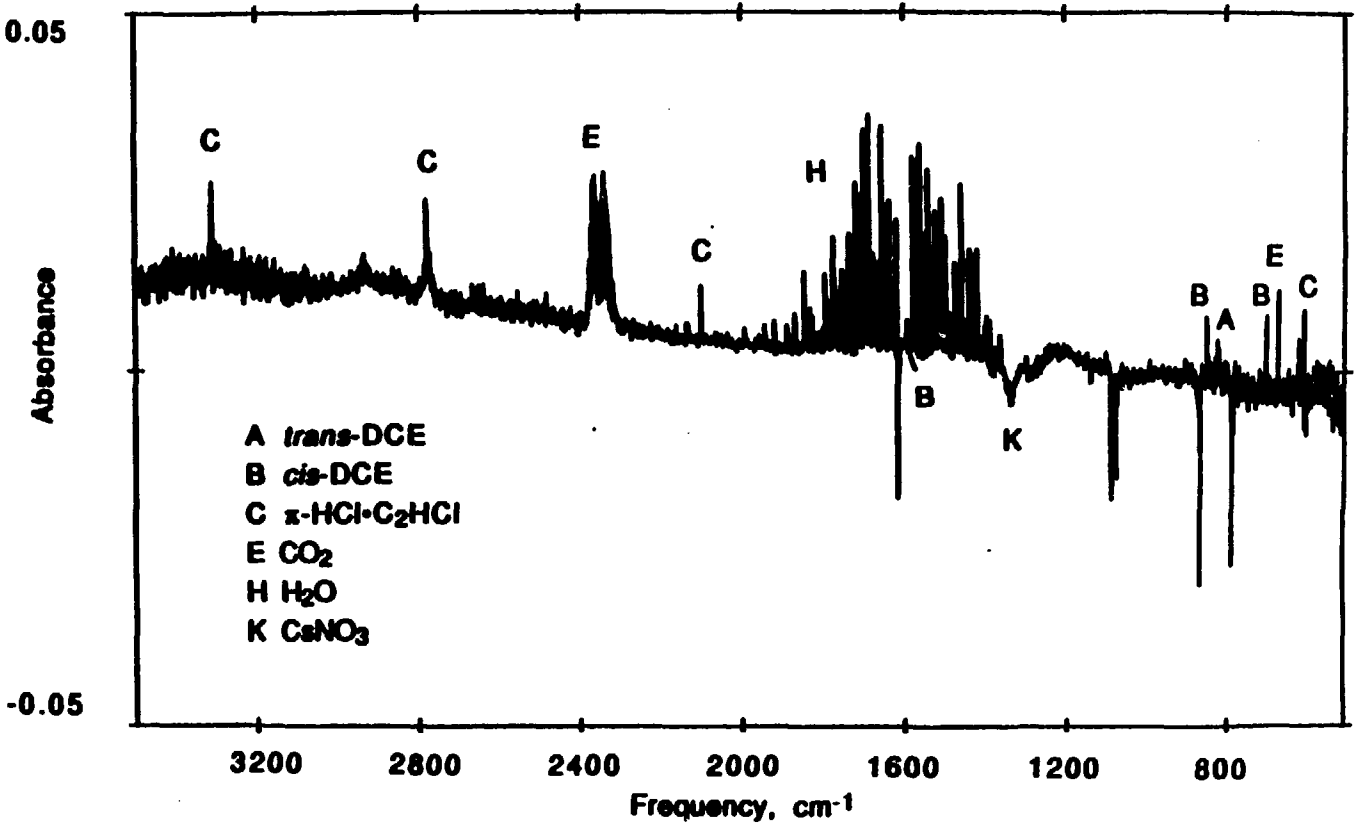

Figure 1: Difference Spectrum of 1,1-DCE/Kr 1:100 at 12 K, after 1.5 mWh laser photolysis at λ = 239 nm

isomerization products *cis*- and *trans*-1,2-dichloroethene are observed, as is the T-shaped complex resulting from hydrogen chloride elimination, $HCl{\cdot}C_2HCl$, while no evidence of the chlorine elimination product, $Cl_2{\cdot}C_2H_2$, is seen. The laser-induced photoproducts are identical with the reaction products observed by Cartland and Pimentel upon broadband ($\lambda > 200$ nm) irradiation with a high-pressure Hg-Xe arc lamp,[2] and, as in that experiment, $HCl{\cdot}C_2HCl$ is the predominant product.

Photolysis in Xe matrix

Upon 239 nm photolysis of an 0.56 mmol 1,1-DCE/Xe matrix with M/R = 100, the photoproduct spectrum presented in Figures 2a and 2b develops. Table 3 displays the frequencies and intensities for these absorptions, a number of which are again readily assigned to photoproducts *cis*-DCE, *trans*-DCE, and $HCl{\cdot}C_2HCl$. In addition, a strong new doublet at 728.5/736.8 cm^{-1} and an additional doublet at 3264.0/3277.8 cm^{-1} are present in the spectrum and identifiable as $Cl_2{\cdot}C_2H_2$ by comparison to the analogous *cis*- and *trans*-DCE experiments. Product growth curves, shown in Figure 3, indicate that all four products are primary photoproducts. In particular, the characteristic ν_5 doublet of the acetylene complex is distinguishable at very short photolysis times, demonstrating that $Cl_2{\cdot}C_2H_2$ is not formed solely via secondary photolysis of *cis*- or *trans*-DCE.

As seen in Figure 4, broadband ($\lambda > 200$ nm) irradiation of 0.50 mmol 1,1-DCE in Xe results in strong absorptions corresponding to both isomerization products and the HCl elimination product. Sometimes a weak absorption at 729 cm^{-1} was also distinguishable, suggesting the presence of a small quantity of $Cl_2{\cdot}C_2H_2$. In addition to these previously identified products, a sharp new band at 3212.1 cm^{-1} was observed in all broadband photolysis

Table 3: Products of 239 nm and Broadband Photolysis of 1,1-DCE/Xe

1,1-DCE/Xe 1:100 (3.8 mWh) ν, cm^{-1}	d_2-1,1-DCE/Xe 1:100 (2.4 mWh) ν, cm^{-1}	Assignment		
	2599.9 (.005)[a]			
3313.6 (.016)[a]	2596.4 (.008)			
3310.9 (.014)	2594.0 (.008)			
3308.7 (.024)	2590.1 (.034)	C	ν_1	$HCl{\cdot}C_2HCl$ (π)
3277.8 (.003)[b,c]				
3264.0 (.013)	2424.4 (.005)[b]	D	ν_3	$Cl_2{\cdot}C_2H_2$
	2284 (.002)	A	ν_9	*trans*-DCE
3084 d	2276.7 (.003)	B	ν_8	*cis*-DCE
2772.1 (.019)	2009.7 (.013)	C	ν_8[e]	$HCl{\cdot}C_2HCl$ (π)
	2006.9 (.009)			
2106.3 (.004)				
2103.1 (.005)				
2098.4 (.003)	1964.4 (.010)	C	ν_2	$HCl{\cdot}C_2HCl$
1588.7 (.007)	1576[f]	B	ν_2	*cis*-DCE
1297.5 (.004)	1042.2 (.017)	B	ν_9	*cis*-DCE
1196.5 (.011)	910.7 (.012)	A	ν_{10}	*trans*-DCE
904.8 (.005)				
900.9 (.008)	665.2 (.007)	A	ν_6	*trans*-DCE
898.5 (.005)				
895.4 (.004)				
850.0 (.019)[g]	762.9 (.011)[g]	B	ν_{10}	*cis*-DCE
848.0 (.013)	761.3 (.008)			
846.1 (.004)	759.8 d			
818.9 (.024)[g]	786.1 (.008)[g]	A	ν_{11}	*trans*-DCE
815.7 (.016)	783.4 (.004)			
813.4 (.005)	781.0 (.002)			
756.1 (.006)	740.5 (.004)	B	ν_3	*cis*-DCE
736.8 (.019)[b,h]	543.3 (.010)[b,h]	D	ν_5	$Cl_2{\cdot}C_2H_2$
728.5 (.024)	537.4 (.012)			
714.1 (.004)[g]	703[f]	B	ν_4	*cis*-DCE
710.8 d				

697.2 (.028)		540.9 (.016)		B	ν_{12}	*cis*-DCE
615.0 (.016)[h] 601[f]		475 (.012)[h] 466 (.012)		C	ν_4	HCl•C_2HCl
3212.1	i	2541.6	i	F	ν_1	HCl•C_2HCl (σ)
2742	i	1990.0	i	F	ν_5[e]	HCl•C_2HCl (σ)

[a]Absorbances in parentheses refer to peak heights after 239 nm photolysis.

[b]Peak height given is for 239 nm photolysis; weak or absent after broadband photolysis.

[c]Splitting due to Fermi resonance with combination band $\nu_2 + \nu_4 + \nu_5$.

[d]weak

[e]Stretching frequency for HCl submolecule.

[f]band obscured by parent absorption; frequency predicted from isotope shift.

[g]Splitting due to $^{35/37}$Cl isotopes.

[h]Splitting of degenerate bend due to presence of cage partner.

[i]Observed only upon broadband ($\lambda > 200$ nm) photolysis; intensity relative to equivalent band of π complex varies (see text).

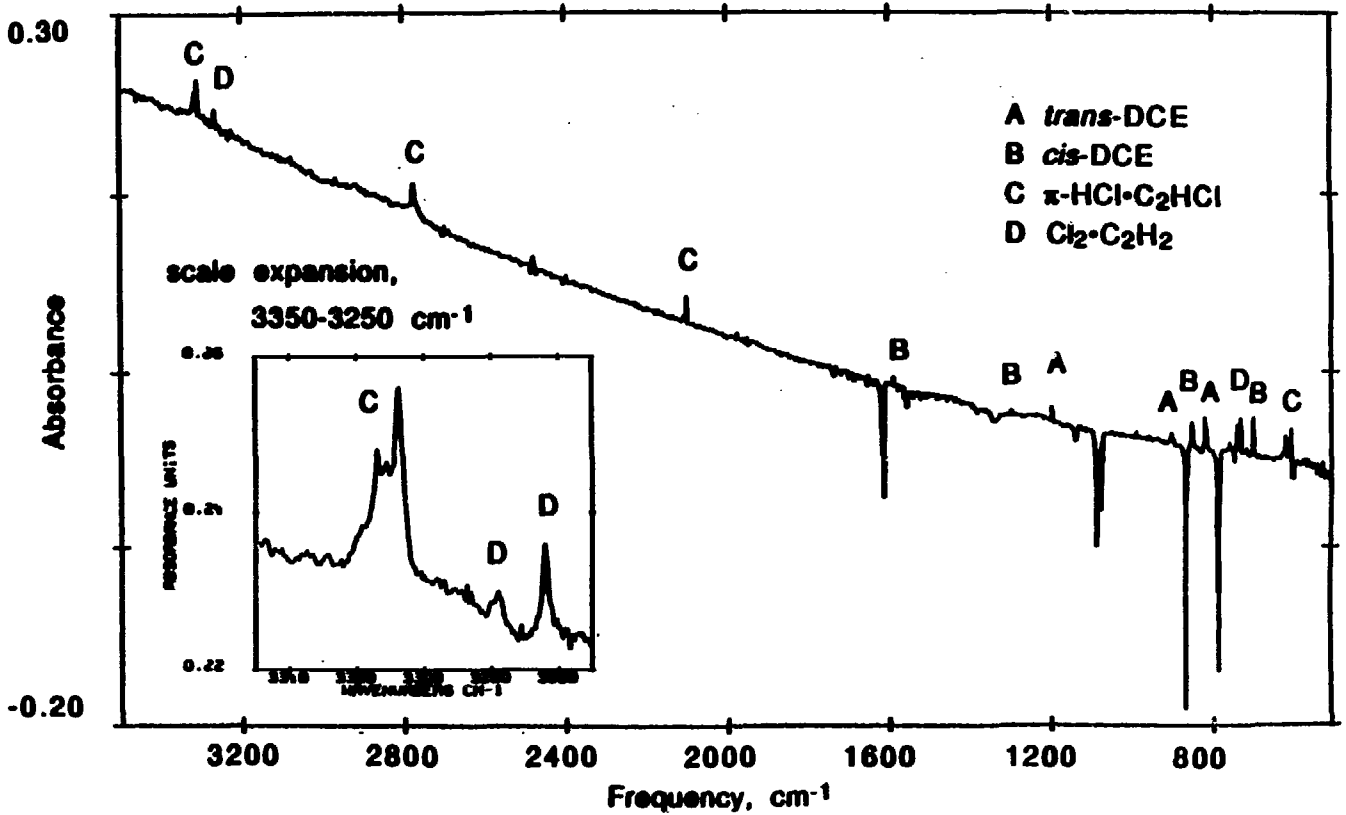

Figure 2a: Difference Spectrum of 1,1-DCE/Xe 1:100 at 12 K, after 3.8 mWh laser photolysis at λ = 239 nm

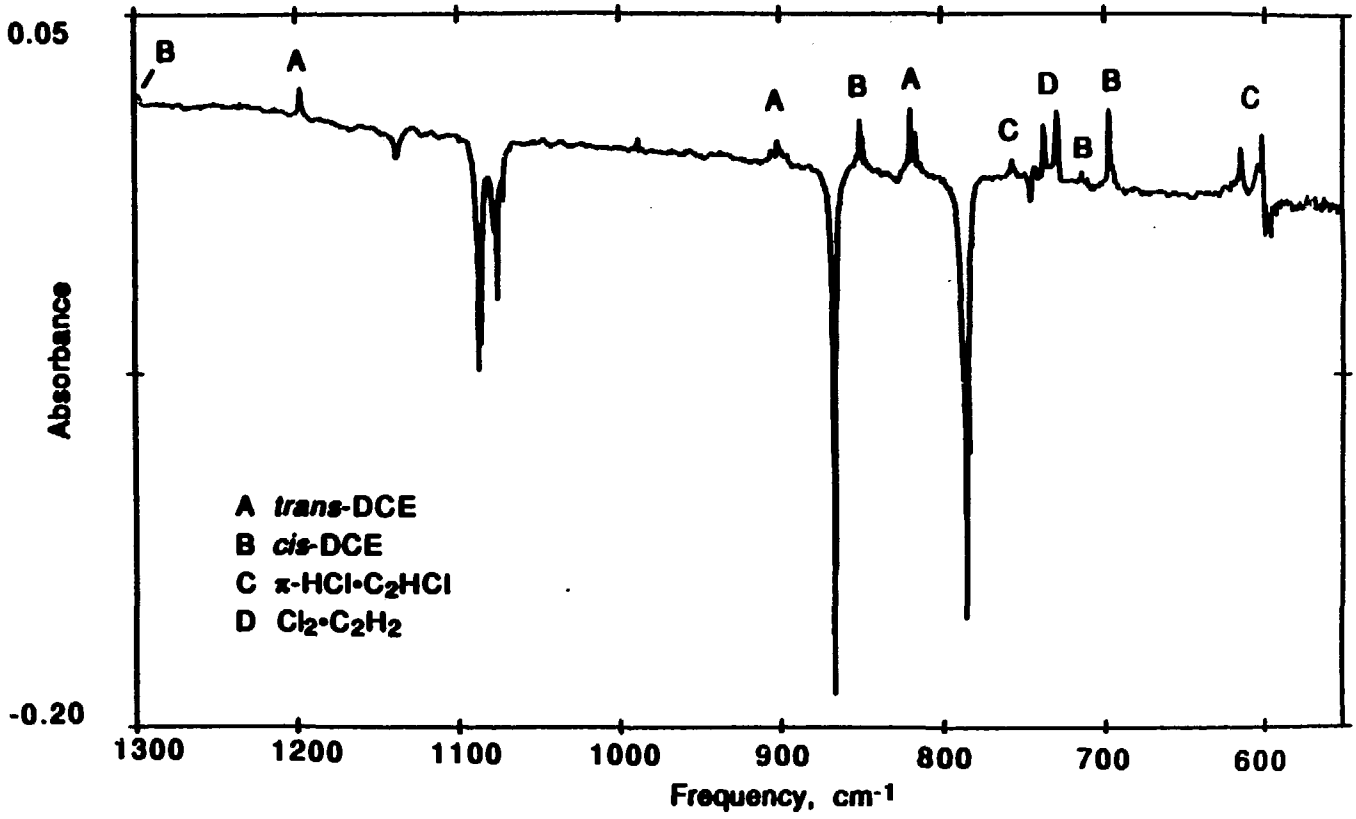

Figure 2b: Low-Frequency Region from Difference Spectrum 2a; 1,1-DCE/Xe 1:100 at 12 K, after 3.8 mWh laser photolysis at λ = 239 nm

Figure 3: 1,1-DCE/Xe Photoproduct Growth at λ = 239 nm

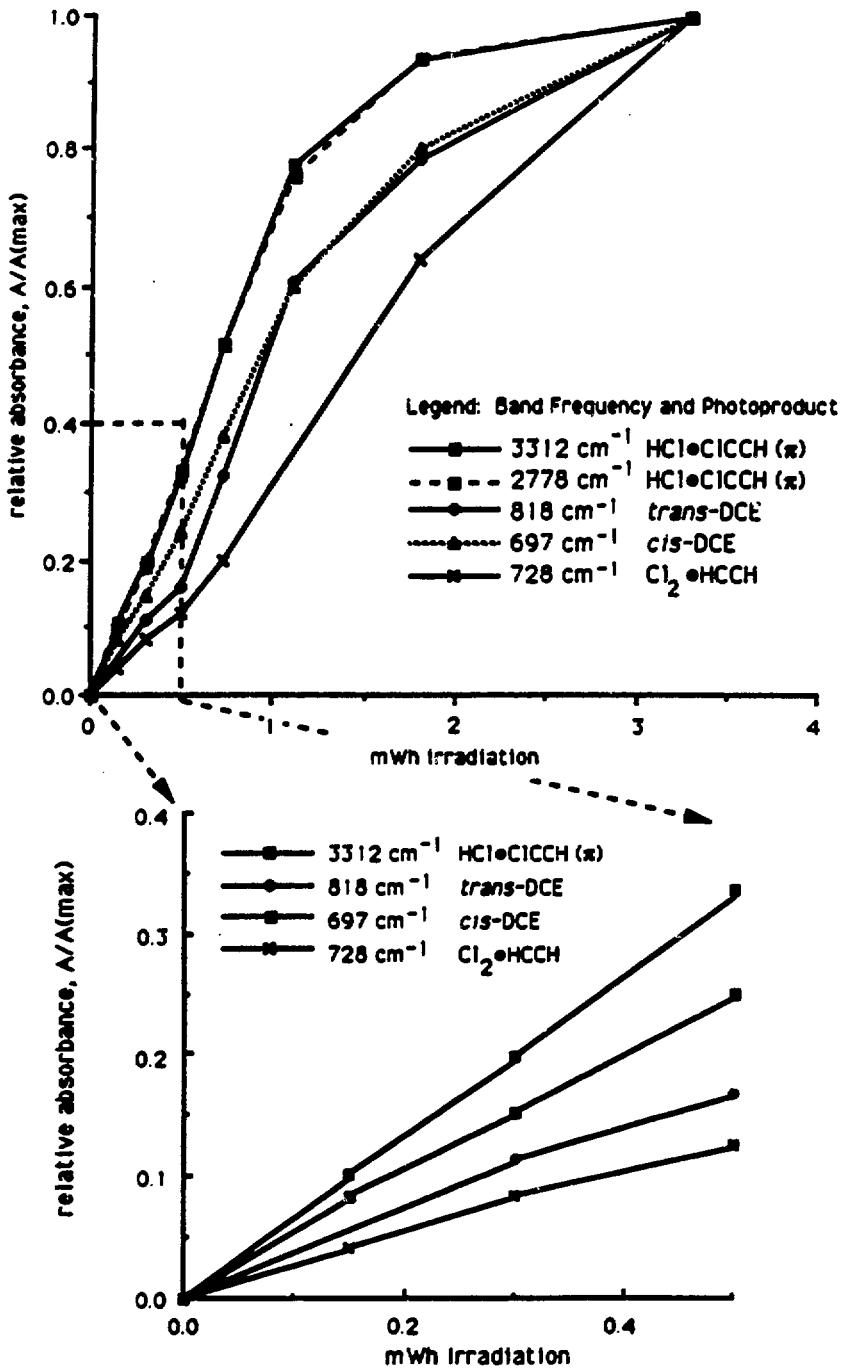

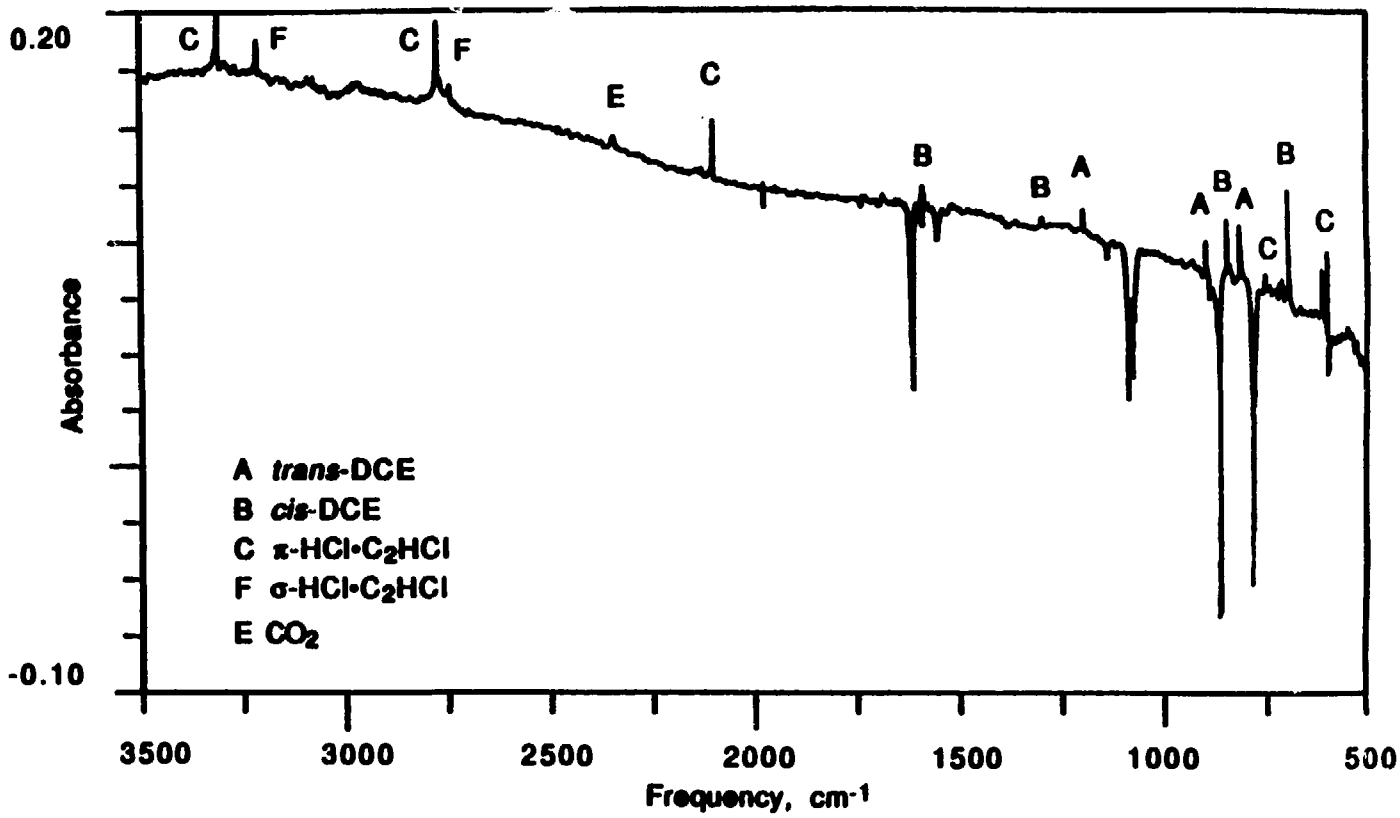

Figure 4: Difference Spectrum of 1,1-DCE/Xe 1:100 at 12 K, after 1.0 h Hg-Xe lamp photolysis at $\lambda > 200$ nm

experiments and, weakly, in one laser photolysis experiment. The relative intensity of this band varied significantly from experiment to experiment, but in some cases was as high as 70% of the intensity of the strong ν_1 band of $HCl \cdot C_2HCl$ nearby at 3308 cm^{-1}. The behavior over time of this feature was like that of the other products, smoothly approaching an asymptotic limit with no evidence of an induction period, as seen in Figure 5. A slight frequency shift of this product band, but no decrease in intensity o. other change, was observed after annealing to 45 K a 1,1-DCE/Xe matrix which had been previously irradiated at $\lambda > 200$ nm. A maximum at 2742 cm^{-1}, superimposed on the sloping baseline of the stronger absorption at 2772 cm^{-1}, had the same wavelength-dependent behavior as the 3212 cm^{-1} feature, but its intensity relative to that of the higher-frequency feature did not appear to be constant.

Photolysis through the 12 K CsI window ($\lambda > 218$ nm, determined from UV spectrum) gave the same three known products, *cis*- and *trans*-DCE and $HCl \cdot C_2HCl$, along with bands at 3212.5 and 2742 cm^{-1}, while continuing irradiation through a Corning 7-54 filter ($400 > \lambda > 224$ nm) produced mostly $HCl \cdot C_2HCl$ and *trans*-DCE. Direct initial photolysis with the 7-54 filter, however, gave all four products. The photoproduct spectrum of a more dilute 1:500 matrix showed no spectral differences from the more concentrated sample, except a narrowing of product features and diminishing of some features due to multimers.

Pyrex-filtered irradiation ($\lambda > 300$ nm) of 1,1-DCE/Xe 1:100 for 3.5 h induced no spectral changes due to unimolecular photochemistry of 1,1-DCE. In one case, however, $\lambda > 300$ nm photolysis gave a weak absorption at 1100.6 cm^{-1} that was depleted upon subsequent irradiation through a 254 nm

Figure 5: 1,1-DCE/Xe Photoproduct Growth at $\lambda > 200$ nm

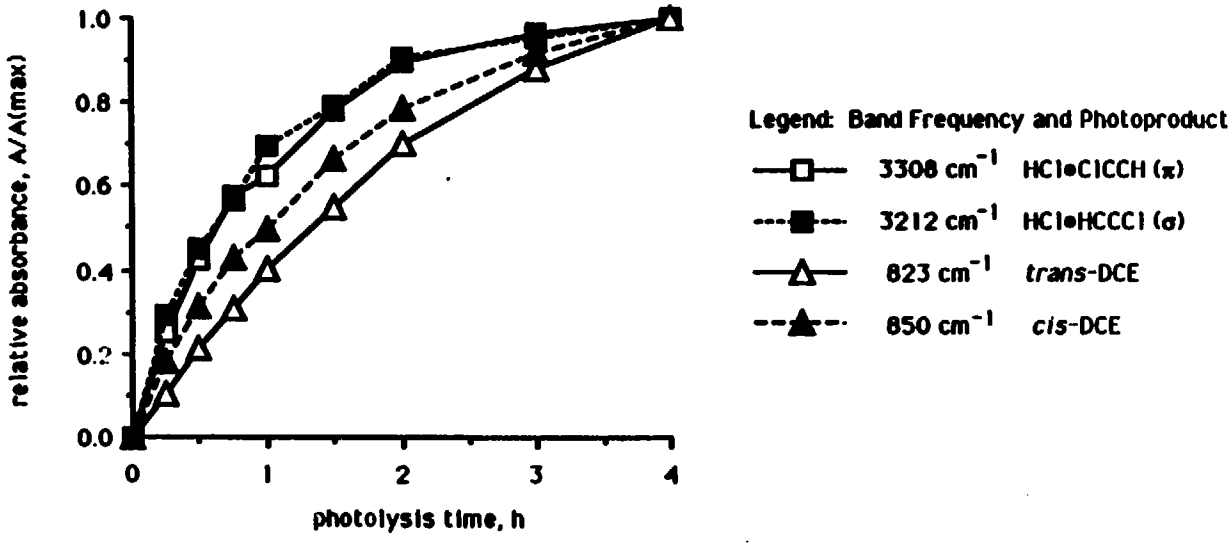

interference filter (247 < λ < 258 nm) as a doublet at 1234.4/1231.9 cm^{-1} grew in. The proximity of these features to the strongest absorptions of OClO (1105 cm^{-1} in solid N_2)[9] and HOCl (1239 cm^{-1} in solid Ar)[10] suggests both some production of Cl atoms and the presence of a minor air leak, source of O_2 and/or H_2O.

In one case, as mentioned above, prolonged laser photolysis (11.6 mWh) at 239 nm did produce a small but definite absorption (.0031, 12% of 3308 band) at 3211.8 cm^{-1}, which exhibited essentially identical growth behavior to the other photoproduct absorptions (*cis*-DCE, *trans*-DCE, $HCl{\cdot}C_2HCl$, $Cl_2{\cdot}C_2H_2$). The sample containing the laser-produced photoproducts was then irradiated with the broadband source for five minutes, resulting in a dramatic decrease in the intensity of the ν_5 and ν_3 bands of the chlorine-acetylene complex, while all other product absorptions, including the unidentified 3212 cm^{-1} feature, continue to increase, and the parent 1,1-DCE absorptions continued to disappear. These kinetic data are plotted in Figure 6 and clearly demonstrate the different behavior of the $Cl_2{\cdot}C_2H_2$ bands from those of the other products.

One experiment was performed to investigate the effect of infrared irradiation on the unknown photoproduct. A sample of 1,1-DCE/Xe 1:100 was photolyzed for 1.5 h at λ > 200 nm to produce the usual array of photoproducts. The sample was then exposed to the Ge-filtered globar source of the spectrometer (ν < 5500 cm^{-1}) for 12 h. Neither depletion of the 3212 and 2742 cm^{-1} bands nor growth of other existing or new bands was detected.

An 0.53 mmol sample containing d_2-1,1-dichloroethene 1:100 in Xe was irradiated with the laser at 239 nm and developed the product spectrum

Figure 6: Growth Kinetics of Photoproducts of 1,1-DCE/Xe
With 239 nm Photolysis and Subsequent λ > 200 nm Photolysis

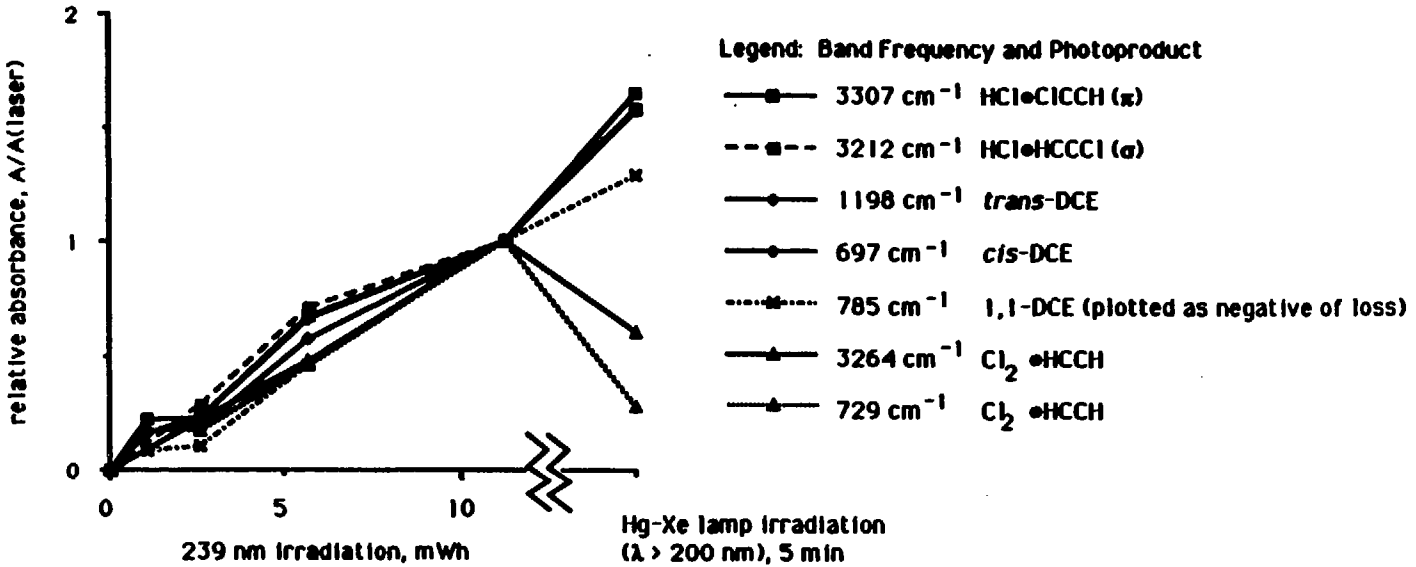

shown in Figure 7. Photolysis with the high pressure Hg-Xe lamp or a medium pressure Hg source produced a similar difference spectrum, lacking the 537 and 2424 cm^{-1} absorptions of the laser experiment, but containing an additional, sharp band at 2541.7 cm^{-1} and another at 1990.0 cm^{-1}, as seen in Figure 8 (0.45 mmol sample). Photoproduct absorptions for both 239 nm and broadband photolyses are included in Table 3. For one preirradiated sample of d_2-1,1-DCE/Xe, the temperature dependence of the photoproduct spectrum was studied, with spectra collected at ten-degree intervals from 30 to 60 K after photolysis at 12 K. The temperature dependence of selected bands is plotted in Figure 9.

Other Molecules

Unfiltered arc lamp irradiation of a sample of trichloroethene (TCE)/Xe 1:100 resulted in rapid growth of product absorptions at 2794.9, 2229.4, and a triplet at 987.5/984.5/980.9 cm^{-1} with relative intensities of 8:4:1. These absorptions are in good agreement with TCE photoproducts observed by Cartland in Kr matrix[3,11] and identified as the HCl stretch, ν_2 (CC stretch, activated by complexation with HCl), and ν_3 (CCl stretch, with isotope splitting) of the HCl elimination product, $HCl{\cdot}C_2Cl_2$. Photolysis through Corning glass filter 7-54 gave much slower growth of the same features. Neither 1.5 h irradiation through a Pyrex filter ($\lambda > 300$ nm) nor 4.0 h through a 290 nm interference filter (bandpass 260-335 nm) caused any spectral changes.

Hg-Xe arc lamp irradiation of 2-chloro-1,1-difluoroethene (CDFE)/Xe 1:100 through a 254 nm interference filter (bandpass 247-258 nm) for 3 hours caused no photoproduct growth. Unfiltered photolysis induced features at 1906.5, 1252.0, 1935, 1230, and 766 cm^{-1}. These were assigned to F_2CO by

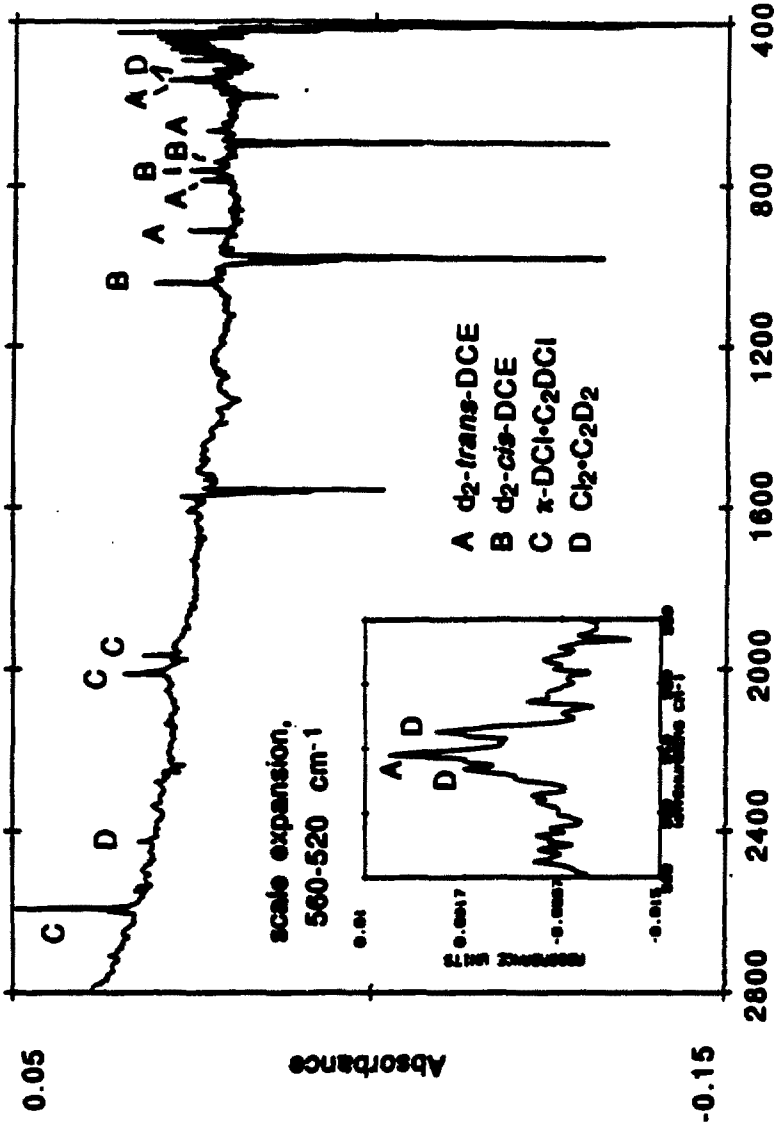

Figure 7: Difference Spectrum of d_2-1,1-DCE/Xe 1:100 at 12 K, after 2.4 mWh laser photolysis at λ = 239 nm

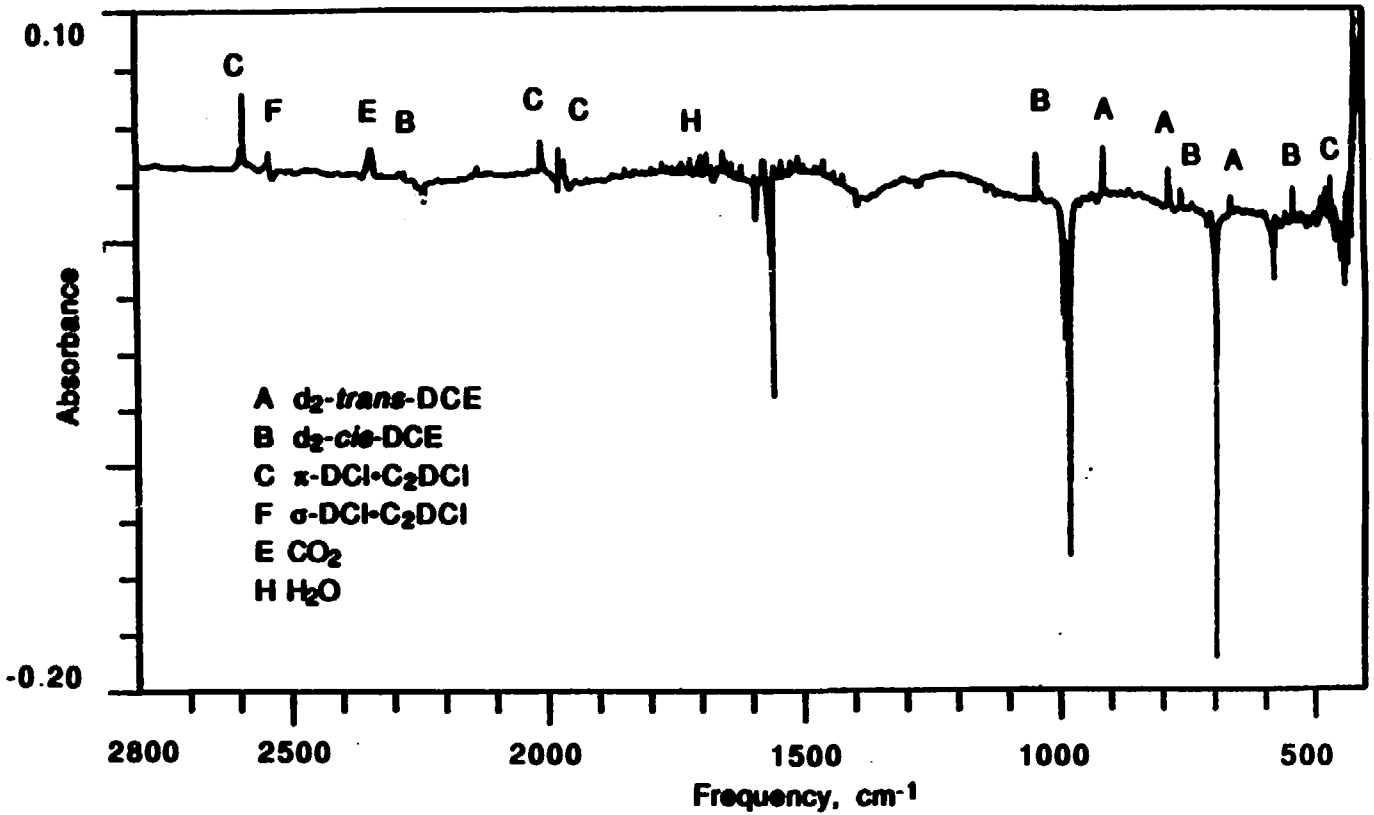

Figure 8: Difference Spectrum of d_2-1,1-DCE/Xe 1:100 at 12 K, after 1.0 h Hg-Xe lamp photolysis at $\lambda > 200$ nm

Figure 9: Temperature Dependence
of 1,1-d_2-DCE/Xe Photoproduct Bands

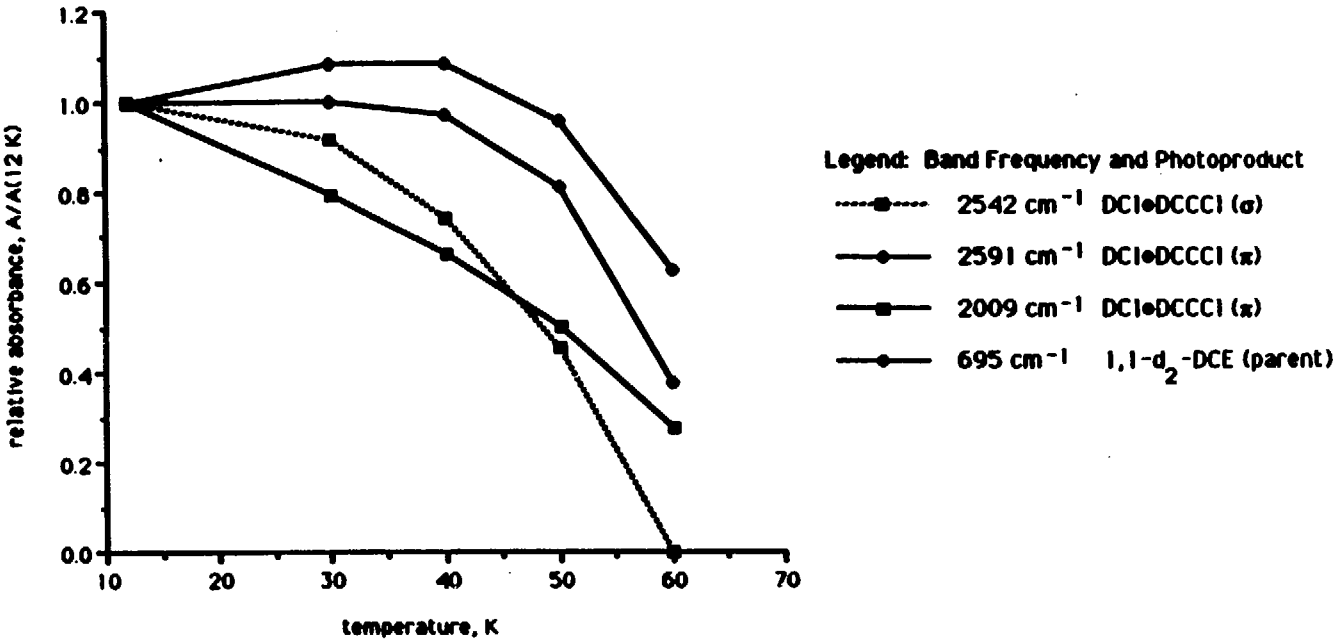

comparison with the Ar-matrix spectrum of that molecule[12,13] and thus indicate the presence of an air leak.

Branching Ratios

In order to estimate branching ratios for the laser photolysis experiments, relative absorption coefficients were calculated as in Chapter I. For a matrix containing 0.43 mmol of 1,1-DCE/Kr 1:106, the integrated absorbance of the ν_2 feature at 1613.8 cm^{-1} was found to equal 0.593 cm^{-1}. This gives an effective absorption coefficient of 145 cm^{-1}/mmol, in rather poor agreement with Cartland's Kr-matrix value of 64 cm^{-1}/mmol. The same feature, at 1612.4 cm^{-1}, in a 1:105 sample of 1,1-DCE/Xe (0.56 mmol deposited) had an integrated absorbance of 0.441 cm^{-1}, for a coefficient of 83 cm^{-1}/mmol, still some 30% larger than Cartland's value in Kr and quite different from the new Kr coefficient. Although some variation in extinction coefficient with matrix gas may be expected, this is a larger deviation than the 15-20% observed for *cis*- and *trans*-dichloroethenes. Due to the possibility of spectral interference from H_2O in the 1600 cm^{-1} region, the ν_{11} parent feature near 867 cm^{-1} was also integrated in each matrix, and the ratio of those absorbances in Kr and Xe was found to agree to within 5% with the ratio of the ν_2 bands, thus indicating that water interference was not the source of the discrepancy.

After 0.42 h 239 nm photolysis (1.5 mWh) of the 1,1-DCE/Kr sample, the 1614 cm^{-1} feature was depleted by 8%, and integrated absorbances of the photoproducts were determined to be 0.0089 cm^{-1} for ν_2 of *cis*-DCE (1590.5 cm^{-1}) and 0.0119 cm^{-1} for ν_2 of the π-$HCl{\cdot}C_2HCl$ complex (2099.9 cm^{-1}). The *trans*-DCE feature for which an extinction coefficient was available, ν_{10} at 1197.6 cm^{-1}, was not strong enough in this spectrum to be measured,

although ν_6 and ν_{11} absorptions indicate that *trans*-DCE was present. Using the extinction coefficients for *cis*-DCE and the HCl product in Kr from Chapter I, 94 cm^{-1}/mmol and 128 cm^{-1}/mmol, yields are obtained of 30% *cis*-DCE and 29% $HCl \cdot C_2HCl$. From the noise level, the yield of *trans*-DCE is estimated at no more than 15%. The three products thus account for ≤74% of the loss of starting material.

The 1,1-DCE/Xe matrix was depleted by 58% after 0.75 h 239 nm photolysis (3.8 mWh). Photoproduct integrated absorbances were measured: 0.0177 cm^{-1} for ν_2 of *cis*-DCE (1588.7 cm^{-1}); 0.0270 cm^{-1} for ν_{10} of *trans*-DCE (1196.5 cm^{-1}); 0.0260 cm^{-1} for ν_2 of $HCl \cdot C_2HCl$ (2098.4 cm^{-1}); 0.341 cm^{-1} for ν_3 of $Cl_2 \cdot C_2H_2$ (3264.0 cm^{-1}). Following the same procedure and using extinction coefficients of 82 and 65 cm^{-1} for *cis*- and *trans*-DCE in Xe, and 128 and 35 cm^{-1}/mmol for the HCl and Cl_2 elimination products, respectively, yields resulted as follows: 7% *cis*-DCE, 14% *trans*-DCE, 7% $HCl \cdot C_2HCl$, 32% $Cl_2 \cdot C_2H_2$; which together account for 60% of the depleted 1,1-DCE parent.

DISCUSSION I: Spectroscopic Identification of Photoproducts

The photoproducts of 1,1-dichloroethene in krypton and xenon after 239 nm irradiation have already been identified, as their infrared spectra are quite familiar from studies of the 1,2-dichloroethenes. However, the matrix infrared spectra of the products in the deuterated experiment were unknown, and thus a more careful analysis of the d_2-1,1-DCE/Xe photoproduct spectrum was required. The spectral assignments are discussed below and the data collected in Table 3.

Photoproducts of 239 nm Photolysis of d_2-1,1-DCE

The 239 nm photoproduct spectrum of d_2-1,1-DCE/Xe can be assigned by comparison of product frequencies with gas phase spectra and published matrix spectra of expected products, bearing in mind the previously studied photoproducts of the undeuterated molecule.[2] Gas phase frequencies are available for the two dichloroethene isomers, d_2-*cis*-DCE and d_2-*trans*-DCE,[8] and isotopic shifts calculated from the gas phase absorptions predict very well the isotopic shifts for the xenon matrix spectra. Dideutero-*cis*-DCE is clearly formed, as seen by the presence of the strong ν_{12} 540.9 cm^{-1} CD bend and the triplet at 762.9/761.3/759.8 cm^{-1}, which exhibits the $^{35}Cl/^{37}Cl$ isotope splitting expected in the ν_{10} symmetric CCl stretch. The ν_8 CD stretch appears at 2276.7 cm^{-1}, while the ν_2 C=C stretch and the ν_4 asymmetric CCl stretch, predicted to fall at 1576 and 703 cm^{-1}, respectively, are obscured by overlapping bands of the parent molecule. A strong band at 1042.2 cm^{-1} is assigned to the ν_9 in-plane CD bend, although in H_2CCCl_2 this band (1297.5 cm^{-1}) is relatively much weaker. The intensity of this band in the dideutero species is enhanced through mixing with another band of the same (a_2)

symmetry moved nearer upon substitution, probably the strong ν_{10} CCl stretch. In support of this hypothesis, a weaker feature at 1033.8 cm^{-1} can be distinguished in some spectra and may be due to $^{35}Cl/^{37}Cl$ splitting (shift of 1.0081; 1.0070 predicted). The presence of d_2-*trans*-DCE can be ascertained from bands at 910.7 and 665.2 cm^{-1}, corresponding to the ν_{10} and ν_6 CD bends, and the ν_{11} CCl stretch at 786.1/783.4/781.0 cm^{-1}, showing chlorine isotope splitting and an intensity ratio of 10:5:1, close to the predicted 9:6:1. The ν_9 CD stretch is also weakly present at 2284 cm^{-1}.

The π-bonded deuterium chloride elimination product, DCl•C_2DCl, is identified by comparison of the photoproduct frequencies with the data of Andrews, *et al.* for variously substituted hydrogen-bonded HX•C_2HX complexes in argon matrix.[14] The strong ν_1 CD stretch of the chloroacetylene moiety shifts to 2590.1 cm^{-1} by a factor of 1.277, identical with the deuterium shift of the same hydrogen-bonded species in Ar. Similarly, the ν_4 CD bend, split into in-plane and out-of-plane components by the presence of the DCl partner, is observed at 475/466 cm^{-1}, shifted by a factor of 1.29 as predicted. Andrews *et al.* point out that, although the *absolute* vibrational frequencies depend on whether the submolecule is isolated or complexed, the ν^H/ν^D *ratio* is identical in both cases. Thus the ν^H/ν^D ratio of 1.068 obtained by assigning the 1964.4 cm^{-1} product band to the ν_2 C≡C stretch of the DCl•C_2DCl complex is in excellent agreement with the 1.067 ratio they obtain for uncomplexed C_2HCl. These workers do not report a value for ν_3, the CCl stretch, but the slight shift from 756.1 cm^{-1} to 740.5 cm^{-1} of this band (ν^H/ν^D = 1.02) is reasonable, given the isotopic shift of 1.01 which they report for the equivalent vibration of fluoroacetylene. Finally, assignment of the strong band at 2009.7 cm^{-1} to vibration of the hydrogen-bonded DCl submolecule, to obtain a

ν^H/ν^D ratio of 1.38, gives good agreement with the 1.39 value obtained for this species in Ar as well as with the value of 1.38 for the isolated hydrogen halide in Kr.[15] This product clearly has the same T-shaped structure observed before, with DCl hydrogen-bonded to the π bond of deuterochloroacetylene.

The deuterated version of the fourth product observed in Xe, $Cl_2 \cdot C_2D_2$, can also be identified by comparison with the Ar matrix data of Andrews and coworkers. The symmetry-broken doublet of the ν_5 CD bend of C_2D_2 is observed at 537.4/543.3 cm^{-1}, each component shifted a factor of 1.356 from its 728.5/736.8 cm^{-1} counterpart in the C_2H_2 complex, just as in the $HCl \cdot C_2H_2$ complex studied by Andrews *et al.* The two acetylene bands are distinguished from the 540.9 cm^{-1} band of d_2-*cis*-DCE by their intensity ratio of 1.25 (537.4/543.3), identical to the ratio of absorbances (728.5/736.8) in the equivalent ^1H experiment. The ν_3 CD stretch, observed as a doublet in the $Cl_2 \cdot C_2H_2$ product, is seen here as a singlet at 2424.4 cm^{-1}, the Fermi resonance removed upon isotopic substitution. This photoproduct, too, is easily identified as the same chlorine-acetylene complex seen upon 1,2-DCE photolysis in Xe.

Thus 239 nm photolysis of dideuterated 1,1-DCE isolated in Xe causes isomerization to *cis*- and *trans*-DCE, elimination of DCl to give the π-hydrogen-bonded chloroacetylene complex, and elimination of Cl_2 to form the dideuteroacetylene-chlorine complex. In other words, d_2-1,1-DCE/Xe undergoes the same primary photoprocesses as does the unsubstituted molecule at this wavelength, surely no great surprise. The excited-state reaction pathways which lead to these products will be discussed in detail in a later section.

Photoproducts of d_2-1,1-DCE/Xe at $\lambda > 200$ nm

Now that the two isomers and two elimination products have been identified in both protonated and deuterated versions, much of the photoproduct spectrum at $\lambda > 200$ nm can be assigned by inspection. Elimination of HCl to form the π-bonded complex has clearly occurred upon broadband photolysis, as has isomerization to *cis*- and *trans*-dichloroethene. The C_2D_2 doublet at 537/543 cm^{-1} is not detected, although chlorine elimination no doubt occurs, as it does in 1,1-$C_2H_2Cl_2$/Xe. As seen before, secondary photolysis is efficient in destroying chlorine-acetylene pairs, and in addition deuterium-substituted vibrations are less intense than hydrogen motions.

The photoproduct with a band at 3212.1 cm^{-1} remains to be identified—certainly a problematic task in the absence of other features definitely assignable to the same species. The observed frequency suggests a CH stretch, but it falls just between the normal frequency ranges for acetylenic (e.g. C_2H_2: 3374, 3289 cm^{-1}; C_2HCl: 3340 cm^{-1}) and ethylenic (e.g. C_2H_4: 3106, 3103 cm^{-1}) CH stretches.[8] In fact, this frequency is more typical of species with allenic bonding, such as ketene, $H_2C{=}C{=}O$ (3155 cm^{-1}),[16] and the linear diradical $HC{=}C{=}N$ (3229 cm^{-1}),[17] but it is difficult to imagine an allene-like product of 1,1-DCE decomposition. The relative strength of this feature in the more dilute 1:500 experiment does not decrease enough to support a contention that the unknown product is a reaction product of dimers or higher multimers.

More exotic species, such as chlorovinyl radicals or the biradical vinylidene, are also eliminated on further consideration. Jacox reports a CH stretch of 3178 cm^{-1} for the fluorovinyl radical,[18] whereas Engdahl and Nelander

observe a value of 3093.8 cm^{-1} for the bromovinyl CH stretch;[19] thus the CH stretch for a classical, asymmetric, chlorovinyl radical such as these would probably fall in between, substantially below the observed frequency. However, the chlorovinyl radical might also take a cyclic or bridged form, the chlorine interacting with both the doubly-bonded carbons. Such a structure has been suggested by various workers[20,21] to be a lower-energy form than the classical, unbridged structure, and the bridged bromovinyl radical is long known.[22,23] The 3207 cm^{-1} CH stretch of matrix-isolated thiirene,[24,25] the bond-satisfied sulfur analog, gives weight to this possibility, but the absence of any other vibrational absorptions makes bridged chlorovinyl an unlikely claimant to the observed absorption. In any case, the stability of the 3212 cm^{-1} feature toward annealing and prolonged photolysis discounts the possibility that it belongs to a very unstable species, as cage recombination with the Cl atom would be expected to occur under these conditions. Vinylidene, $:C=CH_2$, has been predicted to have CH vibrations in an appropriate frequency range,[26] but, as in the cases of other unusual species, the lack of features corresponding to other motions of this molecule—for example, the C=C stretch or CH_2 bends—rules it out.

The experiments with d_2-1,1-DCE were conducted to aid in identifying this product, and in fact they prove illuminating. The 2542 cm^{-1} band produced upon shorter-wavelength photolysis, but not with 239 nm laser photolysis, is assigned to the deuterium-shifted 3212 cm^{-1} band, based both on its frequency and on its wavelength-dependent behavior like that of the 3212 cm^{-1} feature. The isotopic shift of 1.26 confirms that this feature is a CH/CD stretch, with some of the predicted $\sqrt{2}$ shift "missing" and presumably taken up by another vibration. The similarity of this shift to that of ν_1 of

chloroacetylene—1.28 for both isolated and π-hydrogen-bonded species[14]—suggests that this motion is a chloroacetylene CH stretch. Hypothesis of an additional chloroacetylene product must also account for the hydrogen chloride cage partner, consideration of which calls attention to the 2742 and 1990 cm^{-1} bands with the same photolysis source dependence as the above bands. The ν^H/ν^D ratio for this pair is 1.38, exactly in accord with the HCl/DCl shift as discussed above. Although the absorbance ratio of the 3212 and 2742 cm^{-1} features did not remain constant over time, as should be true if both belong to a single species, the underlying band at 2772 cm^{-1}, quite strong and broad, makes intensity measurement difficult for the HCl stretch. In summary, the isotopic data reveal the presence of a product that, like the π complex, incorporates both chloroacetylene and hydrogen chloride, but is somehow different from the π complex.

Viewed alongside the π complex, the very large frequency change in the CH stretch (3309 vs. 3212 cm^{-1}) and the smaller but substantial red shift of the HCl vibration (2772 vs. 2742 cm^{-1}) indicate that the interaction of the two submolecules in the new species is quite different, especially with respect to the CH bond. This in turn suggests a complex of the form denoted "σ-hydrogen-bonded" below, in which the acetylenic CH bond acts as acid and the chlorine atom of HCl acts as base. The hydrogen now shares its single electron with the hydrogen bond as well as the CH σ bond, thus electron density in the CH bond is reduced and its vibrational frequency red-shifted, while the chlorine donates electrons from its *p* lone pairs, slightly lowering the strength of the HCl bond.

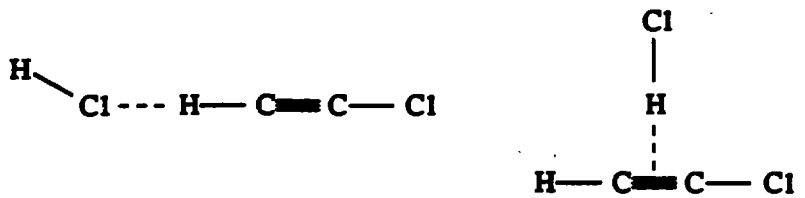

σ-H-bonded complex π-H-bonded complex

It is well known that in many monosubstituted acetylenes the CH proton is sufficiently acidic to participate in hydrogen bonding.[27] The postulated structure of this species is also consistent with the lack of additional bands corresponding to the 3212 cm^{-1} feature, as only the CH and HCl bonds should be noticeably affected by this hydrogen bond. The other vibrations, essentially those of the chloroacetylene submolecule, are expected to fall in the same regions as the corresponding motions in the π complex, and no doubt account for some of the spectral complexity of these features.

Ault and coworkers have extensively studied acetylenic hydrogen-bonded complexes in argon matrices,[28,29,30] although not, to our knowledge, with a hydrogen halide base. The CH stretching frequencies for such complexes lie near 3200 cm^{-1}, in the same frequency range as the observed absorption. As shown in Table 4, the frequency shift in the CH stretching frequency also falls within the range of shifts observed for similarly bonded species. Jeng *et al.* discuss these shifts in terms of the proton affinity, PA, of the base and conclude that the trends in frequency shift "correlate well with the gas-phase basicity of the bases, as measured by proton affinities,"[30] although other authors do not find that such correlation holds.[31] The HCl complex does not fit into this pattern, as the frequency shift is larger than would be predicted from the low proton affinity of HCl. Prior studies have observed

Table 4: Comparison of CH Stretch Frequency Shifts and Proton Affinities for σ Complexes of Chloroacetylene with Various Bases

Base	ν_1, cm^{-1} [a]	$\Delta\nu_1$, cm^{-1} [a]	PA, kcal/mol[b]	Reference
$(CH_3)_3N$	3187	138[c]	225	30
$(CH_3)_2CO$	3230	95	197	30
$(CH_3)_2O$	3222	103	192	30
CH_3CN	3256	69	188	30
HCl	3212	106[d]	135	this work

[a] CH stretch of chloroacetylene, complexed with base; $\Delta\nu_1 = \nu_1$(uncomplexed) - ν_1(complexed).

[b] proton affinity; from reference 39.

[c] in Ar matrix.

[d] in Xe matrix. No data available for uncomplexed C_2HCl; Δν estimated as 96 cm^{-1} shift from π complex, observed in this work, + 10 cm^{-1} shift from uncomplexed C_2HCl to π complex in Ar, reference 14.

only π-bonded complexes of hydrogen halides with acetylenes, both in matrices[14,32] and in the gas phase.[33,34]

However, other data on related complexes increase the chemical plausibility of the proposed second structure for $HCl{\cdot}C_2HCl$. In a matrix, hydrogen cyanide, HCN, forms a complex with HF in which the hydrogen halide is the base.[35]

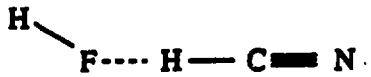

I

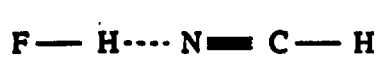

II

The predominant product of codeposition of HCN and HF in Ar is complex I, while the amount of complex II increases upon warming, indicating that it is the thermodynamically more stable structure, a fact predicted by *ab initio* calculations.[36,37] As with the acetylene-HX complexes, only the structure in which HF takes the acidic role (II) is observed in the gas phase.[38] Johnson and Andrews also report "evidence for an analog to I" upon codeposition of HCl and HCN in Ar. Clearly the matrix environment can stabilize species which represent only very shallow minima on the potential surface and are thus not seen in higher-temperature studies.

Furthermore, the electronic structure of the HF•HCN complex is quite similar to that of HCl•HCCl. While a chemist would expect HCN to be more acidic than HCCCl, proton affinities indicate that HCl (135 kcal/mol) is a better base than HF (117 kcal/mol),[39] and in fact the acidities of HCN and HCCCl, as measured by electron affinities of CN and CCCl, are probably not very different. Although no literature value for EA of CCCl was discovered, that for the related species CCF is about 80 kcal/mol (± 18), and for CCH the best values are

about 69 kcal/mol,[40a] compared with 85-88 kcal/mol for CN.[40] Thus the sum (EA_{acid} + PA_{base}), used to estimate the magnitude of the difference in ΔH for the proton transfer reactions and thus to indicate the strength of the acid-base interaction, may be nearly identical for the two systems. The calculations in Appendix B of ΔH for the relevant proton transfer reactions, confirm this prediction quite well.

Again, compared with the HF•HCN complex, the much greater polarizability of HCl improves its ability to donate electron density to the hydrogen bond, since in HCl the hydrogen-bonding orbitals are nonbonding 3*p* orbitals, more spatially extended from the nucleus than the 2*p* orbitals which are involved in the HF hydrogen bond. The relative magnitudes of the frequency shifts in the two complexes, HF•HCN and HCl•HCCCl, suggest that this difference contributes significantly to the extent of bimolecular interaction: Both the HX and CH stretches in the HCl•HCCCl species experience larger red shifts from the uncomplexed frequencies (HCl 3.9%; CH 3.2%) than do their counterparts in HF•HCN (HF 1.6%; CH 1.0%). Johnson and Andrews observe splittings in the HCN bend which enable them to determine a nonlinear structure for I; very likely the HCl•HCCl complex is also bent, but no attempt has been made to distinguish such splittings in the 1,1-dichloroethene photoproduct spectrum.

The magnitude of the frequency shift, traditionally used as an indication of the strength of the hydrogen bond,[41] would seem to indicate that the HCl•HCCCl hydrogen bond is quite strong, comparable to hydrogen bonds formed by rather stronger bases. Why should this be the case? One important difference to keep in mind is that the HCl•HCCCl complex is formed photochemically rather than by codeposition. Not only might this give

access to a different portion of the potential energy surface, but it means that the matrix cage size is predetermined by the parent molecule, rather than by the two submolecules. Thus the cage may be artificially "tighter" than cages formed randomly when acid and base stick in neighboring matrix sites, especially compared to the bulkier organic bases used by Ault's group. The fact that this complex is only formed in xenon may also be important, as the high polarizability of the matrix itself may help stabilize the complex.

While these arguments are not entirely convincing ones for the apparent strength of the σ-bonded $HCl{\cdot}C_2HCl$ complex, perhaps more important is the possibility that they are not even relevant. Klemperer[42] has recently noted that, upon examining the increasingly available experimental values for hydrogen bond strengths, the correlation between Δν and hydrogen bond strength pertains only incompletely. Recent matrix studies of the complexes of CO with HF conclude likewise that the frequency shift has little relation to the stability of the complex.[43] The linear OC•HF isomer, just 0.3 kJ/mol lower in energy than the other linear isomer, CO•HF, exhibits a shift of 130 cm^{-1} from the isolated hydrogen fluoride stretch, while the HF stretch of the latter shifts but 12 cm^{-1}. This complex is another good example of the ability of matrix isolation to trap isomers not detected by other means: As many as four structures were observed in Ar matrix, while only the OC•HF structure has been determined by microwave spectroscopists.[44,45]

Whether it is more or less strongly hydrogen-bonded, the σ-bonded isomer seems to be less thermodynamically stable overall than the π complex, as witnessed by the temperature dependence study of d_2-1,1-DCE. Figure 9 shows a plot of peak heights versus temperature, and although broadening and aggregation cause all the bands listed to decline irreversibly in intensity

with temperature, the band for the σ complex decreases faster than the others. This suggests that the HCl•HCCCl species is disappearing by a mechanism supplemental to those causing the apparent depletion of the parent molecule and π complex. The most obvious possibility is conversion to the other form, although with the overall broadening, no evidence for such isomerization, or any other reaction, could be observed.

Schriver and coworkers have found several base:HI systems which exist in matrices in both hydrogen-bonded and uncomplexed (but still cage-paired) forms.[46,47] Infrared radiation is effective in converting the complexed form C into the uncomplexed form U, while U can be back-reacted to make C by annealing the matrix. A particularly interesting example is that of the H_2O•HI complex, two distinct complexed forms of which are detected in addition to the uncomplexed form.[47] Both C_1 and C_2 are converted to U by photoexcitation of either the HI or the OH stretching mode, and annealing to 20 K recovers both, destroying U. However, a thermal cycle to 30 K results in an irreversible increase of the C_2 population at the expense of C_1. The authors suggest that the two forms arise from two trapping sites, the more stable form C_2 corresponding to a larger frequency shift in the HI submolecule and therefore, they conclude, a stronger hydrogen bond. They do not propose structures for the complexes, but certainly the amphoteric nature of H_2O allows for the alternate possibility of both a water-acid and water-base complex. The sole infrared photolysis performed on the 1,1-DCE/Xe photoproducts revealed no such interconversion in this system. This might indicate that the barrier to interconversion exceeds 5500 cm^{-1} (16 kcal/mol), or it may simply mean that the globar source was not sufficiently intense to cause detectable isomerization on the time scale studied.

With chemical arguments to bolster the spectroscopic evidence, the identity of the σ-hydrogen-bonded HCl•HCCCl complex is established. Less obvious is the mechanism of formation of this new photoproduct. As will be discussed later, its appearance only in Xe matrix and only from the 1,1 starting material, in a specific energy regime, hints at an interesting dynamical origin. That this complex is observed only under matrix conditions demonstrates once again the value of this technique, even in an age of supersonically cooled molecular beams and femtosecond pulses, for trapping and interrogating unstable or very weakly bound species.

DISCUSSION II: Photochemical Dynamics

Photochemistry of 1,1-dichloroethene at 239 nm in Kr Matrix

The photoreactions of Kr-isolated 1,1-DCE upon 239 nm irradiation, isomerization to *cis*- and *trans*-DCE and elimination of HCl to give the π-hydrogen-bonded complex of hydrogen chloride and chloroacetylene, are the same as those seen by Cartland and Pimentel with broadband photolysis.[2] The role of free radical photochemistry is most apparent in the 1,1-DCE isomer, since, as Cartland and Pimentel pointed out, the two isomerization products must be formed through CCl bond-breaking instead of simple rotation about the CC bond. This might occur via direct excitation of one of the dissociative surfaces underlying the dominant $^1(\pi,\pi^*)$ transition or after curve-crossing to one of these surfaces from the $^1(\pi,\pi^*)$ state.[4,8] Rearrangement of the hot α-chlorovinyl radical to the β-chloro radical prior to readdition of the Cl atom and relaxation would then give both *cis*- and *trans*-dichloroethene products, while loss of a hydrogen atom provides a route to the HCl-C_2HCl product. Chlorine atom readdition without rearrangement simply gives the parent again.

Excited-state elimination of HCl is not energetically feasible, and ground-state elimination is believed unlikely, as discussed in Chapter I. Interestingly, although for 1,1-DCE chlorine elimination on a singlet surface is energetically allowed via the Cl_2-$^1CCH_2$ state, it does not occur. Figure 10 shows the energy relationships and reaction channels for the 1,1-DCE/Kr system with 239 nm photolysis. Energies for the various species are derived and fully referenced in Appendix A and are relative to the ground state of 1,1-DCE.

Figure 10: Energy Level Diagram for 1,1-DCE/Kr at λ = 239 nm

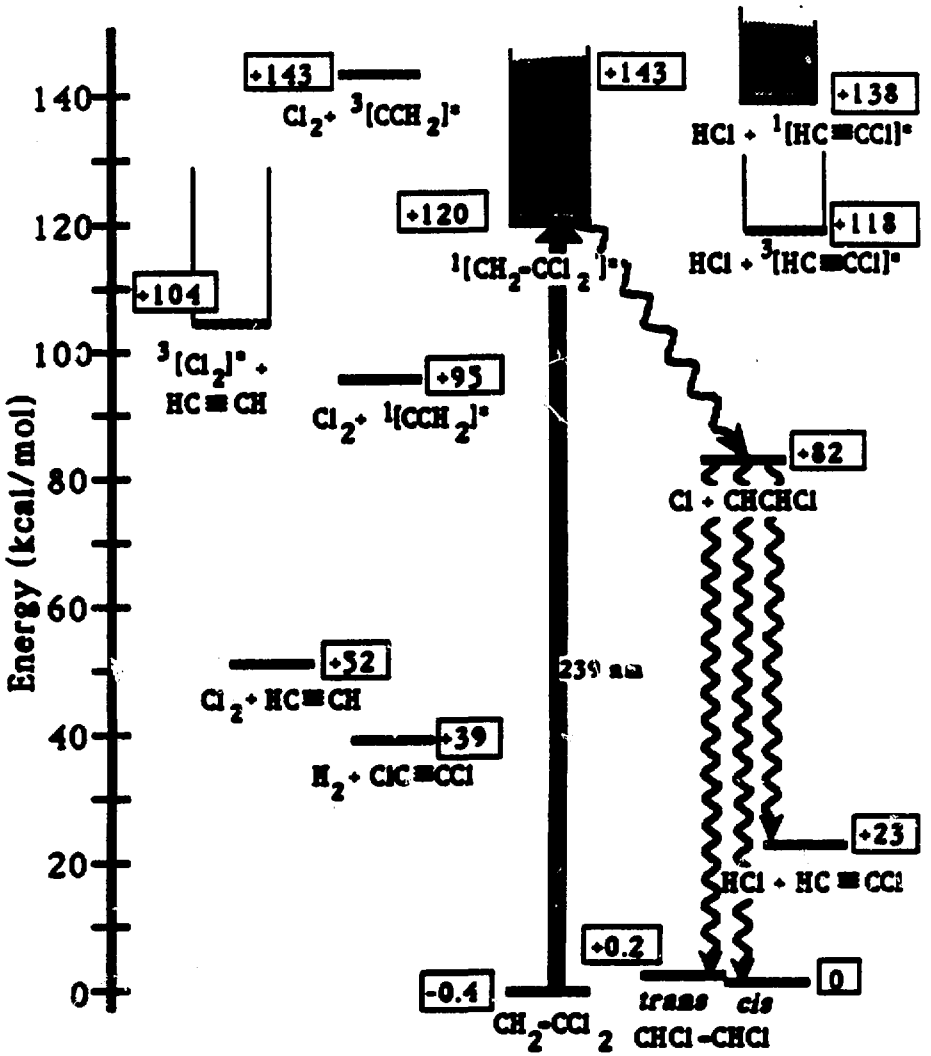

Photochemistry of 1,1-dichloroethene at 239 nm in Xe Matrix

Upon 239 nm excitation, the xenon matrix photochemistry of 1,1-dichloroethene and its deuterated counterpart is analogous to the photochemistry of the 1,2-dichloroethenes in xenon, already discussed. The energy level diagram in Figure 11 illustrates the excited-state processes which lead to the observed reaction products. The formation of $Cl_2 \cdot C_2H_2$ in Xe but not in Kr shows that, as in the cases of *cis*- and *trans*-1,2-dichloroethene in xenon, chlorine is eliminated on a triplet state reaction surface made accessible by the enhanced spin-orbit coupling of the heavy-atom xenon matrix. Molecular elimination of HCl can occur on the triplet surface as well, through the $HCl \cdot {}^3[HCCl]^*$ state. Again, the presence of the two 1,2 isomers indicates the importance of free radical chemistry for this molecule, as hydrogen abstraction to form $HCl \cdot C_2HCl$ competes with chlorovinyl rearrangement and Cl readdition to give the 1,2 isomers. The more extensive reaction in Xe (58% parent depletion in Xe at 3.8 mWh, 8% maximum in Kr) may be due to the opening of new reaction channels in Xe, a higher absorption coefficient in Xe at 239 nm as evidenced by the red-shifted absorption spectrum of 1,1-DCE, or both factors.

Photochemistry of 1,1-dichloroethene at $\lambda > 200$ nm in Xe Matrix

While the 239 nm photochemistry of 1,1-DCE/Xe is important additional evidence of matrix enhancement of intersystem crossing, its photochemistry at shorter excitation wavelengths is rather more interesting. The isomerization and π-HCl elimination products are formed as described above, with the additional availability of the $HCl \cdot {}^1[C_2HCl]^*$ channel at the higher energy. However, the formation of a second, distinct $HCl \cdot C_2HCl$ species from

Figure 11: Energy Level Diagram for 1,1-DCE/Xe at λ = 239 nm

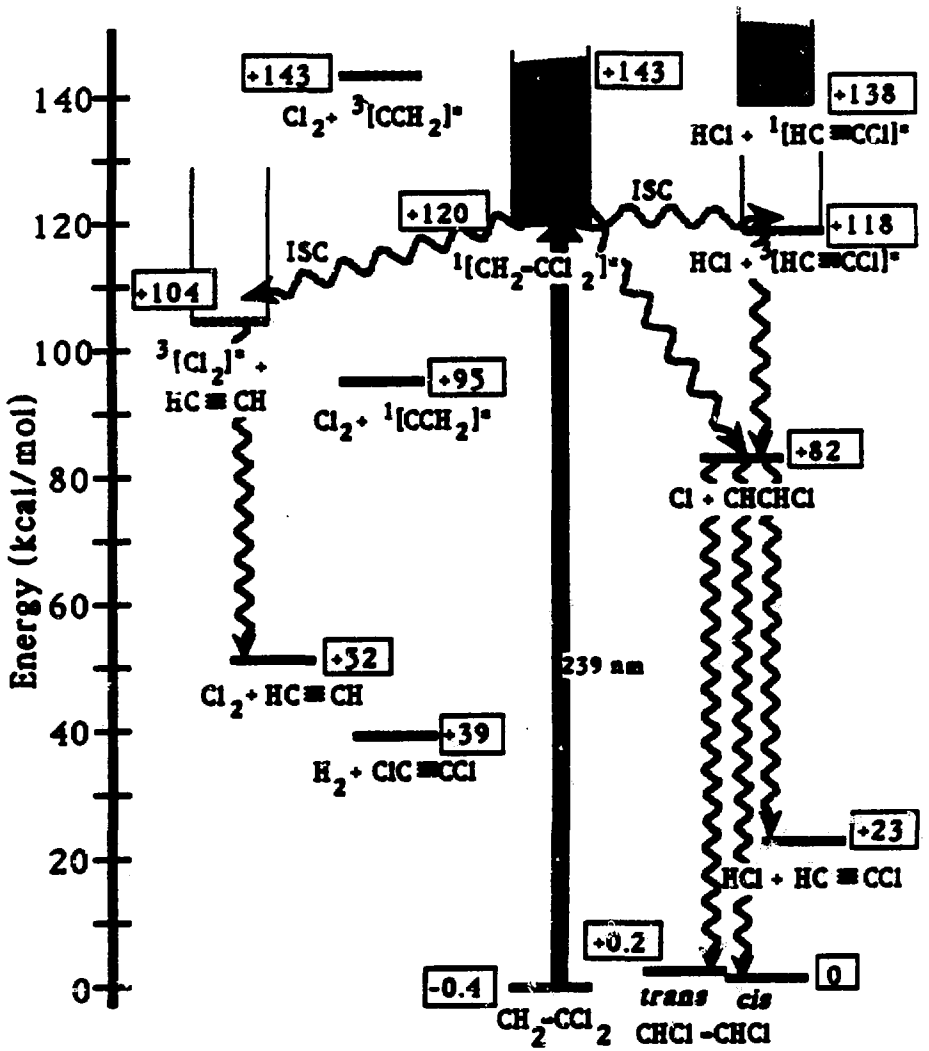

1,1-DCE implies access to a new pathway, one not available to the other isomers.

Certainly the wavelength dependence of the formation of this species and its appearance in xenon but not in krypton are two salient facts which must be considered crucial in interpreting the results. Perhaps in this instance, cage size is the important factor in determining the photoproducts, rather than the ability of xenon to enhance intersystem crossing to a triplet surface. A larger cage size should reduce geometric barriers to formation of the most thermodynamically stable complex, as seen by the structural change in $Cl_2 \cdot C_2H_2$ in Kr and Xe, but here a xenon environment permits formation of a less stable species. This explanation, too, does not account for the energy dependence. That and the uniqueness of this product to the 1,1-dichloroethene precursor point toward an intermediate or product state as yet left out of our survey, while the matrix dependence suggests that we should not forget the possible role of triplet surfaces.

Secondary reactions of any of the familiar photoproducts (*cis*-DCE, *trans*-DCE, π-$HCl \cdot C_2HCl$, $Cl_2 \cdot C_2H_2$) can be ruled out from the previous studies. Thus systematic evaluation of the various possible primary reaction channels should not be overly difficult—after all, the system has only six atoms—and will hopefully lead to an explanation of the reaction dynamics that is consistent with the experimental findings. Frequent reference should be made to the energy level diagram for $\lambda > 200$ nm photolysis in Figure 12. For clarity, some non-participating states that can be seen in previous diagrams have been left out of this figure.

Figure 12: Energy Level Diagram for 1,1-DCE/Xe at $\lambda > 200$ nm

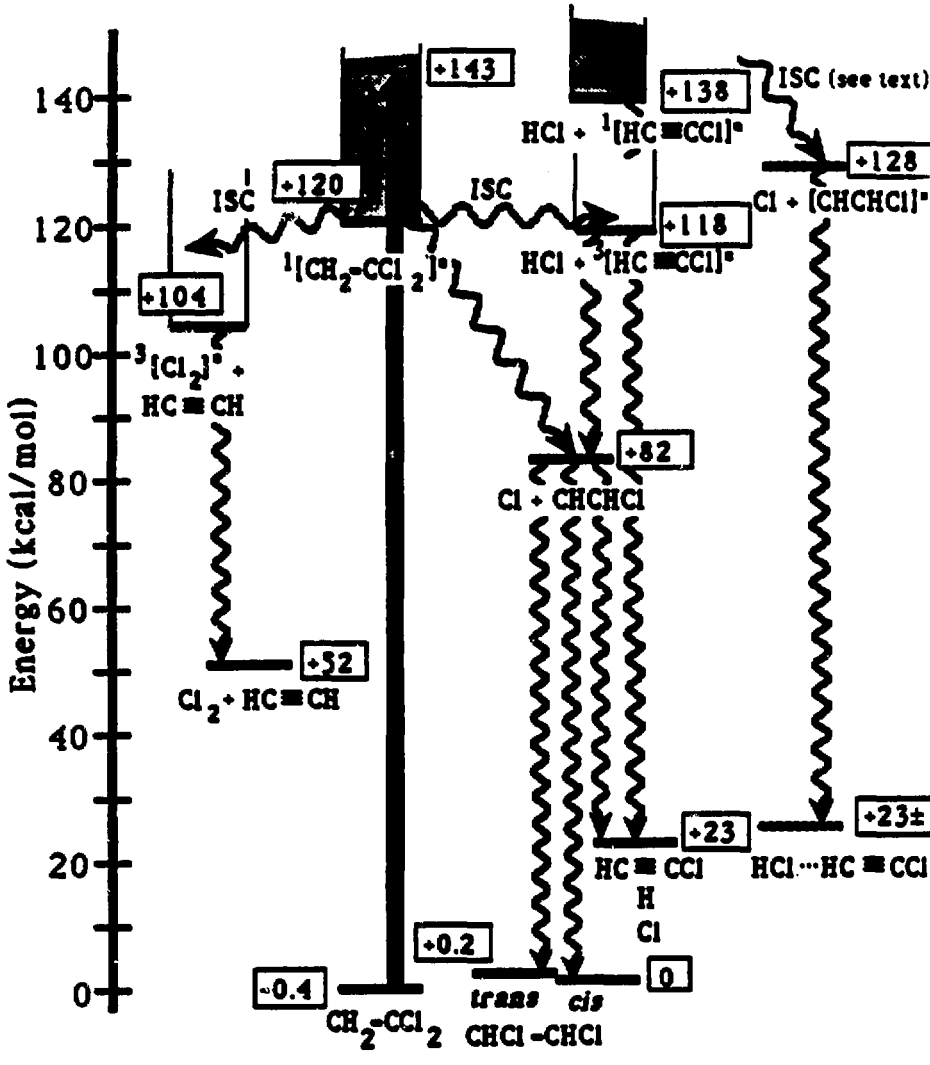

The simplest pathway for HCl production is the molecular elimination channel. Since the various DCE isomers are structurally inequivalent both in the ground and excited states, differing geometries of elimination might account for the differing product geometries. But in 1,1-DCE, only α,β elimination of HCl is possible, whereas both α,α and α,β elimination can, and do, occur from either 1,2 isomer.[49] Thus if molecular elimination geometries were responsible for the product differences observed, the *two* varieties of HCl product would be observed in the 1,2-DCE reactions and only *one* for 1,1-DCE decomposition—exactly opposite to the results. Like Berry and Pimentel,[49] we conclude that the relative amounts of α,α and α,β elimination cannot solely account for the differences reported here. Furthermore, since the eliminations are occuring through nonplanar excited states, considerations of *syn* and *anti* stereospecificity are no longer helpful.

Another molecular elimination channel, while not directly yielding chloroacetylene and HCl, is of possible consequence. Molecular chlorine elimination occurs, as seen, at 239 nm, and can be explained by the presence of a $^3[Cl_2]^*\cdot C_2H_2$ state lying below the available photon energy. Secondary photolysis of the ground-state product is facile, as demonstrated by the difficulty in detecting $Cl_2\cdot C_2H_2$ after $\lambda > 200$ nm irradiation of *cis*- and *trans*-dichloroethene in Xe. But for 1,1-DCE, molecular chlorine elimination can also occur through another triplet state, a $Cl_2\cdot{}^3[CCH_2]^*$ state theoretically predicted to lie at 135 kcal/mol,[50] well above the photon energy used with the laser, but below the air cutoff which limits broadband photolysis with the Hg-Xe arc. This triplet state of vinylidene is predicted to be rather stable, as the barrier to rearrangement to HCCH on the triplet surface is quite high, about 55 kcal/mol.[51] Thus, in theory, photolysis at $\lambda > 200$ nm could produce

metastable $Cl_2 \cdot {}^3CCH_2$ pairs, which, like $Cl_2 \cdot HCCH$, would undergo secondary photolysis to form $HCl \cdot C_2HCl$. By virtue of a different starting geometry, such a procedure might afford a distinct secondary product, at least in the restricted arena of the matrix cage.[52]

In practice, however, this scheme is subject to several limitations. First of all, growth kinetics of the σ-HCl•HCCCl product show no sign of the induction period characteristic of a secondary photoproduct (figure 3). Nor was any evidence of a stable vinylidene intermediate detected: With the low photon intensities employed, if $Cl_2 \cdot {}^3CCH_2$ lasts long enough to absorb a second photon, it might live long enough to appear in the IR spectrum. In fact, the use of Xe as host creates a dynamical Catch-22, as the very property of Xe which is necessary to access the ${}^3CCH_2$ potential surface, its enhancement of intersystem crossing rates, will also hasten $T_1 \rightarrow S_0$ relaxation to the singlet surface, where CCH_2 will rapidly[50c] rearrange to acetylene. Furthermore, a second photon striking the complex may be just as likely to isomerize the vinylidene as to excite the chlorine, again resulting in the ground state product $Cl_2 \cdot HCCH$ instead of the novel $HCl \cdot C_2HCl$ isomer. As a final blow to this hypothesis, recent photoelectron measurements[53] provide a singlet-surface isomerization energy, 44 kcal/mol, and vinylidene singlet-triplet splitting, 48 kcal/mol, which readjust the energy total of the $Cl_2 \cdot {}^3[CCH_2]^*$ state to 143 kcal/mol, at the energy limit of the laboratory photolysis sources. Nonetheless, the possibility of trapping ${}^3CCH_2$ in a matrix via triplet-surface photochemistry of 1,1-dichloroethene remains intriguing, although a narrow-band VUV photolysis source and perhaps a more rapid detection scheme than steady-state FTIR spectroscopy would be required to perform the experiment.

Another possible explanation for the two $HCl{\cdot}C_2HCl$ products lies in the free radical route for HCl elimination, outlined in the discussion of 1,1-DCE/Kr photochemistry. The chlorovinyl radicals formed by Cl dissociation from the three DCE isomers are dissimilar: Chlorine atom detachment from 1,1-DCE gives an α-chlorovinyl radical, $H_2C{=}CCl$, whereas the same process in *cis*- and *trans*-1,2-DCE gives a β-chloro species, $HClC{=}CH$.[54] In order to form the *cis*- and *trans*-DCE products from the 1,1 parent, migration of a hydrogen atom must occur prior to Cl atom readdition. That significant amounts of these two products are observed shows that this migration does occur on a time scale competitive with or faster than other processes such as H abstraction to form $HCl{\cdot}C_2HCl$; in other words, both α- and β-chlorovinyl are formed, however briefly, by 1,1-DCE photolysis. However, 1,1-dichlorethene is not a photoproduct of either 1,2-DCE isomer in these experiments, implying that H migration in the reverse direction, to form α-chlorovinyl from the initial β-chlorovinyl, does *not* occur more rapidly than other deactivation processes. This is not simply because no chlorovinyl radicals are formed, because, as discussed in Chapter I, $HCl{\cdot}C_2HCl$ production from 1,2-DCE with 239 nm irradiation must proceed through chlorine atom loss and subsequent hydrogen abstraction. Thus the β-chlorovinyl radical cannot be responsible for the novel photoproduct, as it is an intermediate in both 1,1- and 1,2-dichloroethene photoreactions.

The α-chlorovinyl radical, initially formed from 1,1-DCE but evidently not formed from 1,2-DCE, must then be examined as potential source of the difference. Loss of a hydrogen atom from $H_2C{=}CCl$ before rearrangement leaves bent HCCCl, just as does loss of the β hydrogen from $HClC{=}CH$. With these seemingly identical precursors, it seems unlikely that two structurally

distinct $HCl{\cdot}C_2HCl$ forms could be engendered, especially since both fragments are formed in the matrix cage with a significant amount of excess energy between them, presumably enough to overcome any geometry-related barriers. Most importantly, if *either* ground-state chlorovinyl structure were the precursor to the new HCl isomer, broadband photolysis of 1,1-DCE should give this product regardless of matrix. Since the second isomer was not observed in Kr,[2] ground-state chlorovinyl radicals are ruled out as sources of the geometric change in the product.

Since these molecules contain chlorine, the special interactions of Xe with Cl must be considered for possible influence on the photochemical dynamics. The charge-transfer excimer $XeCl^*$, well known for its laser emission, is strongly bound and a possible reaction product. The energy required to form this species in solid Xe, some 90 kcal/mol,[55,56] added to the energy of $[Cl + C_2H_2Cl]$, puts this species out of reach with the photolysis sources in use. Likewise, the bound excited states of Xe_2Cl^* and $Xe_{12}Cl^*$ are too high in energy to come into play here.[56] In the ground state, such Xe_nCl species are still bound, but rather weakly compared to the excited states.[57] Thus, free chlorine atoms may be longer-lived in Xe than in other matrices but are not so strongly bound to Xe as to inhibit their participation in other reaction channels. In summary, xenon-chlorine chemistry is not believed to play a major role in dichloroethene photoreactions at the photolysis energies studied.

While ground-state chlorovinyl radicals do not seem to be the source of the dual HCl elimination products, the dissociative excited states involved in their production may well be involved. Asymmetry on the red edge of the absorption band,[48] pre-resonance Raman effects,[58] and photoelectron

spectra[59,60,61] are among the evidence for $^1(n,\sigma^*)$ and $^1(n,\pi^*)$ states underlying the strong $^1(\pi,\pi^*)$ transition in the chloroethenes, but little is in fact known about their energies and oscillator strengths. Calculations agree on the vertical ordering of the lowest singlet transitions: (π,σ^*), (π,π^*), (n,σ^*);[62,63] but the numbers differ, and crossing points and potential surface contours are left to the imagination. Kato *et al.* predict both (π,σ^*) and (n,σ^*) transitions to lie at somewhat higher energies for 1,1-DCE than for the 1,2 isomers,[62] while Umemoto and coworkers find that 1,1-DCE has the lowest-energy $^1(n,\sigma^*)$ state of the three.[63] No energy estimates are available for the $^1(n,\pi^*)$ state.

Experimental information about the low-lying triplet states is even scantier than for the singlets; only the $^3(\pi,\pi^*)$ state has been located in ion and electron impact measurements.[64,65] SCF calculations[62] place $^3(\pi,\sigma^*)$ and $^3(n,\sigma^*)$ transitions about 10 kcal/mol below the associated singlets, and, again, no estimates are available for the $^3(n,\pi^*)$ state. All estimates are, however, in an appropriate energy range for present considerations.

Although these states are not well characterized, they do participate in the photochemical dynamics of the chloroethenes. Ausubel and Wijnen have suggested the involvement of two excited states in 1,1-DCE decomposition at $\lambda > 200$ nm,[66] and Warren *et al.* point to (n,σ^*) states as possible players in the inter-isomer changes observed in their matrix studies.[67] Details of the gas-phase photofragmentation results contain evidence for two distinct excited-state Cl dissociation channels in some species.[63] Time-of-flight spectra of vinyl chloride and *cis*-1,2-dichloroethene contain only single peaks for both HCl and Cl product channels, whereas for *trans*-1,2- and 1,1-dichloroethene, the Cl atom TOF spectrum has an additional low-energy component. The

authors postulate internal conversion from the (π,π^*) state to a low-lying (n,σ^*) state as the Cl-producing pathway common to all four molecules, much as suggested before. They attribute the low-energy component to dissociation from another (n,σ^*) state not directly coupled to the (π,π^*) state, with a $^1(\pi,\sigma^*)$ state serving as intermediate to the dissociative state and the initial $^1(\pi,\pi^*)$ state. This deactivation pathway does not, however, suitably explain the matrix data, since in the beam work both *trans*-DCE and 1,1-DCE show evidence of a second Cl-atom channel. Moreover, the reaction they postulate proceeds solely through singlet excited states, so in a matrix it will be open in Kr and Xe alike. Since the σ-bonded HCl isomer is manifested only in Xe, its origin must not be identical to the route they suggest. However, the beam study does indicate the importance of other DCE excited states besides the predominant $^1(\pi,\pi^*)$ state.

The similarity of this system to the $HI{\cdot}C_2H_2$ system studied in detail by Abrash and Pimentel should not go unheeded. Photolysis of $HI{\cdot}C_2D_2$ and $DI{\cdot}C_2H_2$ pairs gave, in addition to vinyl iodide and isotopically scrambled acetylene-HI, very selective production of DCCI and HCCI, such that the hydrogen iodide H(D) atom always ended up in the molecular hydrogen product.[52] In addition, the reaction product distribution was strongly wavelength-dependent.[68] Since we are starting from little-known dichloroethene excited states and do not have a well-defined reaction coordinate like the HI dissociation in the $HI{\cdot}C_2H_2$ studies,[68] and have also added a second large (Cl) atom to the system, increasing both the number and complexity of product and reactant states, we are unable to derive such an elegant correlation diagram for $C_2H_2Cl_2$ as do Abrash and Pimentel for the C_2H_3I system. Nonetheless their general approach and certain of their

conclusions, as well as some of the particular excited states invoked, apply here too. They find that a Franck-Condon bias—better matching of ground and excited state geometries along the reaction coordinate—strongly favors one excited electronic surface over another at long wavelength, and much less strongly at shorter wavelength, although both potential surfaces are energetically accessible at either wavelength. Because these dissociative surfaces correlate to different $[I + C_2H_3]$ states, different "continued cage chemistry" from the reactive iodine atom-vinyl radical cage pair follows.

In the DCE system, different states of the chlorovinyl-chlorine atom pair are also likely to be energetically within reach. Using the *A* state of vinyl radical (46 kcal/mol) as a model,[69] the first excited state of chlorovinyl lies at about 128 kcal/mol. This falls quite satisfactorily into the very energy range of interest for σ-HCl•C_2HCl production, above the 239 nm laser photolysis energy but accessible with the Hg-Xe lamp. For vinyl, the *A* state is characterized as a "π radical" and the ground state as a "σ radical,"[70] which may be expected to have different chemistries. If the analogy continues to hold, different reactions may likewise be anticipated from the ground and excited states of chlorovinyl.

Furthermore, Abrash and Pimentel suggest that the excited vinyl radical (e.g. HC=CDH) rearranges to the specific product isomer (HD•DCCl) via α,α elimination followed by recombination of C_2D with I "at leisure." An analogous process for the DCE case would be elimination of HCl to give C_2H, which then recombines with the Cl cage partner. Although $\Delta H_f(C_2H)$ is a subject of controversy in the literature,[71] the exothermicity associated with HCl formation lowers the reaction enthalpy of HCl elimination from chlorovinyl, relative to ΔH of H_2 elimination from vinyl. Using the most

recent value for D_0(HCC-H),[72,73] the state [Cl + CCH + HCl] is energetically accessible (135 kcal/mol) for the $C_2H_2Cl_2$ system at $\lambda > 200$ nm, whereas for the C_2H_3I system the energetics of the analogous channel were problematic. However, the formation at $\lambda > 224$ nm, and in one experiment with 239 nm light, of a small amount of the σ-bonded product argues against this mechanism. Perhaps, instead, this result indicates that an unfavorable Franck-Condon factor, rather than a true thermochemical barrier, inhibits the reaction at the longer wavelength. This would imply that the threshold for the relevant photoactive DCE state is near 120 kcal/mol and, additionally, would require that the excited state of chlorovinyl be a few kcal/mol lower in energy than estimated—not an unreasonable result, recalling that the estimate is based on excited vinyl. Further information about this mechanism might be obtained from a study of d_1-1,1-DCE, unfortunately a very demanding experiment from a synthetic vantage, or from a more thorough scan of photolysis wavelength from 239 to 200 nm to obtain the reaction excitation spectrum.

Now that it is clear that the excited chlorovinyl channel satisifies the energy constraints linked with the production of the σ-HCl elimination product, why is this product specific to 1,1-DCE/Xe? The Xe matrix dependence suggests that the [Cl + $C_2H_2Cl^*$] state correlates with a molecular triplet state, presumably one of the σ* states discussed above rather than a π* state. The unique formation of the product from 1,1-DCE may stem from excited-state properties of either the molecule or of the radical. The energy, extinction coefficient, or Franck-Condon profile of the 1,1-DCE triplet surface in question may simply be more favorable than for the equivalent state(s) of the 1,2-DCEs. Or, the reaction mechanism may require formation of an

excited α-chlorovinyl radical. Without knowledge of the full correlation diagram, it is impossible to do more than guess, but the empirical observations make it plain that these or other premises are influential.

In summary, it is proposed that the second, σ-bonded, $HCl \cdot C_2HCl$ isomer is formed at $\lambda > 200$ nm via an electronically excited chlorovinyl radical, $[Cl + C_2H_2Cl^*]$, after Cl dissociation from a molecular triplet state. Decomposition of excited chlorovinyl might proceed through HCl elimination and subsequent cage readdition of Cl to C_2H. The product is formed only in Xe matrix because the enhanced spin-orbit coupling in the heavy-atom matrix is necessary to gain access to the triplet reaction surface.

Photochemistry of 1,1-dichloroethene at Longer Wavelengths

It should be recalled from the earlier chapter that for the 1,2-dichloroethenes, photoisomerization occurred in Xe but not in Kr at energies below the singlet absorption threshold. This was taken as definitive evidence that Xe enhances access to a triplet reaction surface, since only direct excitation of the twisted $^3(\pi,\pi^*)$ state and relaxation into either *cis* or *trans* potential wells could effect such a change. Furthermore, 266 nm irradiation induced both isomerization and chlorine elimination, providing further confirmation of triplet-surface reaction and a guide to the energy placement of the $^3[Cl_2]^* \cdot C_2H_2$ state. In contrast, prolonged exposure of 1,1-DCE/Xe to light of wavelengths above 300 nm causes no photochemical changes. This is precisely as expected: The $^3(\pi,\pi^*)$ state of 1,1-DCE surely has the same, ethylenic, nonplanar geometry as do the 1,2-DCE (π,π^*) states, but rotation 90° in either direction gives equivalent configurations, so no net photochemical change occurs.

The accidental introduction of an oxygen-bearing impurity into one sample furnishes a hint, however, that the 1,1 isomer is not completely inert at the lower photolysis energies. Observation of what appears to be chlorine-oxygen chemistry has as a prerequisite the production of chlorine atoms, a process that is energetically allowed at this wavelength and that might well occur through a low-lying (n,σ^*) state. By analogy with the longer-wavelength photochemistry of the 1,2-DCEs, this may well be a triplet state, but the equivalent experiment should be performed in Kr to state this with more certainty.

Branching Ratios

As noted in the results section, the sum of the photoproduct yields does not account for all of the photolytically depleted starting material in both Kr and Xe samples. Certainly this fact casts some doubt on the accuracy of the calculated yields. However, the information derived is not without value. Some of the apparent loss of parent is probably real, as the errors are of the same sign and of similar magnitude in both cases (40% in Xe, ≥25% in Kr), and such losses have been observed before.[3] Diffusion out of the region of the matrix sampled by the IR beam, or orientation of the sample by the polarized laser beam, may occur during photolysis. Whatever the mechanism for the loss, assuming it shows no selectivity with regard to photoproduct, the *relative* yields should be accurate: ≥2:1 *cis:trans* and 1:1 *cis*/HCl in Kr. Similarly, in Xe, the branching is 1:2:1:5 *cis*/*trans*/HCl/Cl_2. As with the 1,2-DCEs, the new photoprocess in Xe, Cl_2 elimination, becomes the predominant one.

Moreover, the ratio of elimination yields, Cl_2/HCl, is highest for the 1,1 isomer, nearly 5:1, compared with less than 3:1 for the *cis* isomer and scarcely 1:1 for the *trans* isomer. This is consistent with the suggestion in the first chapter that HCl is principally α,α-eliminated: When, as for 1,1-DCE, the α,α elimination does not produce HCl, the extent of HCl elimination is decreased. Or, it may be that the α,α channel is still geometrically favored, but now instead of HCl, chlorine is the product. Also consistent with this interpretation is the observation that the frequencies of the π-HCl•C_2HCl photoproducts from *cis*- and *trans*-DCE, which can undergo either α,α or α,β elimination, are identical, while the π-complex photoproduct frequencies from 1,1-DCE, with only the α,β route available, are somewhat different. It is not difficult to imagine that the two processes could result in different arrangements of the complex within the cage, giving different complex-cage interactions, and the spectroscopic information thus serving as a record of the elimination mechanism. Although the apparent change in branching to *cis* and *trans* isomers between Kr and Xe is interesting, in view of the uncertainty of these numbers, no conclusions about these yields will be drawn here. The possibility of isomerization via back-reaction of HCl•C_2HCl pairs further complicates interpretation of these ratios.

Photochemistry of Other Molecules

As in solid Kr, trichloroethene undergoes only HCl elimination in Xe, although triplet Cl_2 elimination might be expected from this species too, as did occur with Hg photosensitization.[3,11] Perhaps HCl elimination proceeds so rapidly that chlorine elimination does not compete efficiently, or perhaps Cl_2 elimination requires the chemical mediation of excited Hg.

For 2-chloro-1,1-difluoroethene, the lack of reaction with 254 nm photolysis is consistent with the result of Hg-sensitization of CDFE in Kr, in which the only product was the mercury insertion product.[1] No triplet elimination channels are accessible at this excitation energy, and no Hg is present. In the $\lambda > 200$ nm experiment, bimolecular photoreaction prevented observation of possible direct triplet photochemistry at the higher photon energies.

CONCLUSIONS

The photochemistry of 1,1-dichloroethene has been studied in both krypton and xenon matrices at a variety of wavelengths. Recognizable isomerization and elimination products result from 239 nm photolysis, and changes in the reaction product distribution in Xe are attributed to triplet surface chemistry brought about by heavy-atom enhancement of intersystem crossing from the directly excited singlet state to a triplet surface. This finding supports conclusions from earlier work comparing direct and Hg (^{3}P)-sensitized photochemistry of the dichloroethenes and expands the xenon matrix studies of 1,2-dichloroethenes discussed in the first chapter.

Upon short-wavelength photolysis of 1,1-DCE/Xe, a new reaction product is observed that is wavelength-, matrix- and isomer-dependent. With the aid of isotopic substitution, this product is identified as a second isomer of $HCl{\cdot}C_2HCl$, "σ-hydrogen-bonded" with the acetylenic H interacting with the Cl end of HCl. In detecting the new complex, distinct from the π complex observed in previous matrix and gas-phase work, the combined merits of photochemical preparation of the novel complex and matrix isolation for trapping it are displayed to advantage. The formation of this unique species is believed to proceed via Cl dissociation from a triplet state, giving an excited chlorovinyl radical which subsequently cage-reacts to give the σ HCl complex. Again, a simple but deliberate change of matrix gas effects a dramatic change in the photochemical product distribution and reaction dynamics, exemplifying the potential of the method for reaction selectivity and control.

Additionally, these findings provide an opportunity to reconsider the photochemical role and behavior of excited-state complexes. Abrash and Pimentel, in examining the effect of geometry on photochemistry, take advantage of the fixed geometry and proximity of their starting materials and thus define the "supramolecule."[52,68] Other workers call these "precursor geometry-limited" reactions,[74,75,76,77] but the concept is quite similar: The starting geometry of the reactants determines the photochemistry. Here, the supramolecule is the product, and instead of the initial complex geometry defining the excited-state processes, the excited state defines the final complex geometry. Thus it would seem that excited-surface processes characteristic not just of the two molecular constituents but of the bound excited-state complex can exert control throughout the reaction. This demonstrates microscopic reversibility in the "precursor geometry-limited" case: If reactant geometry leads to product-selective photochemistry, here product geometry indicates a prior photochemical selectivity. To anthropomorphize, the constituent species of the supramolecule not only know where they are going, but remember where they came from too.

Although the details of the route from the initial excited state to the final state are unclear, as is even the identity of the initial state responsible for the new photoprocess reported here, it is evident from the simultaneous production of two different HCl product structures that the excited-state reactions are quite specific: The photochemistries of these molecules depend in a highly detailed manner on the electronically excited reaction surface. The characteristics of the excited electronic surface—energy, geometry, multiplicity—may be quite distinct from those of the ground state surface,

and all of these can influence the photochemistry. Understanding the photochemistry requires consideration of all possible reactant and product states, a difficult task even for a six-atom system, but such detailed examination leads to general conclusions about the nature of the excited-state reaction process and the factors that influence it, as well as to information about the particular reaction surfaces involved.

REFERENCES

[1]Cartland, H. E.; Pimentel, G. C. *J. Phys. Chem.* **1986**, *90*, 1822.

[2]Cartland, H. E.; Pimentel, G. C. *J. Phys. Chem.* **1986**, *90*, 5485.

[3]Cartland, H. E. Ph.D. thesis; University of California, Berkeley, 1985.

[4]Laursen, S. L.; Pimentel, G. C. *J. Phys. Chem.* **1989**, *93*, 2328.

[5]Liebler, D. C.; Guengerich, F. P. *Biochem.* **1983**, *22*, 5482.

[6]Sroog, C. E.; Woodburn, H. M. *Org. Synth.* **1963**, *4*, 271.

[7]Fieser, L. F.; Fieser, M. *Reagents for Organic Synthesis*, vol. I; Wiley: NY, 1967; p. 1180.

[8]Shimanouchi, T. Report NSRDS-NBS 39; National Bureau of Standards, U.S.: Gaithersburg, MD, June 1972.

[9]Rochkind, M. M.; Pimentel, G. C. *J. Chem. Phys.* **1967**, *46*, 4481.

[10]Schwager, I.; Arkell, A. *J. Am. Chem. Soc.* **1967**, *89*, 6006.

[11]Cartland, H. E.; Pimentel, G. C. *J. Phys. Chem.*, in press, 1989.

[12]Jacox, M. E. *J. Mol. Spectrosc.* **1980**, *80*, 257.

[13]Clemitshaw, K. C.; Sodeau, J. R. *J. Phys. Chem.* **1989**, *93*, 3552.

[14]Andrews, L.; Johnson, G. L.; Kelsall, B. J. *J. Phys. Chem.* **1982**, *86*, 3374.

[15]Keyser, L. F.; Robinson, G. W. *J. Chem. Phys.* **1966**, *44*, 3225.

[16]Moore, C. B.; Pimentel, G. C. *J. Chem. Phys.* 1963, *38*, 2816.

[17]Dendramis, A.; Leroi, G. E. *J. Chem. Phys.* 1977, *66*, 4334.

[18]Jacox, M. E. *Chem. Phys.* 1980, *53*, 307.

[19]Engdahl, A.; Nelander, B. *J. Chem. Soc. Perkin Trans. II* 1985, 1747.

[20]March, J. *Advanced Organic Chemistry*, 3rd ed.; Wiley: New York, 1985; p. 612, and references within.

[21]Skell, P. S.; Shea, K. J. Chapter 26 in *Free Radicals*; Wiley: New York, 1973; vol. 2.

[22]Singer, L. A. *Selective Organic Transformations*, ed. B. S. Thyagarajan, vol. 2. Wiley: New York, 1972.

[23]Skell, P. S.; Traynham, J. G. *Acc. Chem. Res.* 1984, *17*, 160.

[24]Krantz, A.; Laureni, J. *J. Am. Chem. Soc.* 1977, *99*, 4842.

[25]Torres, M.; Clement, A.; Bertie, J. E.; Gunning, H. E.; Strausz, O. P. *J. Org. Chem.* 1978, *43*, 2490.

[26]Osamura, Y.; Schaefer, H. F.; Gray, S. K.; Miller, W. H. *J. Am. Chem. Soc.* 1981, *103*, 1904.

[27]Bellamy, L. J. *The Infrared Spectra of Complex Molecules, Volume 1*, 3rd ed.; Chapman and Hall: New York, 1985; p. 66.

[28]DeLaat, A. M.; Ault, B. S. *J. Am. Chem. Soc.* 1987, *109*, 4232.

[29]Jeng, M.-L. H.; DeLaat, A. M.; Ault, B. S. *J. Phys. Chem.* 1989, *93*, 3997.

[30]Jeng, M.-L. H.; Ault, B. S. *J. Phys. Chem.* **1989**, *93*, 5426.

[31]Barnes, A. J. *J. Mol. Struct.* **1983**, *100*, 259, for example.

[32]McDonald, S. A.; Johnson, G. L.; Keelan, B. W.; Andrews, L. *J. Am. Chem. Soc.* **1980**, *102*, 2892.

[33]Legon, A. C.; Aldrich, P. D.; Flygare, W. H. *J. Chem. Phys.* **1981**, *75*, 625.

[34]Read, W. G.; Flygare, W. H. *J. Chem. Phys.* **1982**, *76*, 2238.

[35]Johnson, G. L.; Andrews, L. S. *J. Am. Chem. Soc.* **1983**, *105*, 163.

[36]Curtiss, L. A.; Pople, J. A. *J. Mol. Spectrosc.* **1973**, *48*, 413.

[37]Kollman, P. A. *J. Am. Chem. Soc.* **1972**, *94*, 1837.

[38]Legon, A. C.; Miller, D. J.; Rogers, S. C. *Proc. Roy. Soc. London A* **1980**, *370*, 213.

[39]Lias, S. G.; Liebman, J. F.; Levin, R. D. *J. Phys. Chem. Ref. Data* **1984**, *13*, 695.

[40](a) Lias, S. G.; Bartmess, J. E.; Liebman, J. F.; Holmes, J. L.; Levin, R. D.; Mallard, W. G. *J. Phys. Chem. Ref. Data* **1988**, *17*, supplement 1. (b) Christodoulides, A. A.; McCorkle, D. L.; Christophorou, L. G. *Electron-Molecule Interactions and Their Applications*, vol. 2; Academic Press: Orlando, FL, 1984; p. 423.

[41]Pimentel, G. C.; McClellan, A. L. *The Hydrogen Bond*; Freeman: San Francisco, 1960.

[42]Klemperer, W. Invited lecture; symposium honoring George C. Pimentel, October 6-7, 1989.

[43]Schatte, G.; Willner, H.; Hoge, D.; Knözinger, E.; Schrems, O. *J. Phys. Chem.* **1989**, *93*, 6025.

[44]Legon, A. C.; Soper, P.D.; Keenan, M. R.; Minton, T. K.; Balle, T. J.; Flygare, W. H. *J. Chem. Phys.* **1980**, *73*, 583.

[45]Legon, A. C.; Soper, P. D.; Flygare, W. H. *J. Chem. Phys.* **1981**, *74*, 4944.

[46]Schriver, L.; Schriver, P.; Racine, S.; Perchard, J.-P. *Chem. Phys.* **1988**, *119*, 95.

[47]Hannachi, Y.; Schriver, L.; Schriver, A.; Perchard, J.-P. *Chem. Phys.* **1989**, *135*, 285.

[48]Berry, M. J. *J. Chem. Phys.* **1974**, *61*, 3114.

[49]Berry, M. J.; Pimentel, G. C. *J. Chem. Phys.* **1970**, *53*, 3453.

[50]Calculations of S_0 acetylene-vinylidene isomerization energy: (a) Sakai, S.; Morokuma, K. *J. Phys. Chem.* **1987**, *91*, 3667 (42 kcal/mol); (b) Krishnan, R.; Frisch, M. J.; Pople, J. A.; Schleyer, P. R. *Chem. Phys. Lett.* **1981**, *79*, 408 (42 kcal/mol); (c) Osamura, Y.; Schaefer, H. F., III; Gray, S. K.; Miller, W. H. *J. Am. Chem. Soc.* **1981**, *103*, 1904 (40 kcal/mol). S_0-T_1 splitting: (d) Osamura, Y.; Schaefer, H. F., III. *Chem. Phys. Lett.*. **1981**, *79*, 412 (42 kcal/mol). 51 + 42 + 42 = 135 kcal/mol.

[51]Conrad, M. P.; Schaefer, H. F., III. *J. Am. Chem. Soc.* **1978**, *100*, 7820.

[52]Abrash, S. A.; Pimentel, G. C. *J. Phys. Chem.* 1989, *93*, 5828.

[53]Ervin, K. M.; Ho, J.; Lineberger, W. C. *J. Chem. Phys.* 1989, *91*, 5974.

[54]The inversion barrier between *syn* and *anti* forms is low, < 6 kcal/mol for β-fluorovinyl: Arnaud, R.; Elliager, Y.; Subra, R.; Douady, J. *Theochem* 1984, *110*, 203.

[55]Fajardo, M. E.; Apkarian, V. A. *J. Chem. Phys.* 1986, *85*, 5660.

[56]Last, I.; George, T. F. *J. Chem. Phys.* 1987, *86*, 3787.

[57]Becker, C. H.; Valentini, J. J.; Casavecchia, P.; Sibener, S. J.; Lee, Y. T. *Chem. Phys. Lett.* 1979, *61*, 1, for example.

[58]Takagi, Y.; Udagawa, Y.; Mikami, N.; Kaya, K.; Ito, M. *Chem. Phys. Lett.* 1972, *17*, 227.

[59]Lake, R. F.; Thompson, H. *Proc. Roy. Soc. London A* 1970, *315*, 323.

[60]Klasson, M.; Manne, R. in *Electron Spectroscopy*, ed. D. A. Shirley; North Holland: Amsterdam, 1972.

[61]Chadwick, D.; Frost, D. C.; Katrib, A.; McDowell, C. A.; McLean, R. A. N. *Can. J. Chem.* 1972, *50*, 2642.

[62]Kato, H.; Hirao, K.; Konishi, H.; Yonezawa, T. *Bull. Chem. Soc. Japan* 1971, *44*, 2062.

[63]Umemoto, M.; Seki, K.; Shinohara, H.; Nagashima, U.; Nishi, N.; Kinoshita, M.; Shimada, R. *J. Chem. Phys.* 1985, *83*, 1657.

[64]Moore, J. H. *J. Phys. Chem.* 1972, *76*, 1130.

[65]Koerting, C. F.; Walzl, K. N.; Kuppermann, A. *Chem. Phys. Lett.* 1984, *109*, 140.

[66]Ausubel, R.; Wijnen, M. H. J. *J. Photochem.* 1976, *5*, 233.

[67]Warren, J. A.; Smith, G. R.; Guillory, W. A. *J. Photochem.* 1977, *7*, 263.

[68]Abrash, S. A.; Pimentel, G. C. *J. Phys. Chem.* 1989, *93*, 5834.

[69]Wodtke, A. M.; Hintsa, E. J.; Somorjai, J.; Lee, Y. T. submitted to *Isr. J. Chem.*, February 1989.

[70]Paddon-Row, M. N.; Pople, J. A. *J. Phys. Chem.* 1985, *89*, 2768.

[71]Wodtke and Lee review the literature to 1985 in their paper on C_2H_2 photodissociation; Wodtke, A. M.; Lee, Y. T. *J. Phys. Chem.* 1985, *89*, 4744.

[72]Segall, J.; Lavi, R.; Wen, Y.; Wittig, C. *J. Phys. Chem.* 1989, *93*, 7287.

[73]Green, P. G.; Kinsey, J. L.; Field, R. W. *J. Chem. Phys.* 1989, *91*, 5160.

[74]Wittig, C.; Sharpe, S.; Beaudet, R. A. *Acc. Chem. Res.* 1988, *21*, 341, and references within.

[75]Rettner, C. T.; Zare, R. N. *J. Chem. Phys.* 1981, *75*, 3636.

[76]Rettner, C. T.; Zare, R. N. *J. Chem. Phys.* 1982, *77*, 2416.

[77]Jouvet, C.; Boivineau, M.; Duval, M. C.; Soep, B. *J. Phys. Chem.* 1987, *91*, 5416.

Chapter III

Chemistry of Electronically Excited Cadmium Atoms with Small Molecules

INTRODUCTION

Metal atom photosensitization is one of the more venerable techniques known to photochemists. Since the 1920's,[1] metal atoms, especially the group 12 metals Hg, Cd, and Zn, have been used for collisional transfer of electronic energy to other molecules which do not absorb or absorb only weakly in the spectral region of interest, resulting in a voluminous literature covering a wide variety of organic substrates.[2,3,4] Traditionally this process is described as spin-conserved quenching and includes the processes represented by the equations below, using the example of Hg ($^3P_1$):

$$Hg\ ^3P_1 + Q \rightarrow Hg\ ^3P_0 + Q\dagger \qquad (1)\ \text{quenching to metastable Hg } ^3P_0$$

$$\rightarrow Hg\ ^1S_0 + {}^3Q^* \qquad (2)\ \text{electronic energy transfer}$$

$$\rightarrow Hg\ ^1S_0 + F_1 + F_2 \qquad (3)\ \text{direct dissociation of quencher}$$

$$\rightarrow HgF_1 + F_2 \qquad (4)\ \text{dissociation with compound formation}$$

In the case of chemical reaction, fragments F_1 and F_2, or F_2 and compound HgF_1, must conserve spin as well, forming two doublet states or a singlet plus a triplet.

Although process (4) implicitly recognizes the possibility of chemical reactivity of the excited mercury, little concrete evidence for or serious discussion of this channel is seen in the literature through this early period. A typical example of the formal distinction made by these early workers between photosensitization, referring more strictly to the energy transfer process (2), and chemical reaction such as in (4), is seen in a statement from the 1964 review by Cvetanovic: "The related processes in which the strongly absorbing substance interacts chemically or forms chemically reactive

intermediates by bonding or complexing with the non-absorbing molecules cannot always be distinguished with certainty from simple physical transfer of energy in collisions and are as a rule also considered within the framework of photosensitization."[3]

However, a recent, two-pronged resurgence of interest in this field has reopened the discussion. On the synthetic side, Crabtree and others have rediscovered the utility of Hg photosensitization on a preparative scale.[5,6,7,8] The technique has also proven useful in studies of free radicals, as in the Hg (^3P) photosensitization of ammonia to form NH_2, which is then studied in a supersonic jet using laser-induced fluorescence.[9] Bernath and coworkers have found that excitation of Ca and Sr to triplet states enhances reactivity with a variety of organic species, making this an efficient means of producing inorganic free radicals for laser spectroscopic study.[10,11,12] In addition to these examples, direct evidence for the participation of excited-state complexes in photosensitization is provided by detection of emission from exciplexes of Cd with a number of organic molecules, including ammonia[13] and other amines,[14,15] water, alcohols and ethers.[16]

From a more physical point of view, growing interest in a "state-to-state" picture of energy transfer and chemical reaction dynamics has redirected attention to metal atom photosensitization. The quenching of electronically excited metal atoms by small molecules is an attractive system for such studies, as both experimental and theoretical approaches are feasible. Even traditional "slow" flash kinetic spectroscopic techniques can provide useful information. For example, from their findings of differing isotopic specificity for quenching of excited Cd or Zn ($^1P_1$) and ($^3P_1$) with H_2, HD and D_2, Breckenridge and Realund were able to derive information about

barriers, surface crossings, charge-transfer interactions, and the extent of involvement of chemical interaction surfaces, such as metal hydride surfaces of the type H-M-H.[17,18]

However, new physical techniques, particularly the ability to resolve vibrational and rotational state distributions, have brought about more dramatic advances in the understanding of these reactions. Electronic-to-vibrational energy transfer has been studied by detecting state-resolved products of collisions of Hg ($^3P_1$) with small molecules.[19,20,21] Excited group 2 metal atoms, Ca ($^1P_1$)[22,23,24] and Sr ($^1P_1$),[25] as well as Hg ($^3P_1$),[24] have been used in studies of the effect of orbital alignment on reactivity and energy partitioning. Laser spectroscopy of van der Waals complexes of metal atoms with rare gases yields information about the van der Waals potential energy surfaces, which can be useful in understanding quenching and reaction dynamics.[26,27] Van der Waals complexes are also crucial in the so-called "half-collision" studies, in which a cold complex of the reagent molecules, with a well-defined geometry, is prepared in a supersonic jet and excited with a laser to initiate reaction.[24,28,29,30] These studies allow precise control of the entrance channel conditions, so that detection of the final states permits a high degree of state-to-state correlation, and measurements on the excited complex may provide information on reaction transition states.

Although the group 12 metals are too large for theoretical treatment, the group 2 metals are amenable to *ab initio* methods. The reaction of hydrogen with excited Mg has been theoretically modeled for both $^1P_1$ and $^3P_1$ states and serves as a prototype of these reactions.[31,32] Similar calculations on HF + Mg on S_0, S_1 and T_1 surfaces predict different reactivity on the different

surfaces.[33] Even polyatomic molecules are now tractable, enabling the study of such chemically interesting topics as metal-ethylene exciplexes[34] and metal-mediated acetylene-vinylidene rearrangement.[35,36]

Several recent examples of Hg-sensitized chemistry in a cryogenic matrix have also brought into question the distinction between energy transfer and chemical reactivity as aspects of photosensitization. In studies of the reactions of Hg ($^3P_1$) with various haloethenes, Cartland and Pimentel found that Hg reacted with the substrate, inserting into CCl or CBr bonds.[37,38,39,40] They conclude that chemical reactivity of the excited metal atom is clearly important, and, furthermore, that reaction in the matrix is constrained to the reaction surface of the initial excited state, singlet or triplet. Numerous other works report photoreaction of metal atoms with small molecules,[41] but, with a few exceptions,[42,43] the majority of these have a synthetic orientation and do not evaluate the excited-state chemistry. Thus there is both need and ample opportunity for further physical investigation of the primary photoprocesses and dynamics of these reactions in a matrix.

Remaining in question, then, is the issue of whether chemical reaction competes with spin-conserved energy transfer, or whether the mercury-containing species is an intermediate in the energy transfer process, trapped in the matrix. The xenon-matrix studies addressed the problem of spin-conserving reaction pathways separately from the issue of reactivity, and as shown in Chapters I and II, confirmed the finding that intersystem crossing in these molecules is not facile in the absence of a spin-orbit perturbation. Thus this chapter returns to the topic of metal atom reactivity, with the intention to further examine the primary process(es) in photosensitization with the other group 12 metals, Cd and Zn. Because of the

traditional emphasis on energy transfer, the term "photosensitization" will be avoided in this work when possible, in favor of the term "excited-state chemistry," and will otherwise be used with full cognizance of the chemical as well as energetic aspects of the process.

Several reasons contribute to the selection of Cd and Zn for the continuation of these studies. Cadmium and zinc are in the same group as mercury, and thus have similarly unreactive, closed-shell ground states (ns^2) but reactive lowest excited states (ns^1np^1). However, the spin-orbit coupling factors vary significantly, so ease of singlet-triplet energy transfer increases through the series Zn, Cd, Hg. Thus a comparison of the photoreactions of these species should give an indication of the relative importance of spin-conserved energy transfer and chemical reactivity in the reaction dynamics. An additional advantage of cadmium and zinc is the presence of both singlet and triplet excited states with energies below the air cutoff, making the study of both singlet- and triplet-sensitized reactions experimentally feasible, as is not convenient with mercury.

Nonvolatile Cd and Zn are less readily deposited into a matrix than Hg, so a two-chamber Knudsen oven with several novel features was designed and constructed, enabling controlled quantities of metal atoms to be codeposited with the reactant species and matrix gas. This chapter describes that apparatus and the UV spectroscopic studies conducted to characterize the Knudsen cell, including the observation of some matrix effects on atomic absorption spectra. In addition, results of attempted photosensitized reactions of several small organic molecules with Cd are reported and discussed.

EXPERIMENTAL SECTION

Knudsen cell

Cadmium was introduced into matrix samples using a Knudsen cell, shown in Figure 1. The cell consisted of two independently heated ovens: The temperature of the metal-filled rear oven determined the rate of deposition, according to the Knudsen equation,[44] and the second oven was superheated in order to dissociate the weak (2 kcal/mol) bond of Cd_2[45] and thereby increase the ratio of atomic to diatomic metal species deposited.[46,47] The cell was fabricated of Invar for its low coefficient of thermal expansion and of demountable pieces for ease of cleaning and filling. The two ovens were separated with a ceramic "MaCor" (Corning) spacer, to slow heat transfer and maximize the thermal gradient between the two ovens, and the assembled cell was held together with two Invar bolts. The channel between the two chambers was of relatively large bore, so that the pressure in the two chambers was equal and molecular effusion was impeded only by the 1 mm effusion orifice.[46] Each oven was provided with a heater, made of 1 mm inconel-sheathed "Thermocoax" heater cable (Amperex Electronic Corporation) tightly coiled and brazed onto the oven surface, and with a type K thermocouple, made of matched, 0.10", chromel and alumel wires (Omega) and cemented into the drilled thermocouple wells with Omega "CC" high-temperature cement. Temperatures were measured near the ceramic spacer so that the temperature difference ($T_2 - T_1$) measured was a lower limit.

The cell was mounted inside a stainless steel vacuum chamber, shown in Figure 2, which attached directly to the cryostat vacuum shroud. A quarter-inch O.D. deposition jet entered the chamber about 2" from the substrate. An

Figure 1: Two-Chamber Knudsen Cell for Metal Atom Deposition (twice actual size)

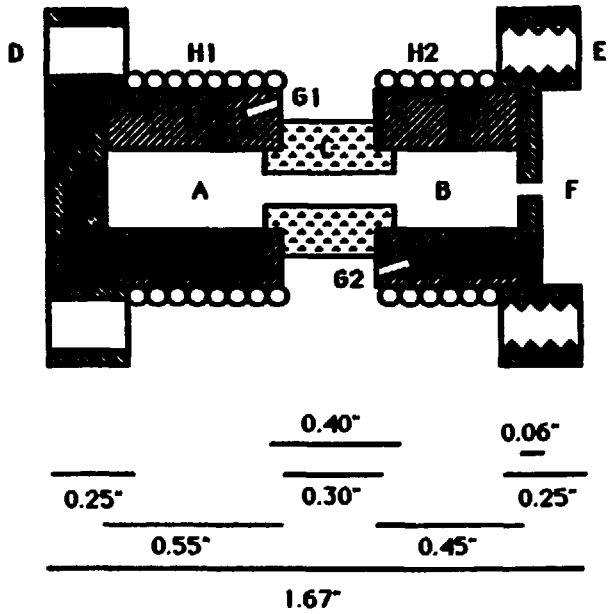

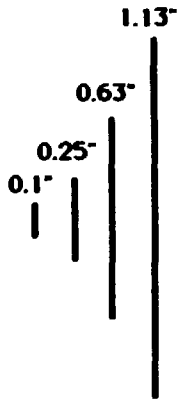

A. chamber 1; filled with metal
B. chamber 2
C. Macor divider
D. bolt holes for invar bolts (2) and mounting rods (2)
E. 10/32 threads
F. 1 mm effusion orifice
G. wells for type K thermocouples
H. brazed thermocoax heaters

(thermocouples and heater leads not shown for clarity)

Figure 2: Vacuum Chamber and Eight-Conductor Flange for Metal Atom Deposition with Knudsen Cell (actual size)

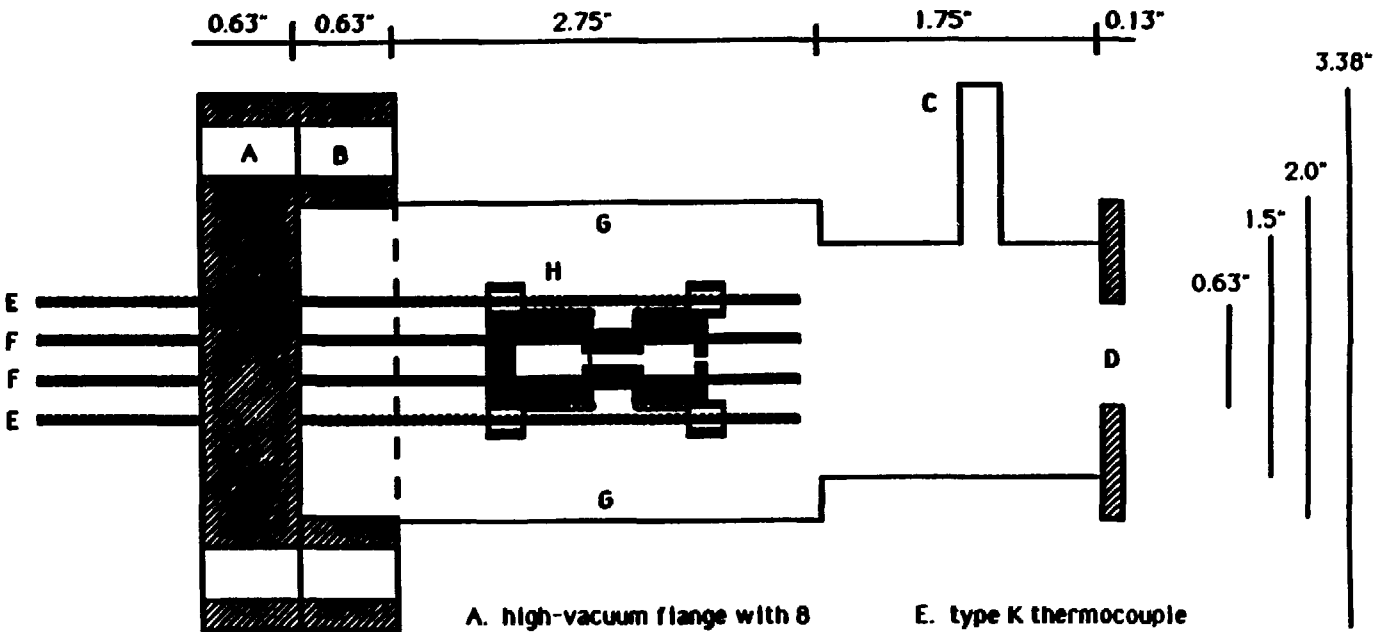

A. high-vacuum flange with 8 feedthroughs for heater and thermocouple conductors
B. high-vacuum flange welded to chamber body
C. deposition port; 0.25" O.D.
D. collimating aperture
E. type K thermocouple conductors (2 pairs)
F. 0.050" Cu conductors for heaters (2 pairs)
G. Al foil radiation shield
H. Knudsen cell, mounted on thermocouple leads with ceramic insulators

eight-conductor "Del-Seal" high-vacuum flange, customized by Insulator Seal, Inc., supplied electrical feedthroughs for the heaters and thermocouples, with two pairs of type K thermocouple leads replacing four of the original eight copper leads. A copper gasket was used in the flange seal. The cell was mounted directly on the flange, facilitating removal and access for maintenance. The stiff chromel leads of the two thermocouples, insulated with a column of small porcelain beads, were inserted through the two open bolt holes of the cell, such that when the flange was attached to the chamber, the cell was suspended axially in the center of the chamber by the chromel rods. The distance of the cell from the substrate could be fixed by the use of larger porcelain beads as spacers.

Connecting the heater and thermocouple leads to the flange conductors proved to be a major challenge, as the constraints of high temperature tolerance and small space requirements were demanding. After some experimentation, the stripped, Nichrome ends of the "Thermocoax" heaters were attached to the heavier copper conductors with crude but effective connectors made of 0.010" copper foil, snipped and folded into pockets which held the two wires in close proximity but could be unfolded for nondestructive disassembly of the cell. Thermocouple wires were spot-welded to the appropriate conductors, a method which necessitated destruction and rewelding upon each cell disassembly, and thus occasional replacement of a damaged thermocouple, but which was nonetheless deemed an acceptably simple solution.

Power to each heater was supplied by a Variac power supply, connected through a transformer (25-28 V output at 3 A). Each thermocouple was connected with insulated, duplex, type K thermocouple wire through a

reference junction held at 0° C in an ice-water bath, to a Keithley digital multimeter, model 177 or 191. Readouts in millivolts were converted to temperature using the reference tables for type K (chromel-alumel) thermocouples supplied by the manufacturer.[48] Deposition temperatures quoted were calculated using a simple computer routine to find the time-weighted average over the entire deposition period, based on periodic readings during the deposition and assuming linear temperature variation between readings.

In a typical deposition for an IR experiment, the cell was preheated with approximate power settings of 10 V for the first oven (P_1 = 10 V) and 25 V for the second (P_2 = 25 V), until T_1 was within 20-40° C of the desired setting. The first power supply was then turned off so that the two ovens could stabilize, such that the power supplied to P_2 was sufficient to maintain both ovens at nearly constant or slightly increasing temperatures, with a difference (T_2 - T_1) of 70 to 100° C. Thus the deposition temperature T_1 was ultimately determined by the power P_2 supplied to the second oven. Under the conditions described above, P_2 = 25 V corresponded to T_1 = 220° C, T_2 = 310° C. For experiments done in the Perkin-Elmer 450 UV spectrometer, optimal metal concentrations were lower, thus a typical setting for P_2 was 20 V, with T_1 = 150° C.

Deposition rates were calculated assuming ideal Knudsen effusion[49] according to the equation[50]

$$N = \frac{\pi d^3}{12l}\sqrt{\frac{8kT}{\pi m}}\left(\frac{P0}{kT}\right)\left(\frac{R^2}{D^2+R^2}\right)$$

where N is the flow rate in particles/s, d and l are the diameter and thickness, respectively, of the effusion orifice, m is the atomic mass of the

metal, k is the Boltzmann constant, p_0 is the vapor pressure of the metal at temperature T, and the last term a collection fraction which accounts for the solid angle covered by the target, in which R is the radius of the target and D is the distance of the effusion source from the target.[44] No correction was made for the fact that some diatomic species were deposited; that is, the deposition rates include all Cd particles rather than just Cd atoms. For this system, d = 1 mm and l = 1.5 mm, assuming the orifice was fabricated to specifications, while R = 1 cm (2 cm substrate) and D = 7.9 cm. The size of the aperture on the plate attaching the chamber to the cryostat was selected to provide the same collection fraction (0.0156) as the assumed substrate size. Calculated deposition rates for various temperatures are shown in Table 1. Rates for temperatures between the known data points[51] were extrapolated assuming a linear slope between the two nearest points.

Materials

Cadmium was obtained as 0.64 mm wire from Alfa, with a stated purity of 99.999%. A f about 0.7 g lasted for several experiments. If the metal-filled cell was exposed to atmospheric moisture for more than a few hours, a greenish coating, presumably CdO, formed on the surface of the metal and inhibited Cd deposition. This could be prevented by storing the filled cell, if removed from the vacuum system, in plastic with $CaCl_2$ desiccant and an occasional nitrogen flush, or corrected by washing the metal with a dilute solution of HCl until the shiny appearance was restored. The metal was then rinsed with water and acetone and dried with a stream of nitrogen before replacement in the cell.

Argon, krypton and xenon were obtained from Matheson (Ar) and Airco (Kr and Xe) and were of 99.995%, 99.995%, and 99.9995% purity, respectively.

Table 1: Knudsen Deposition Rates for Cadmium Atoms

Temperature, K (°C)[a]	Deposition Rate, mmol/h	M/R[b]
368 (95)	$8.55(10^{-9})$	58,500,000
390 (117)	$8.31(10^{-8})$	6,020,000
400 (127)	$2.14(10^{-7})$	2,340,000
416 (143)	$8.05(10^{-7})$	621,000
447 (174)	$7.76(10^{-6})$	64,400
486 (213)	$7.44(10^{-5})$	6700
500 (227)	$1.53(10^{-4})$	3300
532 (259)	$7.11(10^{-4})$	700
587 (314)	$6.77(10^{-3})$	74

[a]temperatures for which vapor pressure data is available; from reference 51.

[b]matrix/reactant ratio, assuming a typical rate of deposition of matrix gas, 0.5 mmol/h.

Acetylene was obtained from Pacific Oxygen and purified as described in Chapter I. Propyne from Linde, cyclopropane from Matheson (99%), 2-chloro-1,1-difluroethene from PCR Inc., and vinyl chloride of unknown parentage were used without further purification. Cyclobutane was from Columbia Organic (99%) and was treated with two freeze-pump-thaw cycles in liquid nitrogen before use. Matrix gas/organic reactant mixtures were prepared as in Chapter I and at 100:1 concentrations unless otherwise noted.

Spectroscopy

UV spectra were recorded on a Perkin-Elmer model 450 dual-beam spectrophotometer sample compartment modified to accomodate the cryostat described previously. The specified resolution of the double-prism monochromator was 0.1 nm with a wavelength accuracy of 0.08 nm, although in practice the poor signal-to-noise ratio reduced the effective resolution. Wavelength calibration was verified using the visible line spectrum of the D_2 source, with the instrument in single-beam mode and the slits at 0.03 mm. The D_2 source was also used as a narrow-band photolysis source for photoaggregation studies, with the slits opened to 3 mm at the selected wavelength.

The external windows and substrate were BaF_2 or CaF_2 from Harshaw and the baseline was electronically compensated for these elements at room temperature, versus the empty reference compartment, then re-recorded after cooldown. The full optical path was continuously purged with nitrogen to permit collection of data down to 185 nm. Ar samples were deposited at 12 K, Kr at 20 K, and Xe at 25 K, although in later IR experiments deposition of Kr mixtures on an unheated substrate (12 K) was found to produce better-isolated matrices (narrower IR bandwidths) than 20 K deposition, possibly

because the substrate was slightly warmed by deposition of hot Cd atoms or simply by long exposure to the hot Knudsen cell.

For experiments involving codeposition of the metal with an organic reactant, infrared spectra were collected on one of the two IBM FTIR spectrometers described previously, the IR97 or the IR44. Resolution was 0.5 cm^{-1} and 200 scans were collected from 4000 to 400 cm^{-1}. Occasional impurity bands near 2340 and 660 cm^{-1} are easily assigned to CO_2, a common contaminant in matrix samples due to small air leaks. Samples which were doped with Cd, however, habitually exhibited much stronger CO_2 absorptions than undoped samples, suggesting that, despite continuous evacuation of the cryostat assembly, a significant amount of CO_2 was adsorbed on the metal surfaces of the Knudsen cell and chamber and desorbed upon heating of the cell. Frequent opening of the cryostat to clean the substrate or perform repairs no doubt exacerbated the problem.

Another, unidentified, impurity absorption at 1024 cm^{-1} was quite persistent throughout the series of experiments with Cd, but its intensity did not correlate with the CO_2 intensities, Cd concentration, deposition time or rate, or oven temperature, nor was it constant with reactant mixture or substrate cleanliness. The unknown absorption did not diminish with photolysis. This frequency is near the strongest absorption of ozone isolated in Kr, 1033 cm^{-1}.[52] Since this band had not appeared in any of the earlier work, for example, that with the dichloroethenes, the possibility of reaction of Cd with oxygen from an air leak was considered, in analogy to the spontaneous reaction of Ge atoms with O_2 upon codeposition in Kr, to form O_3 and GeO.[53] Too, Cd and O_3 react spontaneously, to form CdO, CdOO or CdO_3,[54] but no CdO_x absorptions were observed in any spectra. Furthermore, an air leak large

enough to produce detectable amounts of ozone, but no detectable increase in the pressure in the cryostat, seems unlikely. Since the impurity was not photochemically active, it was deemed of minimal interest for the present purpose.

Photolysis

For studies done in the UV spectrophotometer, only the D_2 source could be used to irradiate the sample as described above, because the Knudsen cell deposition apparatus was mounted in the only cryostat port not blocked by the spectrometer frame. For IR spectroscopic studies, photolysis was performed with one of two sources. The 1000-W Hg-Xe arc lamp described previously provided a continuum down to 200 nm, the air cutoff, and was used in conjunction with a one-inch aperture near the sample to minimize radiative heating of the sample holder. Interference or cutoff filters were employed to select portions of the wavelength range, with specifications as follows: 325 nm interference filter, λ_{max} = 325 nm, T_{max} = 7.1%, FWHM = 29 nm (same as filter "a" in reference 37); 280 nm cutoff filter, 0% T at 270 nm, 5% at 280 nm, 12% at 290 nm. The Nd:YAG-pumped dye laser was used with DCM dye (Exciton) in electronics-grade methanol; frequency-doubled, this could be tuned to the Cd ($^3P_1$) resonance at 315 nm in Kr matrix.

In the work discussed in Chapters I and II, a matrix sample was deposited from the "back" of the cryostat, so that after rotating the sample 180°, it could be illuminated from the front, with the light directly impinging on the sample. Unfortunately, the geometry of the sample compartment of the IR44 instrument necessitated mounting the Knudsen cell chamber on the front port of the cryostat shroud. Thus irradiation was accomplished by reflecting

the source beam off two mirrors mounted at right angles, as in the diagram below.

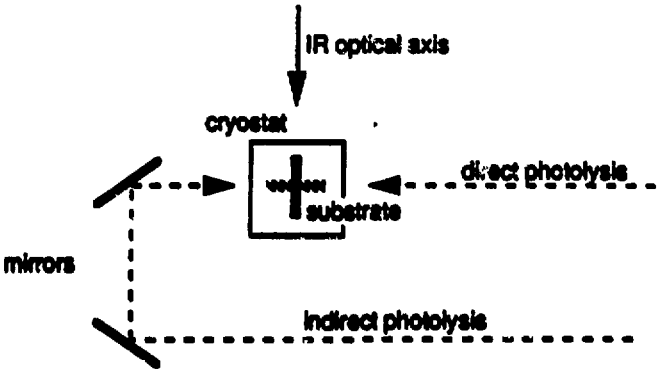

This certainly resulted in a lower photolysis efficiency, due to losses both from imperfect alignment and, particularly in the shorter wavelength regime, from the fact that the mirrors were not selected for high UV reflectance. Since adequacy of the photon flux was of much concern in the sensitization experiments, the optical alignment of the photolysis setup was reproduced and the lamp power measured with a Scientech 380105 meter through various filters. While the actual power levels obtained are not considered accurate, comparison of the power recorded through a Corning 7-54 filter (bandpass 224-400 nm) with and without the mirrors in the optical path (equivalent to direct vs. indirect photolysis) indicates that total mirror losses in the UV were approximately 50%. For the actual experimental setup, fluorescence from a card held in front of the photolysis window indicated that at least some UV light was reaching the sample. It can be assumed that photolysis is direct unless otherwise noted.

RESULTS: Cd Absorption Studies

In order to test the Knudsen cell and determine optimum deposition parameters, samples of cadmium in argon, krypton, and xenon matrices were prepared and UV absorption spectra recorded. Of particular interest was the ability to prepare a sample of isolated Cd atoms at a desired concentration, minimizing the quantities of cadmium dimers and higher aggregates. The majority of the studies were done in Ar matrix, for reasons that will be discussed later, but some experiments were also performed in Kr and Xe.

Cd in Ar Matrix

As the spectra in Figure 3 show, at high dilutions (M/R = 10^{-3}-10^{-5}), a single strong feature was recorded with maxima at 219.6 and 221.5 nm and a tail to 237 nm, and with a full width at half-maximum absorbance (FWHM) of 1150 cm^{-1}. This feature appeared sometimes as a doublet and other times as an uneven triplet. At dilutions from 10^{-5} to 10^{-4}, the relative intensity of the 237 nm tail increased and additional features appeared, a doublet at 204.4/205.6, a broad, stronger band at 272.7 and one at 260.3 nm, as well as a weak, narrow band at 311 nm (FWHM 520 cm^{-1}). A weak, broad band at 247 nm became visible at M/R $\leq 10^{-4}$.

Several absorption features were irradiated with the spectrometer deuterium source in order to look for evidence of photoaggregation. Irradiation at the central wavelength of the strongest feature (221.0 nm, 30 min) and on its shoulder (234.8 nm, 20 min) caused neither bleaching of this feature nor growth of others. Likewise, irradiation of other bands at 273.0 nm (90 min), 261.0 nm (60 min), and 205.0 nm (10.5 h) caused no spectral changes.

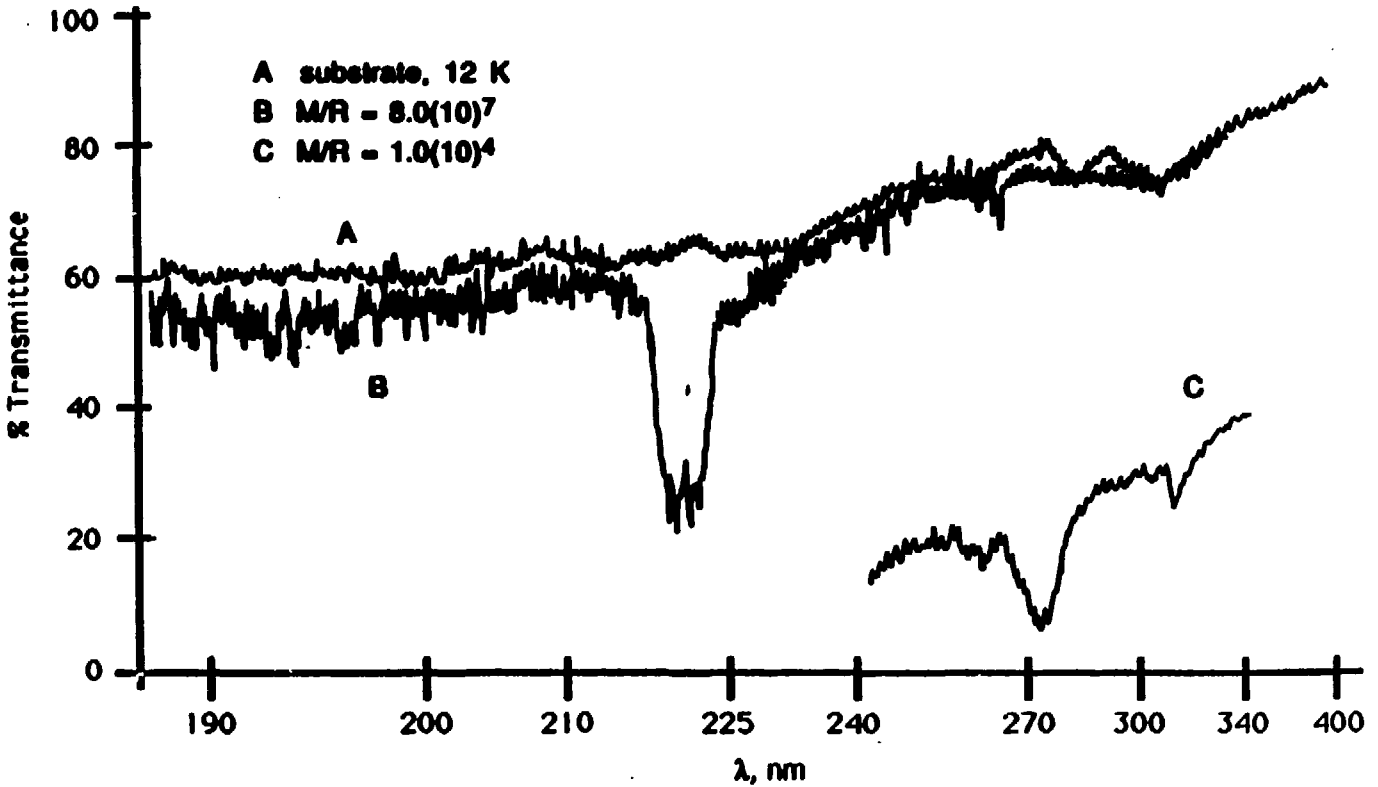

Figure 3: UV Spectra of Cd in Ar Matrix

Cd in Kr Matrix

A single strong absorption appeared at high dilution (M/R = 122,000), a triplet with maxima at 225.4, 226.7, and 228.1 nm and with a shoulder at 236 nm, seen in Figure 4. Continued deposition at M/R = 11,400 resulted in features further to the blue at 201.5 and 209.3/210.7, and higher-wavelength absorptions at 253, 266.5, and 277 nm, while a sharper feature appeared at 315.1 with a shoulder at 316.8 nm.

For one spectrum of a Cd/Kr sample, the integrated absorbance of the principle feature near 226 nm, including shoulders, was determined as follows. Since the data were collected in transmittance units, the spectrum in the region of interest (246-215 nm) was first manually converted to absorbance, the baseline (spectrum of the cold substrate) normalized out, and the scattering due to the matrix (assumed to be linear) subtracted. The spectrum was then plotted linearly in ν and graphically integrated to obtained a total absorbance of 2484 cm^{-1} for this feature.

Cd in Xe Matrix

Only low Cd concentrations could be studied in Xe, as this matrix strongly scatters UV light and samples became optically opaque before sufficient Cd/Xe was deposited for higher-concentration samples. The sole feature observed in Xe at M/R = 146,000 was a strong, sharp triplet at 233.6, 235.0, and 236.3 nm, displayed in Figure 5. The most concentrated sample studied (M/R = 82,000) showed no additional bands.

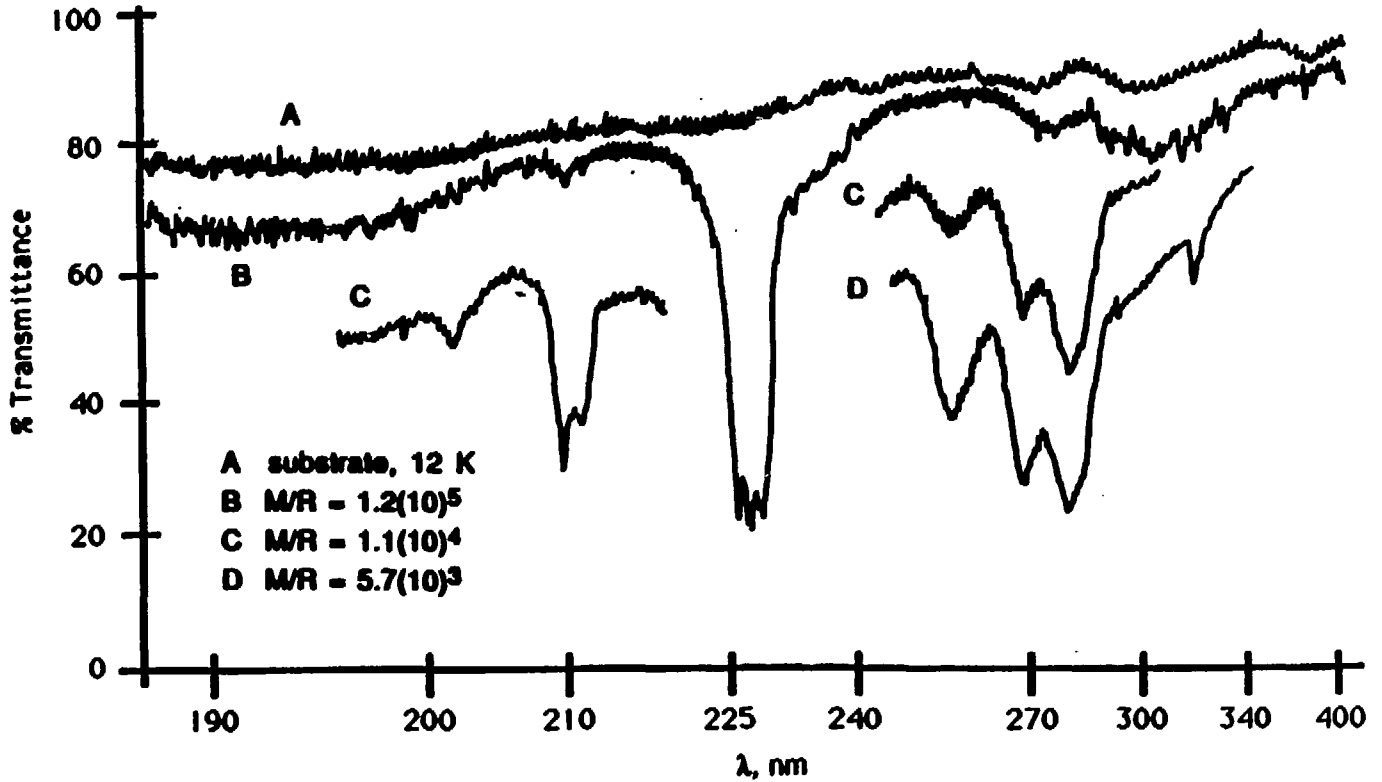

Figure 4: UV Spectra of Cd in Kr Matrix

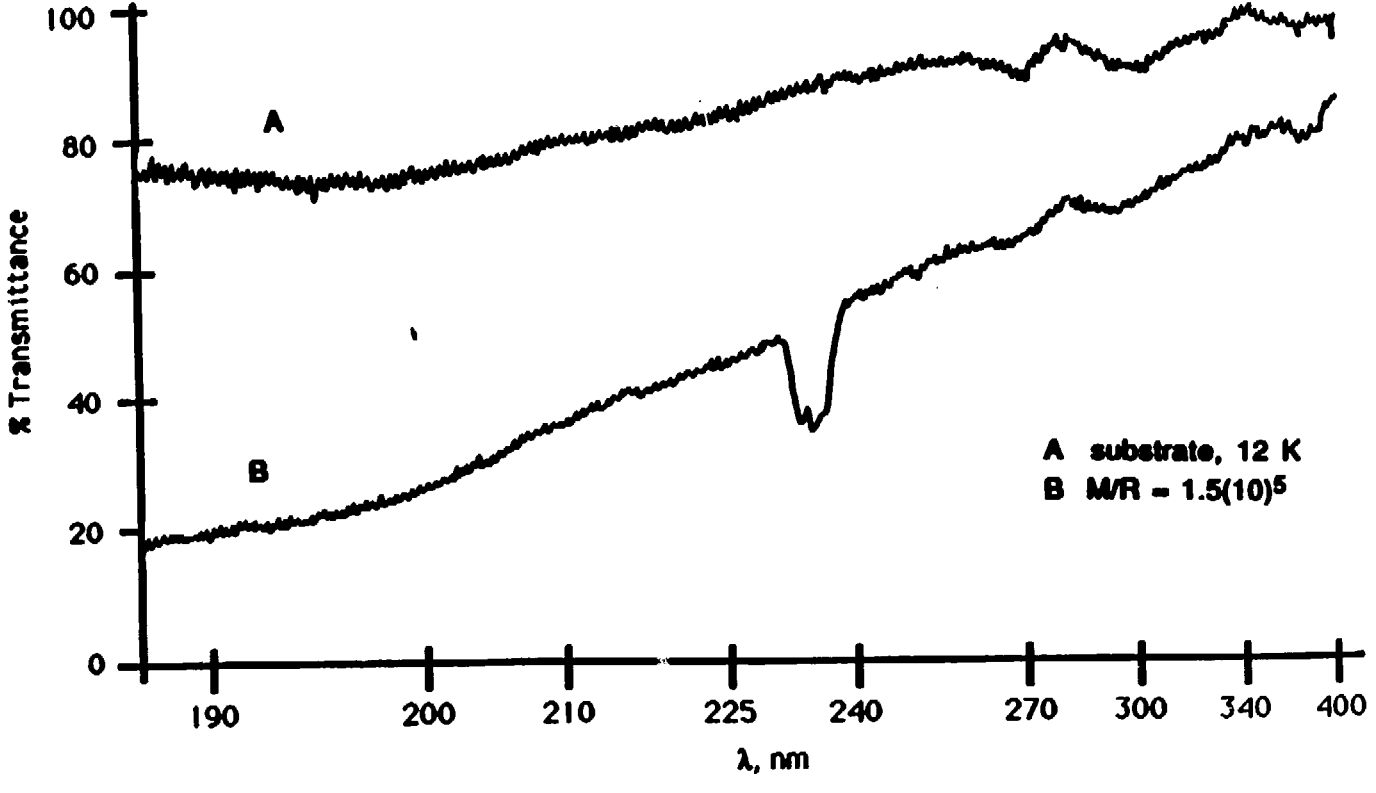

Figure 5: UV Spectrum of Cd in Xe Matrix

DISCUSSION: Cd Absorption Studies

As one of the lower-melting metals, cadmium is experimentally practical and thus its absorption spectrum in rare gas solids has been studied several times previously.[55,56,57] Assignments of both atomic and multimeric features have been made, and no major discrepancies are reported here. Thus the purpose of this section is to analyze the experiments done to characterize the Knudsen cell and to show that the new apparatus gives improved results over the device used in preliminary Cd photosensitization studies.[57] The spectroscopy of Cd will not be discussed in detail, as this was done thoroughly in the earlier work and thus is not new information. Furthermore, the spectrometer has deteriorated such that the present spectral data, although in agreement with that of Cartland and others, is of poorer quality. However, some interesting observations have been made, particularly with regard to matrix effects on oscillator strength and frequency shifts, and are discussed both in terms of their innate interest and their influence on metal atom photochemistry.

Assignment of Absorption Spectra

Cd in Ar Matrix. The positions of the observed absorption features match, within the experimental uncertainty, those seen by Cartland[57] and thus are accordingly assigned, as noted in Table 2. The first spectral feature to appear, at 221 nm, is easily identified as the Cd ($^1P_1 \leftarrow {}^1S_0$) atomic aborption. The triplet structure noted by Cartland and discussed in terms of Jahn-Teller effects[58] is not reproducibly resolved, although the structure which could be resolved in this study is consistent with the previous discussion. The line at

Table 2: Cd Absorption Features in Rare Gas Solids

Cd/Ar[a] λ, nm	Cd/Kr[a] λ, nm	Cd/Xe λ, nm	Assignment
	316.8		
311	315.1		Cd ($^3P_1 \leftarrow {}^1S_0$)
272.7	277		Cd_2 ($^1\Sigma^+_u \leftarrow {}^1\Sigma^+_g$)
260.3	266.5		Cd aggregate
247	253		Cd aggregate
	228.1	236.3	
221.5	226.7	235.0	Cd ($^1P_1 \leftarrow {}^1S_0$)
219.6	225.4	233.6	
205.6	210.7		
204.4	209.3		Cd_2 ($^1\Pi_u \leftarrow {}^1\Sigma^+_g$)
	201.5		Cd aggregate

[a]Not all features observed in all spectra; see text.

311 nm is the ($^3P_1 \leftarrow {}^1S_0$) transition, again with structure that is irreproducible, but not inconsistent with Cartland's findings.

Some of the remaining features are also easily identified, such as the transition to the lowest Cd_2 excited state, ($^1\Sigma^+_u \leftarrow {}^1\Sigma^+_g$), at 272 nm.[59] The signal-to-noise ratio of the data and the inability to perform scale expansion do not permit resolution of the vibronic structure observed in previous studies. The short-wavelength doublet at 204/205 nm is "reasonably" assigned by Ault and Andrews[59] to absorption to the $^1\Pi_u$ state of the Cd_2 molecule, a transition observed at 221.2 nm in the gas phase.[60] They also discuss the 261 nm feature and attribute it to a Cd aggregate, but later workers from the same laboratory reassign this feature to a mixed ZnCd dimer.[61] However, the intensity of this feature in the present spectra would imply that the cadmium wire in use has a large quantity of zinc impurity, contrary to the stated impurity content of less than 10^{-5}. Furthermore, the published spectrum in the mixed-metal study shows a distinct feature at 261 nm in the Cd (no zinc) experiment, similar to that observed here. Thus, we suggest that the strong 261 nm feature observed in the Zn/Cd experiments and assigned to the mixed-metal species overlaps a weaker feature, which the observations indicate is due to a Cd aggregate species alone.

The 247 nm feature was recorded by Cartland but not by other workers, and its appearance only at long deposition times and higher temperatures suggests that it is also due to a cadmium aggregate. Bands reported by Cartland at 347, 305, 296, 286, 198 and 192 nm were not observed here. If these are due to higher Cd multimers, their absence here suggests that the distribution of Cd cluster sizes produced by the Knudsen cell is more strongly weighted toward the monomer than that produced by Cartland's filament, not

a surprising result. Mixed species of Cd with Ni and Cr from the Cd-wrapped nichrome filament perhaps contribute to the spectral complexity in the earlier work.

The insensitivity of the spectrum to UV irradiation confirms Cartland's conclusion that Cd is not subject to the photoinduced clustering observed for other metal atoms in matrices,[62,63] a fact that was important in the interpretation of the photochemical results.[37,64]

Cd in Kr Matrix. The krypton matrix spectra obtained in the current study agree with the previous work. The spectrum shows transitions to the same atomic ($^1P_1$, $^3P_1$) and dimeric ($^1\Sigma^+_u$, $^1\Pi_u$) states as in Ar, and the 266 nm band corresponds to the 261 nm band in Ar, as indicated in Table 2. Cartland assigns the feature at 202 nm to an aggregate. In contrast to the earlier work, we were unable to observe simultaneously the $^1P_1$ and $^3P_1$ absorptions in Kr or any other matrix.

Cd in Xe Matrix. The ($^1P_1 \leftarrow {}^1S_0$) atomic transition near 235 nm is the only feature observed but is in good agreement with that reported by Cartland. The absence of features due to molecular species and the decreased breadth of the atomic absorption compared to Cartland's data suggest an improvement in the ability to produce a sample of matrix-isolated atoms.

Reduction of Multimer Proportion

The sharpness of the strong absorption first to appear in all matrices, Cd ($^1P_1 \leftarrow {}^1S_0$), indicates that at low concentrations a quite homogeneous sample of isolated atoms is deposited. As deposition proceeds, the atomic absorption develops a significant shoulder and tail, suggesting heterogeneity of substitutional sites (i.e. varying Cd-Xe interactions)[55]

and/or some nonnearest-neighbor (Cd-Cd) interactions which alter the relative energies of the two states involved in the transition.[56]

Due to its intensity, the allowed atomic absorption could not be observed on the same scale as the dimer absorptions, but the forbidden transition to the atomic Cd ($^3P_1$) state and the fully allowed Cd_2 ($^1\Sigma^+_u \leftarrow {}^1\Sigma^+_g$) dimer absorption become visible at similar concentrations. Thus the relative intensities of these two features in Ar were used as a qualitative measure of the proportion of monomer to dimer, although no quantitative study could be done without knowledge of the extinction coefficient for the Cd_2 transition. Since the Cd ($^3P_1$) absorption would be weakest, or most strictly forbidden, in this light medium with lower spin-orbit coupling than Kr or Xe, the absorption spectrum in Ar provided the most severe test of the ability of the oven to dissociate dimers.

Our inability to observe the singlet and triplet atomic features on the same scale is somewhat puzzling, as Cartland was able to do so in both Kr and Xe. One possibility is that in an imperfectly isolated sample, Cd atoms in sites which are neighboring but not within bonding distance may experience a mutual heavy-atom effect. Indeed, interactions of this nature are known to cause electronic perturbations. For example, Ozin's group[65] observes two different Cu_2 species in Xe matrix, one a weakly coupled xenon cage complex, formed in next-nearest-neighbor vacancy sites and with a distinct absorption spectrum from the "normal" dicopper, Cu_2 separated by the gas-phase internuclear distance and isolated in the xenon lattice. If triplet oscillator strengths of such atoms are enhanced relative to a truly isolated atom, excitation of the Cd $^3P_1$ state would be more efficient in the less well-isolated sample. Thus, ironically, technical improvement in the ability to

isolate the metal atom photosensitizer in a matrix may in fact decrease its ability to absorb the light necessary to initiate excited-state chemistry.

Matrix Frequency Shifts

Recent work on the matrix-induced frequency shifts of transition metal atoms in matrices[66] prompted a reexamination of the shifts observed for the group 12 metals. For absorptions of Ru, Os and Ir in Ar, Kr and Xe, as well as for other authors' data on matrix-isolated Ni, Mo, Ag and Au, resonance frequencies correlate linearly with the polarizability of the matrix, whereas Y, Rh, Pd and Pt show strong deviations in Xe from the slopes extrapolated from the Ar and Kr points. Jeong and Klabunde, in agreement with previous discussions,[67,68,69] interpret this to mean that the major source of the frequency shift is van der Waals interaction of the guest and host, but that additional interactions are involved, particularly in Xe, for the species which do not correlate linearly.

A similar plot of the shifts from the gas phase for Zn, Cd and Hg (table 3 and figure 6) also shows essentially linear behavior, consistent with the metals previously studied. One very striking feature of this plot, which differs from the previous study, is that the lines fall into two distinct groups based on slope and degree of linearity. Furthermore, the groupings are related to the upper state of the transition, $^1P_1$ or $^3P_1$. The plots for the triplet transitions are much less steeply sloped than the singlet plots, indicating that the triplet transition frequencies vary less strongly with matrix. Too, all the triplet data points are above zero, or blue-shifted from the gas phase, while the singlet transitions exhibit a red shift in xenon. Finally, the triplet plots are nearly perfectly linear, while the singlet plots show a positive deviation of the xenon points compared to the extrapolated Ar-Kr slopes. The fact that a

Table 3: Atomic Transitions of Group 12 Metals in Rare Gas Solids[a]

Medium	Transition	λ(Zn), nm	λ(Cd), nm	λ(Hg), nm
gas phase[b]	$^3P_1 \leftarrow {}^1S_0$	307.7	326.2	253.7
	$^1P_1 \leftarrow {}^1S_0$	213.9	228.9	184.9
Ar	$^3P_1 \leftarrow {}^1S_0$	297[c]	312.4	245.8[e]
	$^1P_1 \leftarrow {}^1S_0$	206.9	221.0	178.5[d]
Kr	$^3P_1 \leftarrow {}^1S_0$	301[c]	316.0	248.9
	$^1P_1 \leftarrow {}^1S_0$	212.5	226.6	183.5[d]
Xe	$^3P_1 \leftarrow {}^1S_0$	—	322.8	253.2
	$^1P_1 \leftarrow {}^1S_0$	213.9	228.9	184.9

[a]from reference 57; wavelengths listed are approximate band centers.

[b]from reference 70.

[c]from reference 59.

[d]from reference 71.

[e]from reference 72.

Figure 6: Frequency Shifts from the Gas Phase Of Group 12 Metal Atom Absorptions In Rare Gas Matrices

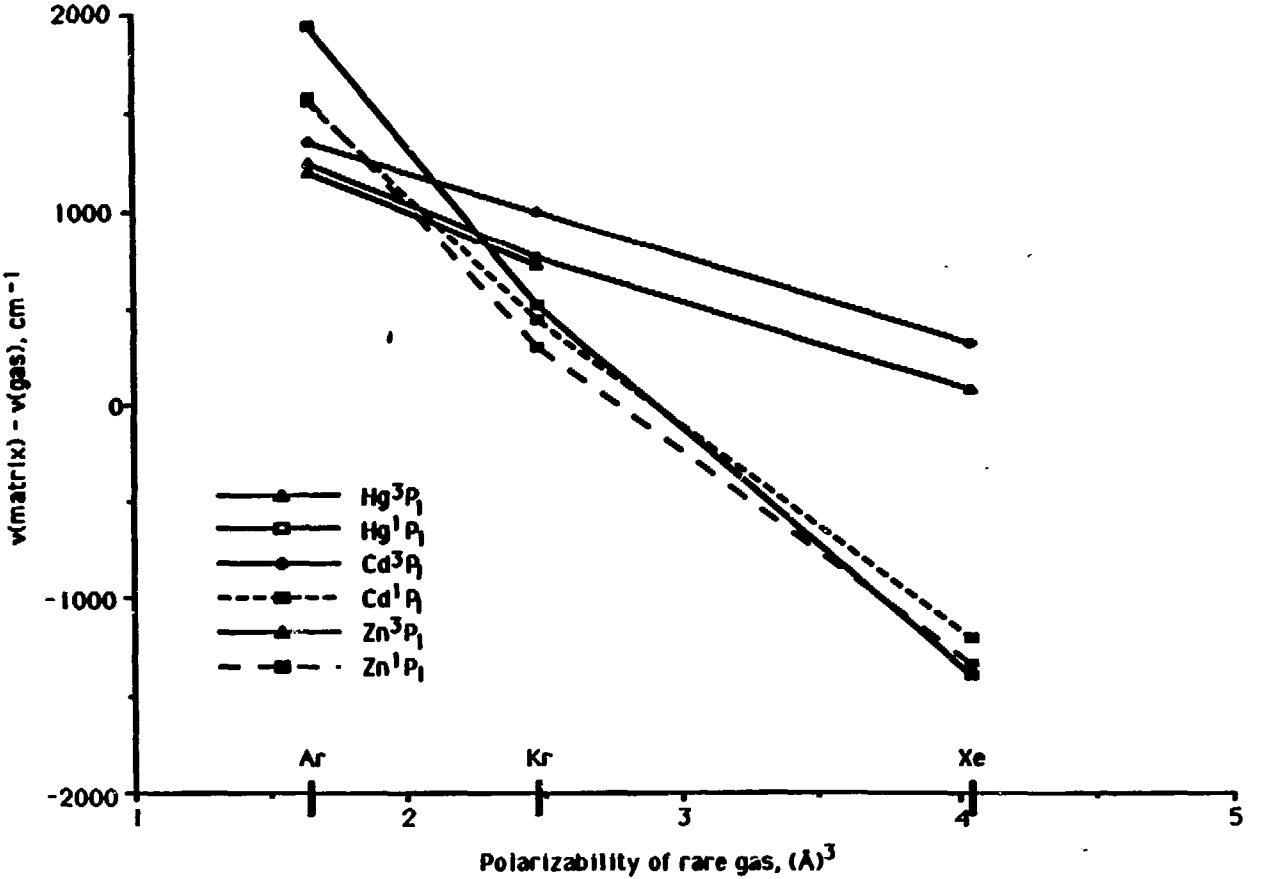

plot of the relative shift, $\Delta\nu/\nu$, shows the same slope and shape characteristics for each group as does Figure 6, demonstrates that these trends are unambiguously related to the states involved in the transition, rather than simply to the absolute absorption frequency.

Jeong and Klabunde attribute the deviations observed for some metal atoms in Xe to formation of a weak complex with the highly polarizable xenon, noting that the more polarizable metals showed greater xenon effects. We observe the same deviation for the singlet transitions of the group 12 metals, yet not for the triplet transitions. Recent molecular beam investigations of excited states of van der Waals complexes formed between Cd and rare gases (Rg)[26,27] are helpful in explaining this behavior. As seen in the table below, the binding energies of the CdRg ground states vary little throughout the rare gas series, while the excited state binding energies are not only larger, but increase quite dramatically as the polarizability of the rare gas increases.

species	D_e, cm^{-1}:	$X\,^1\Sigma^+$	$A\,^3\Pi_0$	$C\,^1\Pi_1$
CdNe		39	77	89
CdAr		96	325	544
CdKr		123	513	1036
CdXe		176	*	*

**data from references 26 and 27; CdXe bound excited states not observed due to competing deactivation processes.*

Since the excited states of the higher members of the molecular series experience greater stabilization, one predicts for the matrix an increase in upper-state stability, and thus a decrease in absorption frequency from the

ground state, with increasing Rg polarizability, precisely as is observed. The particular frequency of absorption, and its relation to the gas-phase resonance, depend on the shape of the upper potential curve in the Franck-Condon-accessible region, and thus cannot be predicted simply from well depths.

The tabulated data also show that the first singlet excited states of the complexes, $C\ ^1\Pi_1$, which correlate with Cd $^1P_1$ + Rg, are strongly bound, while the low-lying $A\ ^3\Pi$ states, which correlate with Cd (^3P_J) + Rg, are more weakly bound. In the matrix, an analogous effect is expected: The singlet states are more strongly influenced by the rare gas than the triplets, hence show much greater variation with matrix, just as seen in Figure 6. As Funk *et al.* note for the van der Waals molecules, the principle difference in the $C\ ^1\Pi_1$ and $A\ ^3\Pi$ states lies in the spatial characteristics of the Cd *p* orbital in the singlet vs. triplet states. Electron correlation causes the ^3P *s* and *p* electrons to spend more time further apart, thus increasing electron-nucleus attraction and shrinking the effective atomic size. Thus the greater bond strengths for the $C\ ^1\Pi_1$ states are due to the larger polarizability of the Cd $^1P_1$ state and the larger spatial extent of the *p* orbital in that state. Upon surrounding the metal atom with a full shell of Rg species, as in a matrix, similar, or even more pronounced, effects are obtained.

Thus, the findings relating the size of the matrix frequency shift to the multiplicity of the excited state are seen to be consistent both with previous findings on matrix frequency shifts and with gas phase investigations of van der Waals bonding. In addition, comparison of stabilities of electronic states of rare gas van der Waals molecules successfully predicts the matrix trends, although not the absolute frequencies. The $M(Rg)_n$ complex present

in a matrix may be modeled, at least qualitatively, by the simpler, monocomplexed, MRg van der Waals molecule. Clearly the interactions between guest and host in a matrix are complex. While, on the one hand, this may complicate the process of identifying and understanding the electronic spectrum, and lessen the directness of its relation to the gas-phase spectrum, it also provides a very sensitive probe of the nature of the interactions between the guest and "inert" host.

Calculation of Cd Oscillator Strength

To test the validity of deposition rates calculated assuming ideal Knudsen effusion, the oscillator strength of the Cd ($^1P_1 \leftarrow {}^1S_0$) absorption in Kr matrix was determined from the UV spectrum, for comparison to the known experimental value in the gas phase. The atomic oscillator strength f_{nm} for a transition between states m and n is

$$f_{nm} = \left(\frac{m_e c^2}{\pi e^2}\right) \int \sigma(\nu) d\nu$$

where m_e and e are the mass and charge of the electron, c is the speed of light, and the integral is the total absorption cross section, with ν in cm^{-1}.[57,73] In the solid state, an electric field correction factor F must be included, which for an isotropic crystal can be expressed in terms of the refractive index n as

$$F = \frac{9n}{(n^2+2)^2}$$

For Kr at 4 K, the refractive index is 1.28,[74] and thus F = 0.87. The absorption cross section can in turn be expressed (here in unintegrated form) as

$$\sigma(\nu) = \frac{A(\nu)}{N l (\ln 10)}$$

where A(v) is the absorbance and Nl is the concentration, expressed in units convenient for matrix samples, atoms/cm^2. When integrated over v, A(v) is just the total absorbance determined from the spectrum, 2484 cm^{-1}, and the constant Nl is calculated via the Knudsen effusion equation, discussed previously. For this particular experiment, the deposition was done in two stages: a 34-minute codeposition at an average temperature of 410 K, followed by a 67-minute deposition at 435 K. This yields a total of 5.95(10^{-6}) mmol deposited over a target area of 2.8 cm^2, to give a concentration Nl of 1.28(10^{15}) atoms/cm^2. The total integrated absorption cross section is thus 8.43(10^{-13}) cm, and the oscillator strength f_{nm} for the observed transition in Kr is 0.829.

This agrees surprisingly well with the gas phase experimental value of 1.20.[75] As an immediate consequence, such agreement inspires confidence in the use of Knudsen effusion rates to determine metal concentrations of matrices deposited with this apparatus. In contrast, the value calculated by Cartland[57] for the Hg ($^3P_1 \leftarrow {}^1S_0$) transition in Kr matrix, 1.8(10^{-3}), was over an 'order of magnitude smaller than the gas phase value of 2.55(10^{-2}).[70] As graphical integration of the absorption feature was employed in the present calculation, rather than the approximation used by Cartland,

$$\int \sigma_v dv \cong \sigma_{max} \Delta v_{1/2}$$

this may have improved the accuracy of the calculation. As Cartland correctly notes, however, the Hg ($^3P_1 \leftarrow {}^1S_0$) line shape is "well-behaved," and thus it seems unlikely that this approximation could be the source of such a large deviation.

More interesting are the possible physical bases for a real difference in the two cases, Hg and Cd. Differences in oscillator strength in solution are usually attributed to a solvent perturbation of the electronic transition.[73] Since the same matrix material, krypton, was used in both experiments, the matrix alone cannot be responsible for the effects demonstrated here. However, the transitions studied were qualitatively quite different, one a fully allowed singlet-singlet transition and the other a singlet-triplet transition. Since the ground state is $^1S_0$ in both cases, if singlet and triplet excited states interact differently with the matrix cage, a large difference in the medium dependence of oscillator strength for the two types of transitions might result, as indeed has been noted for frequency shifts.

Gruen[67] is one of the few authors to discuss oscillator strengths of electronic transitions of metal atoms in matrices, helpfully concluding that "f values can be expected to increase, decrease, or remain relatively unaffected." He notes that for a number of transition metals in matrices, f_{nm} values are one to two orders of magnitude lower than values determined from gas-phase emission measurements. For another example, however, that of Au ($^2P \leftarrow ^2S$) in Ar, Kr and Xe, matrix f_{nm} values are in good agreement with the gas-phase numbers, although with an intriguing downward trend in the order Ar > Kr > Xe, a trend which, if general, may well account for the lack of observation of an external heavy atom effect for Hg absorption spectra.[76] Some gas-phase results are relevant to this problem as well; for example, the decline in oscillator strengths for the Hg ($^3P_1 \leftarrow ^1S_0$) absorption under high pressures of foreign gas. Finally, calculations for the $X \leftarrow A$ transitions of LiHe and NaHe give decreasing f_{nm} values with decreasing M-He distance along the molecular axis, suggesting that matrix f_{nm} values may have a site

dependence as well as the complicated matrix- and transition-dependent behavior already noted. Far more detailed studies with a more versatile spectrometer would clearly be required to verify and understand these effects, but the oscillator strength calculation remains a useful tool in justifying reliance on Knudsen-derived concentrations.

RESULTS AND DISCUSSION: Excited-State Reactions of Cd with Haloethenes

Results

Vinyl chloride (VCl). The cadmium-photosensitized reaction of vinyl chloride was studied as a test of our ability to generate Cd (^{3}P) in a matrix. Cartland had previously studied this reaction and found that, in krypton matrix, vinyl chloride was inert to direct photolysis (λ > 200 nm), but that strong absorbances due to reaction products were observed when the sample was doped with Cd and illuminated at 325 nm to selectively excite the Cd (^{3}P) state.[40,57]

Indirect photolysis through a 325 nm interference filter for 1.5 h of a 1:340:34,000 Cd/VCl/Kr sample resulted in no products, while continued irradiation for 4.0 h with a 280 nm cutoff filter yielded distinct photoproduct features, a doublet at 746.7 and 734.0 cm^{-1} and another feature at 2766.6 cm^{-1}. An additional 4.7 h unfiltered photolysis (λ > 200 nm) caused growth of these features and of an additional band at 3276.6 cm^{-1}. Samples with a tenfold higher concentration of Cd gave the same, weak, product absorptions after similarly lengthy photolysis times, while an undoped sample of VCl/Kr 1:100 developed no product absorptions after 1.2 h of broadband photolysis, in agreement with the prior work.

2-chloro-1,1-difluoroethene (CDFE). Due to limited success in reproducing previous results with vinyl chloride, another previously studied molecule, 2-chloro-1,1-difluoroethene,[37] was selected to further verify Cd (^{3}P) generation in the matrix. A sample of Cd/CDFE/Kr 1:20:2000, irradiated directly through a 325 nm interference filter for 3.0 h, developed broad infrared absorptions at 1678, 1071, 913, 1253, and 771 cm^{-1}. Continued

photolysis (3.9 h) with the glass cutoff filter (λ > 280 nm) resulted in further growth and sharpening of these features, and additional features at 1732, 656, and 542 cm^{-1} became apparent as well. These features are listed in Table 4 and compared with the previous work, and the difference spectrum is presented in Figure 7.

Discussion of Individual Systems

Vinyl chloride. The initial photoproduct features are readily identified as the HCl stretch (2766.6 cm^{-1}) and ν_3 band of C_2H_2 (746.7, 734.0 cm^{-1}) in the T-shaped complex $HCl{\cdot}C_2H_2$, the degeneracy of the band removed by the HCl cage partner. The less intense ν_5 CH stretch (3276.6 cm^{-1}) appears at longer photolysis times and confirms the product identification. As this hydrogen-bonded complex, the result of HCl elimination, was the primary product observed by Cartland,[40,57] its appearance is a favorable indication of our ability to create Cd-VCl pairs in the matrix and to selectively excite Cd to its triplet state.

However, agreement with the previous work is incomplete, and this discrepancy is rather disturbing. Cartland observed a second product, $(CH_2CH)CdCl$, the product of Cd insertion into the CCl bond, but we observed here no absorptions corresponding to those product frequencies (1380.4, 1347.9, 1337.7, 1242.1, 1004.3/993 cm^{-1}). In addition, for a 1:55:5500 sample Cartland saw the complete photoproduct spectrum after only 0.5 h irradiation through a 325 nm interference filter with a maximum transmittance of just 10.3%, while full lamp intensity and much longer photolysis times were required in these experiments.

Table 4: Product of 325 nm Photolysis of Cd/CDFE/Kr

Cd-CDFE this work ν, cm^{-1}	Cd-CDFE ref. 37 ν, cm^{-1}	parent CDFE ref. 37[a] ν, cm^{-1}	Assignment
3260	3253.9		?
		3134.8	CH stretch
1732	1711.0	1771.9	?
1678	1679.7	1742.2	CC stretch
1659			
1253	1250.0	1325.0	CF_2 sym. stretch
1071	1092.2	1195.3	CH i.p. bend
913	917.2	968.8	CF_2 asym. stretch
771	770.3	840.6	CH o.o.p bend
	567.2	764.0	
656	655.2	753.1	CCl stretch
542	560.9	576.5	CF_2 wag

[a]Parent spectrum verified experimentally in this work.

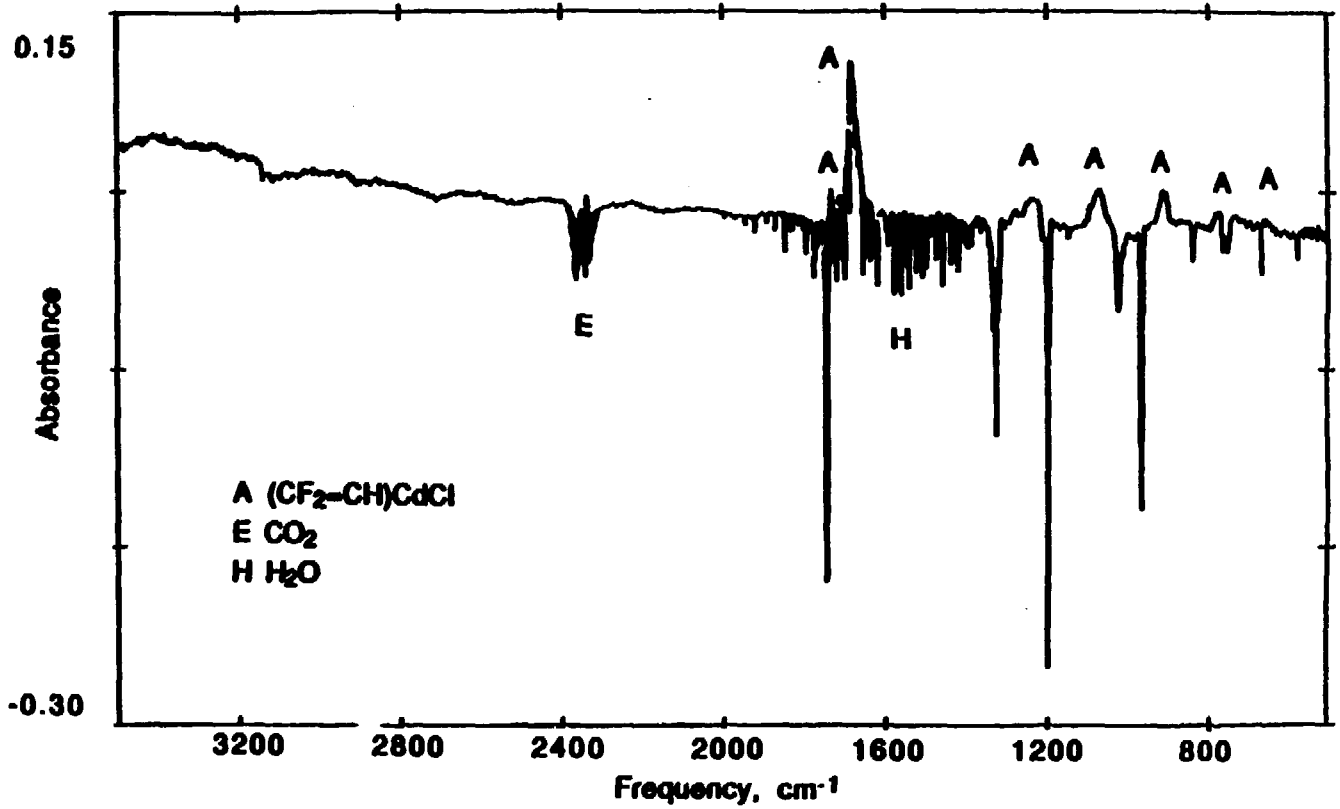

Figure 7: Difference Spectrum of Cd/CDFE/Kr 1:20:2000 at 12 K, after 3.0 h λ = 325 nm and 3.9 h λ > 280 nm photolysis

2-chloro-1,1-difluoroethene. Comparison of the product frequencies with those seen before (table 4) shows that the photoproduct formed in these experiments has similar, but not identical, absorptions to the product identified by Cartland as $(CF_2CH)CdCl$.[37] Most bands undergo frequency shifts of 2-21 cm^{-1}. However, as the bandwidths are broad in both this and the prior work, both sets of frequencies fall within the bandwidth and thus can be considered the same within experimental error. Thus it is concluded that the photoproduct observed here is the same Cd insertion product previously reported, with a slightly perturbed infrared spectrum perhaps related to the different deposition and photolysis conditions of the experiment. The observation of metal atom photochemistry is reassuring. Hydrogen chloride elimination from vinyl chloride gives only indirect evidence of Cd (^3P) participation, but the metallorganic product requires the involvement of both the cadmium atom and the energy it carries, and thus affirms the presence of triplet Cd in the matrix. Again, though, the long photolysis times required to distinguish the product spectrum indicate that Cd (^3P) excitation is rather inefficient, as in the case of vinyl chloride.

General Discussion

The experiments with vinyl chloride and chlorodifluoroethene were intended merely to confirm that the experimental apparatus was operating as expected, but given the difficulty in reproducing the previous results, some general discussion is warranted. Two main experimental parameters control the generation of Cd (^3P) in the matrix: the number of photons available at the sample, and the ability of deposited Cd to absorb them. As noted above, the necessity of adding two mirrors to the optical train reduced photolysis efficiency, but only by a factor of two, much less than the

observed slowdown. Furthermore, experiments done with the photolysis beam directly impinging on the sample did not give significantly different results. The elderly 325 nm interference filter accounts for another inhibition, as its maximum transmittance had decreased to 7.1% from 10.3% in the earlier study. However, use of a cutoff filter in lieu of the narrow bandpass filter increased the photon flux by over an order of magnitude, yet photolysis times were not significantly reduced. This procedure would compensate as well for any loss of wattage due to aging of the Hg-Xe source.

The other factor, the ability of Cd to absorb the resonant photons, is a more likely culprit. One possibility, insufficient Cd concentration, received much attention but was satisfactorily eliminated by variation of the concentration among samples and verification of the Knudsen concentration by the oscillator strength calculation discussed earlier. Severe inhomogeneity of the sample, such that the concentration of Cd atoms was locally low in the area of the substrate sampled by the IR beam, also seems unlikely. Typically, upon removal from the cryostat after an experiment, the substrate appeared to be evenly coated with a metal film. A remaining possibility involves the extinction coefficient of the ($^3P_1 \leftarrow {}^1S_0$) Cd transition in the sample. If, for reasons of more thorough Cd isolation as mentioned in the discussion of absorption spectra, this coefficient were lower in these samples than in those prepared by Cartland, the population of excited cadmium in the sample would be diminished and perhaps inadequate to cause product formation in amounts detectable in these experiments.

RESULTS AND DISCUSSION: Excited-State Reactions of Cd with Hydrocarbons

Results: Cycloalkanes

Cyclopropane (CP). The infrared spectrum for a sample of cyclopropane (CP) 1:100 in Kr agreed with literature spectra.[77,78] Doping with Cd did not alter the spectrum.

Two hours of glass-filtered irradiation ($\lambda > 280$ nm) of Cd/CP/Kr 1:41:4100 induced two very weak infrared bands at 1182.1 and 905.5 cm^{-1}, the former near a parent absorption at 872.5 and the latter near an weak, unidentified band at 1185 cm^{-1} in the deposition spectrum. These did not intensify with continued photolysis, nor did parent absorptions disappear. These bands were not reproduced, nor were other changes in the spectrum discernible, after 6.1 h of dye laser irradiation at 315.0 nm, with an average power of 2.6 mW (0.26 mJ/pulse at 10 Hz).

Cyclobutane (CB). A matrix of c-C_4H_8/Kr 1:100 at 12 K exhibited infrared bands corresponding to the gas-phase frequencies.[78] No spectral changes were observed when the CB/Kr mixture was codeposited with Cd. Four hours of indirect, filtered ($\lambda > 280$ nm) light from the Hg-Xe arc lamp caused no parent loss or product growth in a 1:6:620 sample of Cd/CB/Kr. Subsequent exposure for 9.7 h to the unfiltered arc had no additional effect.

Results: Alkynes

Acetylene. The infrared spectrum of Cd/C_2H_2/Kr 1:8:800 agreed with previous data for matrix-isolated acetylene.[79] Weak bands at 1964.5 and 630.1 cm^{-1} fall near symmetry-forbidden absorptions of acetylene at 1964 (ν_2, CC stretch) and 631 cm^{-1} (ν_4, symmetric CH bend), possibly indicating

perturbation by a Cd cage partner. Irradiation for 7.0 h with the filtered Hg-Xe lamp ($\lambda > 280$ nm) initiated growth of a strong, broad band at 2098.8 cm^{-1}. Equipment failure prevented reproduction or further investigation of this result.

Methylacetylene (MA). A spectrum of Cd/CH_3CCH/Kr 1:15:1500 was consistent with the argon-matrix spectrum of methylacetylene (MA),[80] taking into account the expected matrix shift of a few wavenumbers. Illumination of this sample for 4.4 h with the 280 nm cutoff filter and 3.5 h unfiltered brought about no spectral differences ascribable to photoproduct formation.

Discussion

Selection of molecules for studies of chemistry with electronically excited metal atoms involves a complex array of factors. As one major interest was to differentiate between singlet- and triplet-sensitized chemistry, molecules were considered good candidates if their photochemistry was known or suspected to be different on singlet and triplet surfaces. Multiple reaction paths, to allow the possibility of changes in product branching ratios, were also favorable indicators. Energy transfer requires excited states with energies less than or equal to the Cd excitation energies, 125 kcal/mol for singlets and 89 kcal/mol for triplets. Finally, the detection scheme necessitates that both parent and possible products have simple and assignable IR spectra.

Cycloalkanes. A number of favorable characteristics led to the selection of cyclopropane as a likely reactant for Cd photosensitization studies. The possibility of formation and trapping of a metallacyclobutane intermediate

was particularly appealing, as such species are of synthetic and catalytic interest.[41,81] Previous matrix workers found that the CC bond of cyclopropane could be activated with relative ease by metal atoms. Iron atoms are reported to insert into the ring when irradiated during codeposition with cyclopropane and argon,[82] and Ni inserts spontaneously upon cocondensation[77] with c-C_3H_6 and Ar. In the gas phase, unligated metallacyclobutane ions have been observed as reaction products of translationally excited metal ions with cyclopropane.[83]

Furthermore, a number of hydrocarbon products can be formed from the starting materials, providing possibilities for photochemical branching. The energetic situation for the various channels is favorable, too. Insertion of a metal atom into the ring is predicted to be no more than a few kcal/mol endothermic, by analogy with a calculation of ΔH = 6 kcal/mol for Pd insertion to form palladacyclobutane.[84] Isomerization of cyclopropane to propene is 8 kcal/mol exothermic,[85] thus placing the lowest propene triplet excited state almost exactly isoenergetic to Cd (^3P) + c-C_3H_6.[86] Other potential product channels within energetic reach of either singlet or triplet cadmium excited-state energies include formation of ethylene + CH_2 or $CdCH_2$; C_3H_4 (propyne or allene) + H_2 or CdH_2; or insertion of Cd into the CH bond. The infrared spectra of these products and the parent are simple, and many are available in the literature.

Encouraging precedent was drawn as well from gas-phase studies of the mercury-sensitized chemistry of cyclopropane. Excitation of Hg (^3P) in the presence of 1,2-dideuterocyclopropane leads to cis-trans isomerization, but no mono- or trideuterocyclopropane formation, meaning that no H-D exchange takes place.[87] Thus reaction is believed to occur not through a

free radical mechanism but via an excited triplet diradical, a species which seemed plausible as a precursor to ring insertion of the metal atom.

One objection to the cyclopropane system is raised by thermochemical considerations. Relief of ring strain has been claimed to drive ring-opening in metal insertion,[88] but since cyclobutane has a higher strain energy (28 kcal/mol) than cyclopropane (27 kcal/mol),[89] it is not clear that the four-membered metallacycle will in fact be significantly lower in energy than cyclopropane. Indeed, Beauchamp and coworkers have determined strain energies of cobaltacyclobutane and ferracyclobutane to be nearly as high as cyclobutane, 22 and 18 kcal/mol, respectively.[83] However, cyclopentane is nearly unstrained (5 kcal/mol),[89] thus insertion of a metal atom into cyclobutane to form a metallacyclopentane is surely energetically favorable, and the ring strain argument is more persuasive. Therefore, cyclobutane was studied for this more advantageous thermochemistry but presumably otherwise similar photochemistry.

Despite all these apparently favorable indications, both cyclopropane and cyclobutane were quite unresponsive to Cd (^{3}P)-sensitized photolysis. The higher excitation energy of Hg (^{3}P) may be necessary to generate the reactive biradical intermediate, while the involvement of the *d* orbitals is evidently important in the iron and nickel matrix reactions. The problems of Cd oscillator strength and photolysis efficiency discussed before with respect to haloethene-cadmium reactions also continue to be relevant here.

Alkynes. Similar reasoning to the cycloalkane case was employed in selecting the alkynes as reactants in the cadmium photosensitization studies. Reactions of alkynes with metals are of catalytic importance, and matrix

studies may help to model surface processes.[81] In a matrix, acetylene interacts to varying degrees with metal atoms. Vinyl-like complexes have been observed for some transition metals[90] and π-type complexes for others,[90,91] while iron forms a third type of adduct, interacting through the hydrogen atom.[81] Upon UV photolysis (360 nm < λ < 280 nm), this complex reacts to form the CH insertion product, ethynyliron hydride. With propyne, however, iron photoinserts into the CC single bond.[92] Thus both CC and CH bonds are potentially reactive sites.

One particularly intriguing prospect for the Cd-C_2H_2 system is the formation of Cd=C=CH_2. The rearrangement of acetylene to vinylidene has a high barrier, but metal η^2-alkyne complexes rearrange with facility near room temperature.[93] In the proposed scheme, this barrier would be overcome photochemically instead of thermally and the vinylidene moiety covalently stabilized by the metal atom. In fact, the π-adduct of nickel with acetylene undergoes just such a reaction, photochemically rearranging to give nickel vinylidene with long-wavelength (λ > 400 nm) irradiation, while shorter wavelengths regenerate the π complex.[94] *Ab initio* calculations show that the rearrangement of Be (^{3}P) + HCCH to BeCCH_2 ($^3B_2$ ground state) on the triplet surface is both barrierless and quite exothermic (ΔH < -60 kcal/mol),[35] suggesting that this scheme is not an irrational one for ^{3}Cd, which has the same (ns, np) outer electronic configuration as ^{3}Be. Another interesting possible channel is the formation of a metallacyclopropene, which can be thought of as a tightly bound metal η^2-alkyne complex.[95] Only metal-ligated examples are known at ordinary temperatures,[96] but matrix conditions provide an optimal opportunity to trap an unligated metallacyclopropene.[95] Finally, like cyclopropane, acetylene has the

advantages of a rich mercury-sensitized chemistry,[3] excited states in the appropriate energy range,[97] and a simple infrared spectrum.

Unfortunately, neither of the alkynes examined yielded substantive evidence of metal atom chemistry. The lone infrared feature observed in one acetylene experiment holds out some possibility of reactivity in that system, but the lengthy photolysis time and lack of accompanying features are not encouraging, although the experiment should be repeated before being written off entirely. Again, perhaps the involvement of *d* orbitals is a prerequisite to reaction, or Cd excitation energies are insufficient, and concentration and oscillator strength problems may again come into play.

CONCLUSIONS

The study of metal atom photochemistry has a long history, yet many questions remain unanswered. The factors that control the competition among the primary photophysical and photochemical events have yet to be fully understood, and for its the ability to stabilize otherwise transient intermediates for leisurely study, matrix isolation photochemistry is one of a number of complementary methods which can contribute to the unraveling of these processes. The group 12 metals are a particularly interesting subset of metal atoms for such investigations, since chemical factors such as valence-shell electron configuration can be held constant while varying spin-orbit coupling and thereby access to reaction surfaces of different multiplicity.

To this end, a Knudsen cell deposition apparatus was designed and found to provide improved control of some parameters involved in matrix sample deposition. As an outgrowth of preliminary spectroscopic studies to characterize the new apparatus, some intriguing matrix- and transition-dependent effects on frequency shift and oscillator strength of matrix-isolated cadmium atoms were recognized. Reactions of excited Cd atoms with several organic substrates were attempted, and despite some experimental difficulties, observation of photoproducts from two haloethenes is evidence that Cd ($^3P_1$) was successfully generated in the matrix. Representatives of other classes of organic molecules, alkynes and the small, highly strained cycloalkanes, were not found to be reactive toward either triplet or singlet excited states of Cd, and some possible reasons, both technical and chemical, for this lack of reaction are suggested.

In summary, although no successful excited-state reactions with cadmium are reported, some promising indications are seen. Clearly selection of appropriate molecules for such studies is a complex endeavor, but one well worth further attention. Thus it is hoped that future studies will provide new details of the dynamics of metal-atom photosensitization and further broaden the understanding of chemistry on electronically excited hypersurfaces.

REFERENCES

[1]Cario, G.; Franck, J. Z. *Phys.* 1922, *11*, 161.

[2]Steacie, E. W. R. *Can J. Res.* 1948, *B26*, 609.

[3]Cvetanovic, R. J. *Prog. React. Kinet.*, ed. G. Porter; Pergamon: Oxford, 1964; pp. 39-119.

[4]Calvert, J. G.; Pitts, J. N., Jr. *Photochemistry*; Wiley: New York, 1966; ch. 2 and references within.

[5]Brown, S. H.; Crabtree, R. H. *J. Chem. Soc., Chem. Comm.* 1987, 970.

[6]Brown, S. H.; Crabtree, R. H. *Tet. Lett.* 1987, 5599.

[7]Brown, S. H.; Crabtree, R. H. *J. Chem. Ed.* 1988, *65*, 290.

[8]Ferguson, R. R.; Crabtree, R. H. *Nouv. J. Chim.* 1989, *13*, 647.

[9]Mayama, S.; Hiraoka, S.; Obi, K. *J. Chem. Phys.* 1984, *80*, 7.

[10]Brazier, C. R.; Ellingboe, L. C.; Kinsey-Nielsen, S.; Bernath, P. F. *J. Am. Chem. Soc.* 1986, *108*, 2126.

[11]O'Brien, L. C.; Bernath, P. F. *J. Am. Chem. Soc.* 1986, *108*, 5017.

[12]Ellingboe, L. C.; Bopegedera, A. M. R. P.; Brazier, C. R.; Bernath, P. F. *Chem. Phys. Lett.* 1986, *126*, 285.

[13]Morten, P. D.; Freeman, C. G.; McEwan, M. J.; Claridge, R. F. C.; Phillips, L. F. *Chem. Phys. Lett.* 1972, *16*, 148.

[14]Yamamoto, S.; Yasunobu, M.; Nishimura, N.; Hasegawa, S. *Mol. Photochem.* **1979**, *9*, 277.

[15]Yamamoto, S.; Yasunobu, M.; Nishimura, N. *Bull. Chem. Soc. Japan* **1981**, *54*, 3677.

[16]Yamamoto, S.; Tanaka, K.; Sato, S. *Bull. Chem. Soc. Japan* **1975**, *48*, 2172.

[17]Breckenridge, W. H.; Realund, A. M. *J. Phys. Chem.* **1978**, *82*, 1484.

[18]Breckenridge, W. H.; Realund, A. M. *J. Phys. Chem.* **1979**, *83*, 1145.

[19]Brady, B. B.; Spector, G. B.; Chia, L.; Flynn, G. W. *J. Chem. Phys.* **1987**, *86*, 3245.

[20]Bras, N.; Butaux, J.; Jeannet, J. C.; Perrin, D. *J. Chem. Phys.* **1986**, *85*, 280.

[21]Bras, N.; Jeannet, J. C.; Perrin, D. *J. Chem. Phys.* **1987**, *87*, 219.

[22]Rettner, C. T.; Zare, R. N. *J. Chem. Phys.* **1981**, *75*, 3636.

[23]Rettner, C. T.; Zare, R. N. *J. Chem. Phys.* **1981**, *77*, 2416.

[24]Jouvet, C.; Duval, M. C.; Soep, B.; Breckenridge, W. H.; Whitham, C.; Visticot, J. P. *J. Chem. Soc., Faraday Trans. II* **1989**, *85*, 1133.

[25]Kovalenko, L. J.; Robinson, R. L.; Leone, S. R. *J. Chem. Soc., Faraday Trans. II* **1989**, *85*, 939.

[26]Funk, D. J.; Kvaran, A.; Breckenridge, W. H. *J. Chem. Phys.* **1989**, *90*, 2915.

[27]Funk, D. J.; Breckenridge, W. H. *J. Chem. Phys.* **1989**, *90*, 2927.

[28]Breckenridge, W. H.; Jouvet, C.; Soep, B. *J. Chem. Phys.* **1986**, *84*, 1443.

[29]Jouvet, C.; Boivineau, M.; Duval, M. C.; Soep, B. *J. Phys. Chem.* **1987**, *91*, 5416.

[30]Wittig, C.; Sharpe, S.; Beaudet, R. A. *Acc. Chem. Res.* **1988**, *21*, 341.

[31]Adams, N.; Breckenridge, W. H.; Simons, J. *Chem. Phys.* **1981**, *56*, 327.

[32]Blickensderfer, R. P.; Jordan, K. D.; Adams, N.; Breckenridge, W. H. *J. Phys. Chem.* **1982**, *86*, 1930.

[33]Chaquin, P. *J. Phys. Chem.* **1987**, *91*, 1440.

[34]Gosavi, R. K.; Strausz, O. P.; Bernardi, F.; Kapur, A.; Mezey, P. G. *J. Phys. Chem.* **1987**, *91*, 283.

[35]Sakai, S.; Morokuma, K. *J. Phys. Chem.* **1987**, *91*, 3661.

[36]Nguyen, M. T. *J. Phys. Chem.* **1988**, *92*, 1426.

[37]Cartland, H. E.; Pimentel, G. C. *J. Phys. Chem.* **1986**, *90*, 1822.

[38]Cartland, H. E.; Pimentel, G. C. *J. Phys. Chem.* **1986**, *90*, 5485.

[39]Cartland, H. E.; Pimentel, G. C. *J. Phys. Chem.* **1989**, *93*, 8021.

[40]Cartland, H. E.; Pimentel, G. C. *J. Phys. Chem.*, in press, 1989.

[41]Hauge, R. H.; Margrave, J. L.; Kafafi, Z. H. *Chemistry and Physics of Matrix-Isolated Species*, eds. L. Andrews and M. Moskovits. Elsevier: Amsterdam and New York, 1989; pp. 277-302, and references within.

[42]Parnis, J. M.; Mitchell, S. A.; García-Prieto, J.; Ozin, G. A. *J. Am. Chem. Soc.* **1985**, *107*, 8169.

[43]Parnis, J. M.; Ozin, G. A. *J. Phys. Chem.* **1989**, *93*, 4023.

[44]Margrave, J. L. *Physicochemical Measurements at High Temperatures*; Butterworths: London, 1959; ch. 10.

[45]Herzberg, G. *Molecular Spectra and Molecular Structure*, 2nd ed.; Van Nostrand: New York, 1950; vol. I, p. 516.

[46]Berkowitz, J.; Tasman, H. A.; Chupka, W. A. *J. Chem. Phys.* **1962**, *36*, 2170.

[47]Ault, B. S. Ph.D. thesis, University of California, Berkeley, 1973.

[48]*1987 Temperature Measurement Handbook and Encyclopedia*; Omega Engineering, Inc.: Stamford, CT, 1986; pp. T54-T56.

[49]Cater, E. D. *Characterization of High Temperature Vapors and Gases*, N. B. S. Special Publication 561, ed. J. W. Hastie. U.S. Department of Commerce: Washington, D. C., 1979.

[50]Vályi, L. *Atom and Ion Sources*; Wiley: London, 1977.

[51]Hultgren, R.; Orr, R. L.; Anderson, P. D.; Kelley, K. K.; eds. *Selected Values of Thermodynamic Properties of Metals and Alloys*; Wiley: New York, 1963.

[52]Spoliti, M.; Nunziante-Cesaro, S.; Mariti, B. *J. Chem. Phys.* **1973**, *59*, 985.

[53]Bos, A.; Ogden, J. S.; Orgee, L. *J. Phys. Chem.* **1974**, *78*, 1763.

[54]Prochaska, E. S.; Andrews, L. *J. Chem. Phys.* **1980**, *72*, 6782.

[55]Duley, W. W. *Nature* **1966**, *210*, 624.

[56]Merrithew, R. B.; Marusak, G. V.; Blount, C. E. *J. Mol Spectrosc.* **1969**, *29*, 54.

[57]Cartland, H. E. Ph.D. thesis, University of California, Berkeley, 1985.

[58]Cartland, H. E. *op. cit.*, pp. 60-63.

[59]Ault, B. S.; Andrews, L. *J. Mol. Spectrosc.* **1977**, *65*, 102.

[60]Cram, S. W. *Phys. Rev.* **1934**, *46*, 205.

[61]Miller, J. C.; Andrews, L. *J. Chem. Phys.* **1978**, *69*, 3034.

[62]Mitchell, S. A.; Farrell, J.; Kenney-Wallace, G. A.; Ozin, G. A. *J. Am. Chem. Soc.* **1980**, *102*, 7702.

[63]Ozin, G. A.; Mitchell, S. A.; García-Prieto, J. *J. Phys. Chem.* **1982**, *86*, 473, and references within.

[64]Cartland, H. E. *op. cit.*, p. 229.

[65]Ozin, G. A.; Mitchell, S. A. *Angew. Chem. Int. Ed. Engl.* **1983**, *22*, 674.

[66]Jeong, G. H.; Klabunde, K. J. *J. Chem. Phys.* **1989**, *91*, 1958, and references within.

[67]Green, D. M. *Cryochemistry*, eds. M. Moskovits and G. A. Ozin; Wiley: New York, 1976; ch. 10, and references within.

[68]Moskovits, M.; Hulse, J. E. *J. Chem. Phys.* **1977**, *66*, 3988.

[69]Grinter, R.; Stern, D. R. *J. Chem. Soc. Farad. Trans.* 2 **1983**, *79*, 1011.

[70]Okabe, H. *Photochemistry of Small Molecules*; Wiley: New York, 1978; pp. 366-67.

[71]Malo, S. A. *J. Chem. Phys.* 1974, *61*, 2408.

[72]Brewer, L.; Meyer, B.; Brabson, G. D. *J. Chem. Phys.* 1965, *43*, 3973.

[73]Calvert, J. G.; Pitts, J. N. *op. cit.*, pp. 172-73.

[74]Hallam, H. E., ed. *Vibrational Spectroscopy of Trapped Species*; Wiley: New York, 1973; p. 45.

[75]King, G. W.; Van Vleck, J. H. *Phys. Rev.* 1939, *55*, 1165.

[76]Cartland, H. E. *op. cit.*, p. 45.

[77]Kline, E. S.; Hauge, R. H.; Kafafi, Z. H.; Margrave, J. L. *Organometallics* 1988, *7*, 1512.

[78]Shimanouchi, T. Report NSRDS-NBS 39; National Bureau of Standards, U.S.: Gaithersburg, MD, June 1972.

[79]Abrash, S. A. Ph. D. thesis, University of California, 1987.

[80]Andrews, L. S. *J. Phys. Chem.* 1984, *88*, 2940.

[81]Kline, E. S.; Kafafi, Z. H.; Hauge, R. H.; Margrave, J. L. *J. Am. Chem. Soc.* 1985, *107*, 7559, and references within.

[82]Kafafi, Z. H.; Hauge, R. H.; Fredin, L.; Billups, W. E.; Margrave, J. L. *J. Chem. Soc., Chem. Comm.* 1983, 1230.

[83]Van Koppen, P. A. M.; Jacobson, D. B.; Illies, A.; Bowers, M. T.; Hanratty, M.; Beauchamp, J. L. *J. Am. Chem. Soc.* 1989, *111*, 1991.

[84]Backvall, J.-E.; Bjorkman, E. E.; Pettersson, L.; Siegbahn, P.; Strich, A. *J. Am. Chem. Soc.* 1985, *107*, 7408.

[85]From bond energies; Mahan, B. H. *University Chemistry*, 3rd ed.; Addison-Wesley: Menlo Park, CA, 1975.

[86]Itoh, M.; Mulliken, R. S. *J. Phys. Chem.* 1969, *73*, 4332.

[87]Setser, D. W.; Rabinovitch, B. S.; Spittler, E. G. *J. Chem. Phys.* 1961, *35*, 1840.

[88]Rajaram, J.; Ibers, J. A. *J. Am. Chem. Soc.* 1978, *100*, 829.

[89]Pimentel, G. C.; Spratley, R. D. *Understanding Chemistry*; Holden-Day: Oakland, CA, 1971; p. 743.

[90]Kasai, P. H.; McLeod, D., Jr.; Watanabe, T. *J. Am. Chem. Soc.* 1980, *102*, 179.

[91]Ozin, G. A.; McIntosh, D. F.; Power, W. J.; Messmer, R. P. *Inorg. Chem.* 1981, *20*, 1782.

[92]Kafafi, Z. H. Personal communication.

[93]Bullock, R. M. *J. Chem. Soc., Chem. Comm.* 1989, 165.

[94]Kline, E. S.; Kafafi, Z. H.; Hauge, J. H.; Margrave, J. L. *J. Am. Chem. Soc.* 1987, *109*, 2402.

[95]Manceron, L.; Andrews, L. *J. Am. Chem. Soc.* 1985, *107*, 563.

[96]March, J. *Advanced Organic Chemistry*, 3rd ed.; Wiley: New York, 1985, and references within.

[97]Lischka, H.; Karpfen, A. *Chem. Phys.* **1986**, *102*, 77.

APPENDIX A:
Thermochemical Relations for the $C_2H_2Cl_2$ System

I. Dichloroethenes.

A. Ground states.

ΔH_f(*trans*-DCE) = +1.2 kcal/mol; ΔH_f(*cis*-DCE) = +1.0 kcal/mol; ΔH_f(1,1-DCE) = +0.6 kcal/mol. Energies for all other species are henceforth relative to *cis*-DCE.

Joshi, R. M. *J. Macromol. Sci. Chem.* **1974**, *18*, 861; cited in Cartland, H. E.; Pimentel, G. C. *J. Phys. Chem.* **1986**, *90*, 5485.

B. Excited states.

1. $^1[C_2H_2Cl_2]^*$: $^1(\pi,\pi^*)$ state, absorption tail to near 240 nm ≈ 120 kcal/mol above ground state.

Berry, M. J. *J. Chem. Phys.* **1974**, *61*, 3114.

2. $^3[C_2H_2Cl_2]^*$: $^3(\pi,\pi^*)$ state, 89-91 kcal/mol above ground state.

Koerting, C. F.; Walzl, K. N.; Kuppermann, A. *Chem. Phys. Lett.* **1984**, *109*, 140.

II. Elimination Products and Related Intermediates.

A. HCl + C_2HCl.

1. Ground state, +23 kcal/mol: from standard bond energies, including -1.8 kcal/mol interaction energy from hydrogen bond.

Barnes, A. J. *J. Mol. Struct.* **1983**, *100*, 259; cited in Cartland, H. E.; Pimentel, G. C. *J. Phys. Chem.* **1986**, *90*, 5485.

2. $^1[HCl]^*$•C_2HCl excited state, +149 kcal/mol: *A* $^1\Pi$ state of HCl, 44,000 cm^{-1} = 126 kcal/mol above ground state.

Herzberg, G. *Molecular Spectra and Molecular Structure*, vol. I; Van Nostrand: New York, 1950; p. 534.

3. HCl•$^1[C_2HCl]^*$ excited state, +138 kcal/mol: from absorption spectrum of C_2HCl, 40,000 cm^{-1} = 115 kcal/mol above ground state.

Evans, K.; Scheps, R. S.; Rice, S. A.; Heller, D. *J. Chem. Soc. Faraday Trans. II* **1973**, *69*, 856.

4. HCl•^{3}[C_2HCl]* excited state, +118 kcal/mol: by analogy with C_2H_2, triplet of same symmetry 20 kcal/mol below lowest singlet.
Lischka, H.; Karpfen, A. *Chem. Phys.* 1986, *102*, 77.

B. $Cl_2 + C_2H_2$.

1. Ground state, +51 kcal/mol: from standard bond energies, including -1 kcal/mol interaction energy.
Carland, H. E.; Pimentel, G. C. *J. Phys. Chem.* 1986, *90*, 5485.

2. ^{1}[Cl_2]•C_2H_2 excited state, +125 kcal/mol or more: $^1\Pi_g$ state, indistinct onset.
Huber, K. P.; Herzberg, G. *Constants of Diatomic Molecules*; Van Nostrand Reinhold: New York, 1979; cited in
Carland, H. E.; Pimentel, G. C. *J. Phys. Chem.* 1986, *90*, 5485.

3. ^{3}[Cl_2]•C_2H_2 excited state, +104 kcal/mol: $^3\Pi_{0^+_u}$ state, 18,310 cm^{-1} = 52 kcal/mol above ground state.
Herzberg, G. *Molecular Spectra and Molecular Structure*, vol. I; Van Nostrand: New York, 1950; p. 519.

4. Cl_2•^{1}[C_2H_2]* excited state, +172 kcal/mol: ^1A_u state, 42,196 cm^{-1} = 121 kcal/mol above ground state.
Herzberg, G. *Molecular Spectra and Molecular Structure*, vol. III; Van Nostrand: New York, 1966; p. 611.

5. Cl_2•^{3}[C_2H_2]* excited state, +146 kcal/mol: ^3B_u ($^3\Sigma^+_u$) state (lowest triplet) 95 kcal/mol above ground state.
Lischka, H.; Karpfen, A. *Chem. Phys.* 1986, *102*, 77.

6. Cl_2•$^1CCH_2$ ground state, +95 kcal/mol: $\Delta E(HCCH \rightarrow CCH_2) = 44$ kcal/mol, plus HCCH ground state energy.
Ervin, K. M.; Ho, J.; Lineberger, W. C. *J. Chem. Phys.* 1989, *91*, 5974; Chen, Y.; Jonas, P. M.; Kinsey, J. L.; Field, R. W. *J. Chem. Phys.* 1989, *91*, 3976.

7. Cl_2•^{3}[CCH_2]* excited state, +143 kcal/mol: $\Delta E(S_0\text{-}T_1) = 48$ kcal/mol, plus Cl_2•$^1CCH_2$ energy.
Ervin, K. M.; Ho, J.; Lineberger, W. C. *J. Chem. Phys.* 1989, *91*, 5974.

C. H_2•C_2Cl_2.

1. Ground state, +39 kcal/mol: from standard bond energies.
Carland, H. E.; Pimentel, G. C. *J. Phys. Chem.* 1986, *90*, 5485.

2. $H_2 \cdot {}^1[C_2Cl_2]^*$ excited state, +154 kcal/mol: by analogy with C_2HCl, 115 kcal/mol above ground state.
Evans, K.; Scheps, R. S.; Rice, S. A.; Heller, D. *J. Chem. Soc. Faraday Trans. II* 1973, *69*, 856.

III. Free Radical Products and Intermediates.

A. H + C_2Cl_2H ground state, +107 kcal/mol: by analogy with H dissociation from vinyl chloride.
Cartland, H. E.; Pimentel, G. C. *J. Phys. Chem.*, in press, 1989.

B. Cl + C_2H_2Cl.
1. Ground state, +82 kcal/mol: from standard bond energies.
Cartland, H. E.; Pimentel, G. C. *J. Phys. Chem.* 1986, *90*, 5485.
2. Cl + $C_2H_2Cl^*$ excited state, +128 kcal/mol: by analogy with C_2H_3 *A* state, 46 kcal/mol above ground state.
Wodtke, A. M.; Hintsa, E. J.; Somorjai, J.; Lee, Y. T. submitted to *Isr. J. Chem.*, February 1989.

C. Cl + Cl + C_2H_2 ground state, +109 kcal/mol: $D_0(Cl_2)$ = 57 kcal/mol, plus ground state energy of $Cl_2 \cdot C_2H_2$ (less interaction energy).
Pimentel, G. C.; Spratley, R. D. *Understanding Chemistry*; Holden-Day: Oakland, 1971; p. 904.

D. Cl + H + C_2HCl ground state, +128 kcal/mol: $D_0(HCl)$ = 103 kcal/mol, plus ground state energy of $HCl \cdot C_2HCl$ (less interaction energy).
Pimentel, G. C.; Spratley, R. D. *Understanding Chemistry*; Holden-Day: Oakland, 1971; p. 902.

E. Cl + HCl + C_2H ground state, +135 kcal/mol:
1. $D_0(HCC\text{-}H)$ = 127 kcal/mol = $\Delta H(C_2H_2 \rightarrow C_2H + H)$
Segall, J.; Lavi, R.; Wen, Y.; Wittig, C. *J. Phys. Chem.* 1989, *93*, 7287; Green, P. G.; Kinsey, J. L.; Field, R. W. *J. Chem. Phys.* 1989, *91*, 5160.
2. $\Delta H_f(C_2H) = \Delta H_f(C_2H_2) + D_0(HCC\text{-}H) - \Delta H_f(H)$
= 54 + 127 - 52 = 129 kcal/mol.

3. $\Delta H(C_2H_2Cl_2 \rightarrow C_2H + HCl + Cl)$
$= \Delta H_f(C_2H) + \Delta H_f(HCl) + \Delta H_f(Cl) - \Delta H_f(C_2H_2Cl_2)$
$= 129 + (-22) + 29 - 1 = 135$ kcal/mol.
Pimentel, G. C.; Spratley, R. D. *Understanding Chemistry*; Holden-Day: Oakland, 1971; pp. 891-900.

IV. Xenon-Complexed Products and Intermediates.

A. $XeCl + C_2H_2Cl$.

1. Ground state, +81 kcal/mol: Xe-Cl interaction energy, 0.8 kcal/mol below free Cl + C_2H_2Cl (+ Xe).
Becker, C. H.; Valentini, *J. J.*; Casavecchia, P.; Sibener, S. *J.*; Lee, Y. T. *Chem. Phys. Lett.* 1979, *61*, 1.

2. $(Xe^+Cl^-)^* + C_2H_2Cl$ excited state, +172 kcal/mol: ≥3.94 eV = 91 kcal/mol above ground state in solid Xe.
Last, I.; George, T. F. *J. Chem. Phys.* 1987, *86*, 3787.

B. $(Xe_2^+Cl^-)^* + C_2H_2Cl$ excited state, +159 kcal/mol: 3.35 eV = 77 kcal/mol above ground state in solid Xe.
Fajardo, M. E.; Apkarian, V. A. *J. Chem. Phys.* 1986, *85*, 5660.

C. $(Xe_{12}^+Cl^-)^* + C_2H_2Cl$ excited state, +172 kcal/mol: 3.89 eV = 90 kcal/mol above ground state in solid Xe.
Last, I.; George, T. F. *J. Chem. Phys.* 1987, *86*, 3787.

APPENDIX B:
Thermochemistry of Selected Proton Transfer Reactions

I. $HF + HCN \rightarrow HFH^+ + CN^-$

$HF + H^+ \rightarrow HFH^+$ $\quad \Delta H_b = -117$ kcal/mol[1]

$HCN \rightarrow H^+ + CN^-$ $\quad \Delta H_a = 351$ kcal/mol[2]

$\Delta H_I = \Delta H_b + \Delta H_a$

$= -117 + 351$

$= 234$ kcal/mol

II. $HCl + HCCCl \rightarrow HClH^+ + CCCl^-$

$HCl + H^+ \rightarrow HClH^+$ $\quad \Delta H_b = -135$ kcal/mol[1]

$HCCCl \rightarrow H^+ + CCCl^-$ $\quad \Delta H_a < 367$ kcal/mol (by analogy with HCCF)[2]

$\Delta H_{II} = \Delta H_b + \Delta H_a$

$< -135 + 367$

< 232 kcal/mol

[1]Lias, S. G.; Liebman, J. F.; Levin, R. D. *J. Phys. Chem. Ref. Data* **1984**, *13*, 695.

[2]Lias, S. G.; Bartmess, J. E.; Liebman, J. F.; Holmes, J. L.; Levin, R. D.; Mallard, W. G. *J. Phys. Chem. Ref. Data* **1988**, *17*, supplement 1.